



## **POLITECNICO DI TORINO**

*Department of Environment, Land and Infrastructure Engineering*  
**Master of Science in Petroleum and Mining Engineering**

### **The Establishment of a Multiphase Flow Leak Detection Experimental Set-Up**

**Supervisor:** Prof. Guido Sassi (Politecnico di Torino)

**Co-Supervisor:** Prof. Mohammad Azizur Rahman (Texas A&M University at Qatar)

Student: Saad Ragab Saleh BELMASHKAN

**October 2020**

Thesis submitted in compliance with the requirements for the Master of Science degree in Petroleum  
Engineering

## Abstract

Pipeline leakage has been one of the most problems for fluid transportation for the oil industry especially when the fluid is multiphase flow. The detection of a leak, in this case, will be difficult to detect leak early. This thesis will explain the modification to convert the multiphase flow loop at Texas A&M University – Qatar from drilling purpose to leak detection flow loop for subsea leakage purpose study. No experimental data collected for this study only design, modification, literature review, and sensitivity analysis included.

The study includes an overview of the recent leak detection methods for a single -phase and multiphase flow that will help to understand the most appropriate method could use for the proposed experimental set-up. Provide a sensitivity analysis for the entrance of length for single-phase and multiphase flow for different pipeline diameters to decide the aquarium tank position at the flow loop. Summaries the recent literature review for the leak detection experimental set-up to understand better the materials and instruments that have been used before.

Provide technical information for the new experimental set-up including the specification and required instruments with aquarium tank design and pressure drop calculation for multiphase flow. A study for research cost including the price for the equipment, model, design for the facility, and the total required budget to implement the new proposed setup. Provide Risk analysis (HAZOP) study for the proposed flow loop and detect the high hazard area with a recommendation to avoid or minimize the risk.

This study will help in the future to collect leak data from the experiment. The leak data helps to better understating the leakage method. The design and modification methodology can be used for other experimental purposes as well. The entrance of length calculation shows the velocity has a big impact on the fluid development while the density considers the minor effect for the entrance of length as compared with other fluid parameters.

**Keywords:** Multiphase flow, Entrance of Length, Differential pressure, Risk Analysis, Leak detection.

## **Acknowledgment**

First of all, I would like to express my sincere gratefulness to God (Allah) Almighty, without whom everything was impossible.

Special thanks to my family and friends, mainly my parents, brothers, and sisters for their affection, continuous provision, and firm faith in me. Without them, I would not be at the position today I am.

I would like to express my gratitude to my internal supervisor, Prof. Guido Sassi, and the external supervisor, Prof. Mohammad Azizur Rahman, for his support, encouragement, commitment, and supervision through this study. I am very grateful to Texas A&M University Qatar for their acceptance and warm welcome.

I want to show gratitude to Ph.D. Student Mr. Burak Celal and Dr. Muhammad Saad Khan, at Texas A&M University - Qatar for the massive assistance and suggestions they provided me during the research.

I would also like to thank to all my respected professors in the Petroleum Department, without their knowledge and guidance it was not even possible to accomplish this research. A big thankful to the Politecnico office for the scholarship to write my thesis abroad and get more experience

Thankful you to the Libyan community office in Qatar for their support during the pandemic Covid -19 issue.

Last but not the least, I would like to give my heartfelt thanks to my sponsorship Ministry of Foreign Affairs and International Cooperation – Italy (MAECI) scholarships program to sponsor my degree.

## **Dedication**

**This Thesis is Dedicated to my Father Soul and my Lovely Mom  
for their Endless Love,  
Support and Encouragement**

# Table of Contents

Abstract.....	ii
Acknowledgment .....	iii
Dedication.....	iv
Table of Contents .....	v
List of Figures.....	ix
List of Tables .....	xiii
Nomenclature and Abbreviation .....	xvii
Chapter 1. Introduction.....	1
1.1 Overview .....	1
1.2 Problem Statement.....	1
1.3 Goals and Objectives of the Thesis .....	2
1.4 Method and Approach .....	3
1.5 Structure of the Thesis .....	3
Chapter 2. Leak Detection Background .....	5
2. Introduction to Pipeline Leakage and Risk.....	5
2.1 Pipeline Leakage and Risk Catastrophes .....	5
2.2 Overview of Leak Detection Systems (LDS).....	7
2.3 Hardware Base Method.....	9
2.3.1 Acoustic Sensor Hardware Base Method.....	9
2.3.2 Vapor Sampling Hardware Base Method.....	10
2.3.3 Fiber Optic Hardware Base Method .....	10
2.3.4 Cable Sensor Hardware Base Method .....	11
2.3.5 Accelerometer Hardware Base Method .....	12

2.3.6 Cable Hardware Base Method .....	12
2.4 Software Based Method .....	12
2.4.1 Mass / Volume Balance Software Based Method.....	12
2.4.2 Real-Time Transient Monitoring (RTTM) Software Based Method.....	13
2.4.3 Negative Pressure Wave Software Based Method .....	14
2.4.4 Pressure Point Analysis (PPA) Software Based Method .....	15
2.4.5 Statistical Analysis Software Based Method.....	15
2.4.6 Digital Signal Processing Software Based Method .....	16
2.4.7 Dynamic Modeling Software Based Method .....	16
2.5 Comparison of Leak Detection Methods. ....	17
Chapter 3. Sensitivity Analysis.....	19
3. Flow Regimes for Horizontal Pipeline .....	19
3.1 Entrance Length for Horizontal Pipeline .....	21
3.1.1 Entrance Length for Single Phase Liquid .....	21
3.1.2 Entrance Length for Single Phase Air.....	23
3.2 Entrance Length for Two-Phase Flow .....	31
3.2.1 Mixture Density .....	32
3.2.2 Mixture Viscosity .....	32
3.3 Entrance Length for Multiphase Flow .....	33
3.4 Entrance Length Calculation for Two-Phase (water and Air).....	34
3.5 Entrance of Length Calculation for Three-Phase (Water, Air, and Solid).....	50
3.5.1 Entrance Length Calculation for Three-Phase (Water, Air, and Solid) Change in density .....	56
3.5.2 Entrance Length Calculation for Three-Phase (Water, Air and Solid) with Change in Viscosity.....	61
Chapter 4. Literature Background.....	66

4. Recent studies for single and Multiphase flow loop with Technical Specifications and Fluids.....	66
4.1 Single Phase Experiments.....	67
4.2 Multiphase Flow Experiments.....	72
Chapter 5. Experimental Setup .....	79
5.1 Current Experimental Design Goal .....	79
5.2 Eventual Experimental Design Goal .....	79
5.3 Equipment Selection.....	82
5.3.1 Pipeline.....	82
5.3.2 Acrylic pipeline material.....	83
5.3.3 Differential Pressure Transducer Availability.....	83
5.3.4 Pressure Drop with Inclination .....	88
5.3.5 Differential Pressure Transducer .....	92
5.3.6 Dynamic Pressure Transducer .....	92
5.3.7 Leak Modeling.....	93
5.3.8 Pressure Regulator and Oil Filter.....	94
5.3.9 Flow and Temperature Sensor .....	94
5.3.10 Tank Design.....	95
5.3.11 Acoustic Data Acquisition.....	96
5.3.12 Air Compressor.....	96
5.3.13 Tilting Frame .....	97
Chapter 6. Cost Analysis .....	99
Chapter 7. Risk Analysis .....	104
7.1 Hazard Identification .....	104
7.2 HAZOP Objective .....	104

7.3 Purpose of Risk Analysis .....	105
7.4 HAZOP Analysis.....	106
7.5 Risk Matrix.....	108
7.6 HAZOP Study Details .....	109
7.6.1 Assumptions and Clarifications.....	111
Chapter 8. Conclusions and Recommendation .....	115
8.1 Conclusions .....	115
8.2 Recommendation .....	116
9. Reference .....	117

## List of Figures

Figure 2. 1 number of the incident per year.....	7
Figure 2. 2 illustrates classifying leak detection systems.....	8
Figure 2. 3 Acoustic leak detection .....	9
Figure 2. 4 sensor hose system for pipeline leak detection .....	10
Figure 2. 5 Schematic Representation of Fiber optic application.....	11
Figure 2. 6 Mass/ Volume Leak Detection Method.....	13
Figure 2. 7 Real-Time Transient Model RTTM . .....	14
Figure 2. 8 Negative Pressure Wave .....	14
Figure 2. 9 Expanded Wave Propagation .....	15
Figure 2. 10 Statistical Analysis .....	16
Figure 3. 1 Shows the bubble flow regime for horizontal pipeline.....	19
Figure 3. 2 Shows the stratified flow regime for horizontal pipeline .....	19
Figure 3. 3 Shows the wavy flow regime for horizontal pipeline.....	20
Figure 3. 4 Shows the slug flow regime for horizontal pipeline.....	20
Figure 3. 5 Shows the Annular flow regime for horizontal pipeline .....	20
Figure 3. 6 Taitel and Dukler dimensionless flow regime map 1976 .....	21
Figure 3. 7 The development of the velocity boundary layer in a pipe. (The developed average velocity profile is parabolic in laminar flow, as shown, but much flatter or fuller in a turbulent flow.).....	22
Figure 3. 8 Developing velocity profiles and pressure changes in the entrance of a duct flow.....	22
Figure 3. 9 shows the change in entrance of length with a diameter at different velocity for single-phase water .....	25

Figure 3. 10 shows the change in entrance of length with a diameter at different velocity for single-phase Air .....	26
Figure 3. 11 shows the change in entrance of length with different air density .....	28
Figure 3. 12 shows the change in entrance of length with different water density.....	29
Figure 3. 13 shows the change in entrance of length with different air viscosity.....	30
Figure 3. 14 shows the change in entrance of length with different water viscosity .....	31
Figure 3. 15 shows a change in entrance of length with different liquid hold up at homogenous velocity 20 m/s .....	36
Figure 3. 16 shows change in entrance of length with different liquid hold up at velocity 40 m/s. ....	38
Figure 3. 17 shows change in entrance of length with different liquid hold up at velocity 80 m/s. ....	39
Figure 3. 18 shows the change in entrance of length with different liquid hold up at variable assumption velocities .....	40
Figure 3. 19 shows the change in entrance of length with different liquid hold up at homogenous velocity 20 m/s and different density.....	42
Figure 3. 20 Shows change in entrance of length with different liquid hold up at homogenous velocity 40 m/s and different density.....	44
Figure 3. 21 shows the change in entrance of length with different liquid hold up at homogenous velocity 80 m/s and different density.....	45
Figure 3. 22 shows the change in entrance of length with different liquid hold up at homogenous velocity 20 m/s and different viscosity.....	47
Figure 3. 23 shows the change in entrance of length with different liquid hold up at homogenous velocity 40 m/s and different viscosity. ....	49
Figure 3. 24 Shows change in entrance of length with different liquid hold up at homogenous velocity 80 m/s and different viscosity.....	50

Figure 3. 25 shows the change in entrance of length for 3-phase flow with different solid fraction at a homogenous velocity 20 m/s .....	52
Figure 3. 26 shows the change in entrance of length for 3-phase flow with different solid fraction at a homogenous velocity 40 m/s .....	53
Figure 3. 27 shows the change in entrance of length for 3-phase flow with different solid fraction at a homogenous velocity 80 m/s .....	54
Figure 3. 28 shows the change in entrance of length for 3-phase flow with different solid fraction at variable velocities .....	55
Figure 3. 29 shows a change in entrance of length for 3-phase flow with different solid fractions and different density at a homogenous velocity 20 m/s .....	57
Figure 3. 30 shows a change in entrance of length for 3-phase flow with different solid fractions and different density at a homogenous velocity 40 m/s .....	58
Figure 3. 31 shows a change in entrance of length for 3-phase flow with different solid fractions and different density at a homogenous velocity 80 m/s .....	59
Figure 3. 32 shows a change in the entrance of length for 3-phase flow with different solid fractions and different density at variable velocities .....	60
Figure 3. 33 shows a change in entrance of length for 3-phase flow with different solid fractions and different viscosity at a homogenous velocity 20 m/s. ....	62
Figure 3. 34 shows a change in entrance of length for 3-phase flow with different solid fractions and different viscosity at a homogenous velocity 40 m/s. ....	63
Figure 3. 35 shows a change in entrance of length for 3-phase flow with different solid fractions and different viscosity at a homogenous velocity 80 m/s. ....	64
Figure 3. 36 shows a change in the entrance of length for 3-phase flow with different solid fractions and different viscosity at variable velocities. ....	65
Figure 4. 1 Current Multiphase flow loop At Texas A&M University – Qatar (ant3Dlab).	66
Figure 4. 2 Experimental Set-Up for Single phase .....	68
Figure 4. 3 Experimental Set-Up for Single phase .....	68

Figure 4. 4 Shows the instrument test rig .....	70
Figure 4. 5 shows the leak sound source (a) external correlation technique (b) in-pipe measurement technique .....	70
Figure 4. 6 shows the experimental set-up .....	71
Figure 4. 7 shows the nodes schematic diagram.....	72
Figure 4. 8 shows a sketch of the experimental set-up .....	74
Figure 4. 9 shows the flow chart of the acoustic leakage experimental .....	75
Figure 5. 1 Show the current multiphase flow loop at Texas A&M University – Qatar (ant3Dlab).....	79
Figure 5. 2 Shows the modified multiphase flow loop leak detection 2D Drawing (ant3Dlab).....	80
Figure 5. 3 Shows the modified multiphase flow loop leak detection 3D Drawing (ant3Dlab).....	80
Figure 5. 4 Shows the Dynamic Pressure Transducer specification .....	93
Figure 5. 5 shows the proposed tank design (ant3Dlab) .....	96
Figure 7. 1 TAMUQ Risk Matrix .....	109

## List of Tables

Table 2. 1 show the Performance comparison Metric.....	17
Table 3. 1 shows the minimum required entrance lengths for fully developed laminar....	23
Table 3. 2 shows the entrance length summary for single-phase Air and Water.....	23
Table 3. 3 shows the entrance length summary for single-phase Air and Water with a change in air and water density.....	27
Table 3. 4 shows the entrance length summary for single-phase Air and Water with a change in air and water viscosity. ....	29
Table 3. 5 shows the original liquid and gas viscosity.....	34
Table 3. 6 shows the original liquid and gas density .....	34
Table 3. 7 shows homogenous velocity for liquid and gas 20 m/s two-phase entrance length summary. ....	35
Table 3. 8 shows the change in velocity for two-phase with liquid and gas hold up 0.7, 0.3 respectively entrance length summary. ....	36
Table 3. 9 shows the change in velocity for two-phase with liquid and gas hold up 0.9, 0.1 respectively entrance length $L_e$ summary.....	37
Table 3. 10 shows the change in velocity for two-phase with liquid and gas hold up 0.5, 0.5 respectively entrance length $L_e$ summary.....	38
Table 3. 11 shows the change in liquid (water) density .....	41
Table 3. 12 shows a summary of the entrance of length with change in density at a homogenous velocity 20 m/s for liquid and gas. ....	41
Table 3. 13 shows 2- phase summary entrance of length with change in density at different velocity with liquid and gas hold up 0.9, 0.1 respectively .....	42
Table 3. 14 shows two-phase summary entrance of length with change in density at different velocity with liquid and gas hold up 0.7, 0.3 respectively .....	43
Table 3. 15 shows two-phase summary entrance of length with change in density at different velocity with liquid and gas hold up 0.5, 0.5 respectively .....	44

Table 3. 16 shows the change in liquid and gas viscosity .....	45
Table 3. 17 shows homogenous velocity for two-phase with different liquid and gas hold up and change in viscosity.....	46
Table 3. 18 shows a summary entrance of length with different velocity for two-phase with variable liquid and gas hold up and change in viscosity .....	47
Table 3. 19 shows a summary entrance of length with different velocity for two-phase with variable liquid and gas hold up and change in viscosity .....	48
Table 3. 20 shows a summary entrance of length with different velocity two-phase with variable liquid and gas hold up and change in viscosity .....	49
Table 3. 21 shows the water, air, and solid viscosity for 3-phase.....	51
Table 3. 22 shows the water, air, and solid density for 3-phase .....	51
Table 3. 23 shows the summary entrance of length with homogenous velocity 20 m/s for three-phase with variable liquid, air, and solid fraction .....	51
Table 3. 24 shows the summary entrance of length with homogenous velocity 40 m/s for three-phase with variable liquid, air, and solid fraction .....	52
Table 3. 25 shows a summary for the entrance of length with homogenous velocity 80 m/s for three-phase with variable liquid, air, and solid fraction.....	53
Table 3. 26 shows the water, air, and solid with a change in density for 3-phase .....	56
Table 3. 27 shows the summary entrance of length with homogenous velocity 20 m/s for three-phase with variable liquid, air, and solid fraction and different density .....	56
Table 3. 28 shows the summary entrance of length with homogenous velocity 40 m/s for three-phase with variable liquid, air, and solid fraction and different density .....	57
Table 3. 29 shows the summary entrance of length with homogenous velocity 80 m/s for three-phase with variable liquid, air, and solid fraction and different density .....	58
Table 3. 30 shows the water, air, and solid with a change in viscosity for 3-phase .....	61
Table 3. 31 shows the summary entrance of length with homogenous velocity 20 m/s for three-phase with variable liquid, air, and solid fraction and different viscosity.....	61

Table 3. 32 shows the summary entrance of length with homogenous velocity 40 m/s for three-phase with variable liquid, air and solid fraction and different viscosity.....	63
Table 3. 33 shows the summary entrance of length with homogenous velocity 80 m/s for three-phase with variable liquid, air and solid fraction and different viscosity.....	64
Table 4. 1 shows the leak flow rate with a change in leak size at different pressure.....	69
Table 4. 2 shows the flow regime perform with specific gas and liquid flow rates .....	75
Table 4. 3 show the experimental component details .....	75
Table 5. 1 show the Modification for the multiphase flow loop to leak detection .....	81
Table 5. 2 show the availability of the pressure gauge ranges .....	83
Table 5. 3 shows Lockhart–Martinelli constant.....	85
Table 5. 4 shows pressure drop for different flow regime.....	87
Table 5. 5 shows a two-phase pressure drop for different flow regime .....	87
Table 5. 6 shows a three-phase pressure drop for different flow regime .....	87
Table 5. 7 shows a three-phase pressure drop for different flow regime .....	88
Table 5. 8 shows the three-phase pressure drop.....	88
Table 5. 9 shows a two-phase pressure drop for different flow regime at an angle 20° ...	89
Table 5. 10 shows a two-phase pressure drop for different flow regime at an angle 20° .	89
Table 5. 11 shows a two-phase pressure drop for different angles 15 ° and 20°.....	90
Table 5. 12 shows three-phase pressure drop for different flow regime at angle 20°.....	90
Table 5. 13 shows a three-phase pressure drop for different flow regime at an angle 20°	91
Table 5. 14 shows a three-phase pressure drop for different flow regime at an angle 20°	91
Table 5. 15 shows a two-phase pressure drop for different angles 15 ° and 20°.....	91
Table 5. 16 Mass Flow rate and volumetric flow rate for Air velocity.....	97
Table 5. 17 Shows the total estimation weight for the flow loop .....	98

Table 6. 1 Experimental components of flow loop for two and three-phase leak detection set-up .....	101
Table 6. 2 Image and data acquisition systems.....	103
Table 6. 3 Workstation for image and data acquisition.....	103
Table 7. 1 HAZOP Worksheet for Inlet Line flow loop.....	112
Table 7. 2 HAZOP Worksheet for slurry pumping system. ....	113
Table 7. 3 HAZOP Worksheet for Tank Bath and Leakage Valve.....	114

## Nomenclature and Abbreviation

D	Diameter	<i>m,ft</i>
$C_v$	Solids volume concentration	<i>v/v</i>
$\rho_f$	Fluid Density	<i>kg/m<sup>3</sup></i>
$\rho_s$	Density of solid particles in mixture	<i>kg/m<sup>3</sup></i>
$\mu_m$	Absolute (dynamic) viscosity of the slurry mixture	<i>Pa.s</i>
$\mu_L$	Absolute viscosity of a liquid phase	<i>Pa.s</i>
$\Phi$	Total solid volume fraction	-
$C_v$	Solids concentration by volume	<i>%</i>
$Re_m$	Mixture Reynold number	-
$\rho_m$	Mixture density	<i>kg/m<sup>3</sup></i>
$U_m$	Mixture superficial velocity	<i>m/s</i>
$\mu_m$	Mixture Viscosity	<i>pa.s</i>
$\lambda$	Fraction of fluid	-
$L_e$	Entrance Length	<i>m/ inch</i>
$Re_e$	Reynold Number	-
P	Pressure	<i>pa/bar</i>
v	Velocity	<i>m/s</i>
$X^2$	Lockhart–Martinelli parameter	-
$f_f$	Darcy- Weisbach frication factor	-
f	Fraction factor	-
A	Area	<i>m<sup>2</sup></i>

$U_m$	Mixture superficial velocity	<i>m/s</i>
$U_{sL}$	Single phase liquid superficial velocity	<i>m/s</i>
$U_{sg}$	Single phase gas superficial velocity	<i>m/s</i>
$\rho_L$	Liquid density	<i>kg/m<sup>3</sup></i>
$\rho_g$	Gas density	<i>kg/m<sup>3</sup></i>
$C_{max}$	Maximum package concentration of the solid	<i>%</i>
$C_s$	In-situ volumetric solid concentration	<i>%</i>
$d^+$	Dimensionless particle diameter	-
$j_s$	Slurry superficial velocity	<i>m/s</i>

### **Abbreviation**

EGIG	European Gas Pipeline Incident Data Group
LDS	Leak Detection System
ASME	American Society of Mechanical Engineering
DTS	Distribution Temperature Sensor
DAS	Distribution Acoustic Sensor
FOC	Fiber Optic Technology
SCADA	Supervisory Control and Data Acquisition
RTTM	Real Time Transient Monitoring
PPA	Pressure Point Analysis
IMF	Intrinsic Mode Analysis
EMD	Empirical Mode Decomposition
ERT	Electric Resistance Tomography
SL	Single Phase Liquid

SG	Single Phase Gas
FPG	Fraction Pressure Gradient
HAZOP	Hazard and Operability Study

## **Chapter 1. Introduction**

### **1.1 Overview**

The global growing still dependent on the hydrocarbon products, it is important to ensure the continuity of new hydrocarbons discovery. At the same time, it is very important to ensure that the hydrocarbons are extracted in an environmentally sustainable manner and the produced quantities are efficiently delivered by assuring their safe transportation and distribution from the place of production to place of consumption. The pipeline transport system is a unique form of transportation that involves the transportation of fluids through pipes. In recent years oil industry program conducted large-scale experiments to evaluate the ability of distributed sensing technologies to detect leaks from subsea pipelines where the subsea leakage problems cost more money for repair and operation. The occurrence of leaks in pipeline systems does not only signify a loss of valuable, hydrocarbon resources but also a source of environmental pollution and the potential of disasters. The recent increase in the utilization of pipeline systems for oil and gas transportation together with the great economic loss and the environmental implication associated with their failure calls for a need to explore cheap, quick, accurate, and reliable leak detection methods in pipeline systems using real-time monitoring technologies. Several experimental facilities have carried out investigations to improve the most appropriate leak detection method for both single and multiphase flow. This thesis mainly will focus on how to establishing flow loop leak detection with a simulation of subsea conditions. The chance to use more leak detection methods in this proposed experiment tool will give more ideas about the proper method for leak detection in subsea conditions.

### **1.2 Problem Statement**

All different kinds of fluids including water and crude oil even solid capsule is being transported through thousands or millions of miles of pipelines all over the world. The transport and distribution network is very elaborate and continuously growing. This network is prone to many risks and hazards. The pipelines are vulnerable to losing their functionality by internal and external corrosion, cracking, third party damage, and manufacturing flaws<sup>1</sup>. especially if the pipeline is located in very harsh conditions such as subsea. However, pipelines consider the safest means of transportation. The most common

threat that happens in pipelines is leakage. The effects of leakage go beyond repair expense and cost of lost oil or gas, it also significantly impacts the human lives, animals, and the environment. To impede these huge costs, designing a reliable leak detection technique is crucial. However, more information is required to achieve a reliable system. Before deciding on any corrective action, the location and size of leakage should be known. Many researches have been done during the last decades to find the location and size of the leakage with high accuracy.

The main problem is how to discover the leak detection in case the flow is a multiphase flow which is consist of three-phase or two-phase flow could be water and oil or oil-water and solid. In the oil industry the flow is coming from the wells through the pipeline then is gathering in the separation station during the flow from well to the separation station the flow is in mixture condition. After a while the pipeline exposure to the corrosion issue and to discover the leak early is a big challenge here and a lot of the failure alarm in the control station will distinguish whether there is a leak or not.

### **1.3 Goals and Objectives of the Thesis**

The vital objective of this research thesis title is to design the required modification tools for the current multiphase flow loop at Texas A&M University- Qatar to multiphase leak detection flow loop. By performing all the required calculations and required searching to come out with comprehensive experiments set-up for leak detection. It is hoped to detect the leak as early as possible to avoid the cost-effective and safe environments. In case the flow is multiphase flow hopes this experiment can give more ideas on how to distinguish between the real and fake leak signals. Another goal to capture and visualize the leak fluid spill when the leak happens with different leak sizes and working pressure.

A list of goals can be included as following:

1. To have a better understanding of leak detection methods with different working fluids.
2. To detect the most appropriate leak detection method for subsea harsh conditions.
3. To have a better understanding of how the fluid propertied effect on the leak flow rate.
4. To understand the distribution of spilled fluid during the leaking.

5. Understand the risk analysis and provide information about the most hazardous equipment for the experiment. Also, provide a safe working area for the workers.

#### **1.4 Method and Approach**

To convert the current flow loop at Texas A&M University- Qatar needs to perform some calculation and analysis to finalize the modification to leak detection correctly.

Starting with the support structure frame of the flow loop needs to be stronger than before to move properly up and down with the tank. Need to perform the entrance of length analysis to decide where to fix the tank in the flow loop. The leak modeling place has to be after fully fluid development so the entrance of length is important here. Another consideration takes into account is the visualization of the fluid at leakage place. Need to calculate the volume rate and mass flow rate to design the required air Compressor for the experiment, another computation is required such as differential pressure, the maximum, and minimum differential pressure to decide the needed pressure gauge for the experiment. Using the differential pressure before and after the leak position to detect the leak with different leak size also using the hydrophone to detect the leakage signal when the leak size been very small.

Finally, the experiment can run with a different scenario such as a change in leak size change in pressure, change in flow loop angles, and change in working pressure. Many different scenarios can be done. Unfortunately, no experimental data are included in this thesis only the experimental set-up for leak detection is included.

#### **1.5 Structure of the Thesis**

The thesis draft is the set-up for a new experimental flow loop leak detection. In the section, a brief overview of the entire thesis is enlisted.

**Chapter 1:** This chapter includes the general overview and problem statement of the thesis. Discuss the method and approach for the thesis purpose and finally summaries the structure of the entire thesis.

**Chapter 2:** This chapter discusses the background of pipeline leak detection methods in land and marine. Also, mentioned the most common method used for leak detection at the different environments with complete comprise between all the common methods.

**Chapter 3:** This chapter discusses the parametric study for the entrance of length calculation and summaries the most effective parameter for the entrance of length for single-phase, two-phase, and three-phase flow. Also mentioned the fundamental equations used to calculate the entrance of length. Provide the graphs that show the entrance of length calculation with the change in pipeline diameter, fluid properties, and velocity.

**Chapter 4:** This chapter summarizes the recent experiments leak detection and flow loop studied in the past recent years for single-phase and multiphase flow (literature review). Including the working fluid and the used equipment with the specification. Also, including more information about the leak detection used method and leak modeling.

**Chapter 5:** This chapter refers to the experimental facility and set-up for a new leak detection flow loop including all the required instruments and tools with the entire specification. The comprehensive information about the new modified flow loop with calculation is used to design and proper selection of the instruments. Types of equipment and techniques are enlisted. Also, the detailed discussion about the tank bath design and new support structure frame setup has been explained.

**Chapter 6:** Summaries cost analysis for all the equipment needed for the modification purpose with the supplier name and model type of instrument. Also included the fitting company cost for assembled and the required total amount of research.

**Chapter 7:** Explanation about the risk analysis and perform HAZOP for the proposed leak detection flow loop including the hazard analysis and ranking the riskiest equipment. Gives warning and awareness about future action with a recommendation to prevent some incidents that might occur.

**Chapter 8:** The last chapter of the thesis involves the significant conclusions of the set-up of the experiments as stated in the previous chapters. The recommendations for future aspects are also mentioned.

Finally, the list of references is arranged using the Mendeley tool and displayed with IEEE format in order by number.

## **Chapter 2. Leak Detection Background**

### **2. Introduction to Pipeline Leakage and Risk**

Nowadays, the growing global dependence on hydrocarbon products, it is very important to ensure the continuity of new hydrocarbons discovery. Also, it is very important to ensure that the hydrocarbons are extracted in an environmentally sustainable manner, and the produced quantities are efficiently delivered by assuring their safe transportation and distribution from the place of production to place of consumption.

Pipelines are important means of transporting petroleum products and the most economical they fulfill high demand for efficiency and reliability. Therefore, leakage monitoring is important in pipeline management for safety and environmental reasons. Any process equipment has a given life cycle, after which maintenance is required. Off-shore (subsea) pipelines may also experience damage or decrease in strength over time. Leaks from these subsea pipelines may result in different oil and gas fluids contaminating the environment, leading to undesired economic and environmental losses. Therefore, early detection and localization of such leaks is critical to maintaining process safety and minimize economic losses.

Multiphase flow is one of the most difficult situations for leak detection in pipelines, due to several reasons: the existence of two different and independent flow rates at each phase, five or more possible flow patterns, different fluid velocities at the phases, and sometimes a non-Newtonian associated behavior, due to the formation of an oil-water emulsion. While the single phase less problem during transportation and not complex as compare with multiphase.

This chapter will examine the pipeline leakage in Europe and risks then show the available leak detection and localization methods for single and multiphase flow.

#### **2.1 Pipeline Leakage and Risk Catastrophes**

The EGIG database contains general information about the European gas transmission pipeline system as well as specific information about the incidents.<sup>2</sup>

Every year the length of the pipeline system is collected for the following parameters:

- Diameter
- Pressure
- Year of construction
- Type of coating
- Depth of cover
- Grade of material
- Wall thickness

In many parts of the world major chemical sides such as chemical parks are connected by pipeline and as the transported chemical raw material such as ethylene, hydrogen, carbon monoxide, and oxygen are potentially hazardous to human and the environment regarding safety and security in case the pipeline located in urban centers.

The characteristics of the pipeline on which the incident happened, namely the general information listed as following.

**The leak size:**

- **Pinhole/crack:** the effective diameter of the hole is smaller than or equal to 2 cm
- **Hole:** the effective diameter of the hole is larger than 2 cm and smaller than or equal to the diameter of the pipe
- **Rupture:** the effective diameter of the hole is larger than the pipeline diameter.

**The initial cause of the incident**

- External interference
- Corrosion
- Construction defect/material failure
- Hot tap made by error
- Ground movement

Trends of the number of incidents in the ninth EGIG report, which covers the period 1970-2013, a total of 1,310 incidents were recorded. In the last three years, 56 incidents were reported by the EGIG members, which brings the total number of incidents to 1,366 for the period 1970-2016. The following figure shows the number of incidents per year. <sup>2</sup>

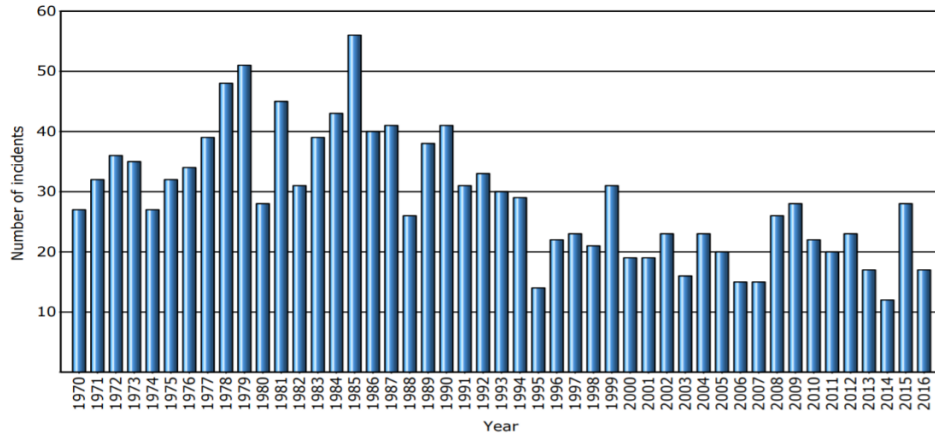


Figure 2. 1 number of the incident per year <sup>2</sup>

Some of the major pipeline leak incidents in Europe through recent past years in July 2004 at *Ghislenghien, Belgium* an explosion cost by a leak in a gas pipeline injures 132 and kills 24 people. This leak for example was existing for almost 14 days before the gas explode.

- In March 2008, a leak in the ethylene pipeline infrastructure network in Germany cost a series of fire.
- In Austria December 2017, A large explosion rocked one of Europe’s biggest gas pipeline hubs at *Baumgarten, Eastern Vienna*, leaving one person dead and 18 injured.
- In March 2012 around one million liters of kerosene leak out of the pipeline because the leak remains undetectable for several weeks in Germany.

At least two of these catastrophes could have been avoided by the state-of-the-art leak detection system.

## 2.2 Overview of Leak Detection Systems (LDS)

The leak detection system could be classified based on their technical approach. There are two general ways for leak detection: hardware-based methods and software-based methods <sup>3</sup>. According to another classification sometimes mentioned as externally or internally based LDSs.

Hardware-based methods depend on mainly the usage of special sensing devices in the detection of fluid leaks. The hardware-based systems detect the leaks from outside of the

pipe using specific sensing devices. These hardware systems can be further classified as optical, acoustic, cable sensor, ultrasonic flow meters, and vapor sampling.

The software base can use different approaches to detect leaks including mass/volume balance, acoustic/negative pressure wave, real-time transient modeling, pressure point analysis, statistics, or digital signal processing <sup>3</sup>. The software-based systems may require flow, pressure, and temperature measurements at the inlet and outlet.

Internal-based (software) systems use field sensor data that monitors internal pipeline parameters, such as pressure, temperature, viscosity, flow rate, density, contamination, product sonic velocity, and product data at interface locations. These inputs are then used for inferring a release leak of fluid by computation. Typically, these systems are installed along with the pipeline and other data acquisition systems. These calculation based technologies usually have a considerable track record for detecting large and some small pipeline leak<sup>4</sup>. Figure 2.2 illustrates classifying leak detection systems.

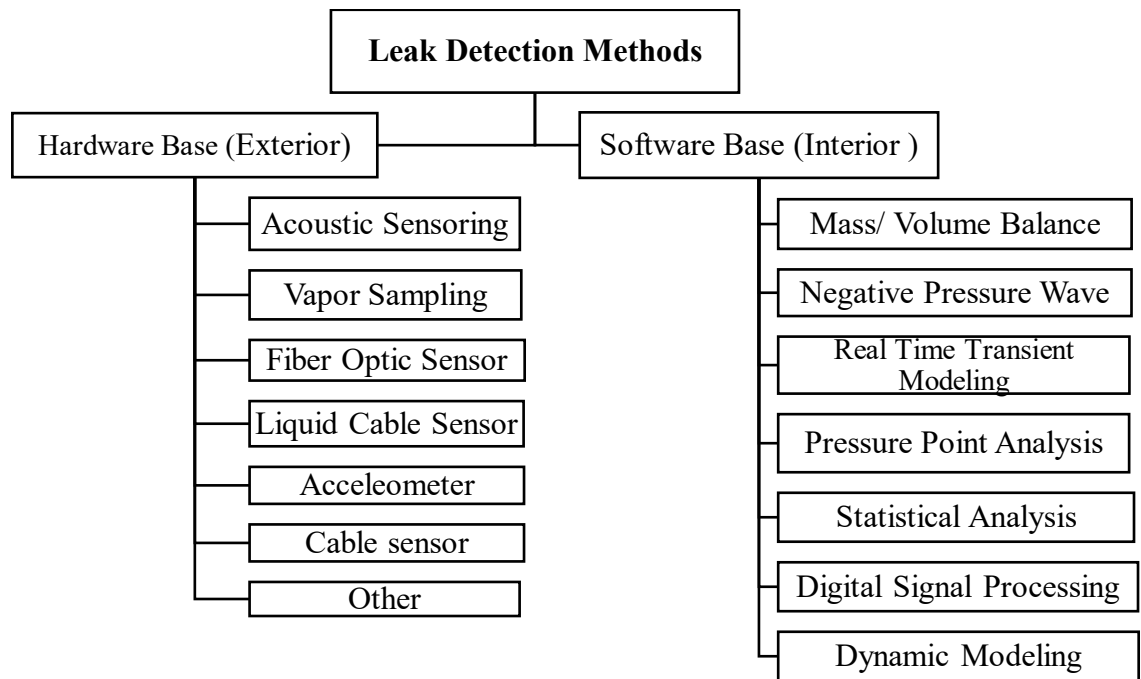


Figure 2. 2 illustrates classifying leak detection systems.

## 2.3 Hardware Base Method

### 2.3.1 Acoustic Sensor Hardware Base Method

Acoustic Emission can be defined according to the American Society of Mechanical Engineering (ASME), which is the “class of phenomena whereby transient elastic waves are generated by the rapid release of energy from localized sources within a material, or the transient waves so generated”<sup>4</sup>. Acoustic based on the fact that when a leak happens, it produces an acoustic noise around the place of leakage. These employ noise or vibration generated as a result of a sudden drop in pressure to detect the occurrence of pipeline leakage.

In this case, the acoustic sensors are installed outside the pipe track and detect the internal noise level and create a baseline with specific features<sup>5</sup>. When a leak occurs, produced low-frequency acoustic signal is detected and investigated. If this signal features different from the baseline signal, an alarm will be activated, and can be concluded that there is a leak in the pipeline based on the change of the baseline signal.

This method can detect small leaks for liquids and gases and has the advantage of both high detection and localization accuracy as well<sup>6</sup>. Most of the work that uses acoustic correlation analysis has been for single-phase liquid systems. The authors in (El-Shiekh 2010) demonstrate the use of acoustic correlation methods pipeline in a vapor-soil environment, and state the acoustic method is only good for lower flow rates, as higher flow rates are contaminated with too much noise<sup>6</sup>.

Acoustic methods enable leaks detection as small as for liquids and gases. The sensors must be located at short distances from one another-not greater than several hundred meters<sup>6</sup>.

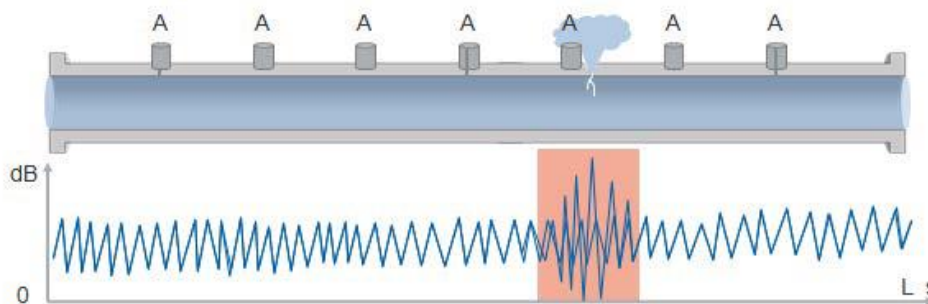


Figure 2. 3 Acoustic leak detection<sup>7</sup>

### 2.3.2 Vapor Sampling Hardware Base Method

In general, Vapor sampling is used to determine the degree of hydrocarbon vapor in the pipeline environment. This method can use a vapor monitoring system or mobile detector. The vapor monitoring system uses a semi-permeable test tube in parallel with the top of the pipeline to be monitored. If the leak occurs the substances to be measured come into contact with the tube in the form of vapor, gas, or dissolved in water. The tube is full of air at atmospheric pressure as shown in the following figure <sup>8</sup>.

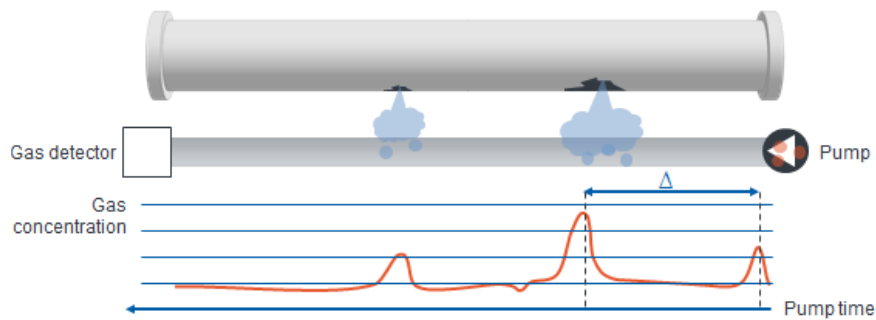


Figure 2. 4 sensor hose system for pipeline leak detection<sup>7</sup>

### 2.3.3 Fiber Optic Hardware Base Method

Fiber Optic Leak Detection Systems are much appropriate to a wide range of single and multiphase liquids and gases pipelines<sup>4</sup>. The fiber optic sensing leak detection method depends on the installation of a fiber optic cable all along the pipeline. The sensors can be installed as a distributed or point sensor to substantially detect the variety of physical and chemical properties of hydrocarbon leakage along the pipelines.

Its principle is as a leak happens in a pipeline the substance inside the pipeline gets in touch with fiber cable. So, the temperature of the cable changes due to this contact. Therefore, the leak could be detected according to the temperature variation in the cable.

Fiber optic sensors have remarkable advantages such as high precision, electromagnetic interference immunity, high sensitivity corrosion resistance, and high reliability. It is noticeable that fiber optic sensors have overcome many conventional difficulties and provide more accurate and steady pipeline monitoring <sup>9</sup>.

Three common distribution of fiber optic technology is used to monitor the pipeline. Distribution Temperature Sensing (DTS), Distribution Acoustic Sensor (DAS), and

Distribution Pressure sensor. Distributed Temperature Sensing (DTS) is one of the most effective solutions based on Fiber Optic cable technology (FOC). FOC itself works as the sensor and data link for the DTS solution. Oil leakage tends to a local temperature increase, but gas leakage will appear to local cooling. DTS uses a temperature analyzing instrument to measure temperature <sup>4</sup>.

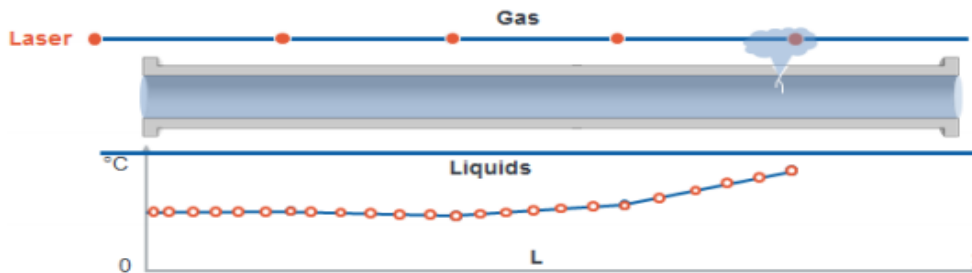


Figure 2. 5 Schematic Representation of Fiber optic application <sup>7</sup>

The advantage of using fiber optic is its insensitivity to electromagnetic interference. However, some drawbacks such as high costs and the stability over time-limited wide range application of this method for pipeline monitoring. This method might be tricky for existing pipelines, as a few pipelines might need to be dug up, to place the optical fiber sensors<sup>3</sup>.

### 2.3.4 Cable Sensor Hardware Base Method

Liquid sensing cables are located or buried close to the pipeline and are specifically designed to reflect variation in transmitted energy pulses as a result of impedance differentials included by contact with hydrocarbon liquid. Safe energy pulses are continuously sent through the cable. The pulses are reflected and a baseline reflection. Fingerprint. Is measured. When a leak occurs, the cable is saturated with fluid, altering the impedance of the sensing cable, which in turn alters the reflection pattern returned. Deviation from the baseline. The fingerprint would signal an alarm. Measuring the time delay between input pulse and reflected pulse enables leak localization. Specific cable types are chosen for each application based on the specific fluid being monitored <sup>8</sup>. This method works well for multiple leak detection and localization for short pipelines.

### **2.3.5 Accelerometer Hardware Base Method**

Accelerometers consider as another type of vibro-acoustic measuring device that is also applicable to monitor low-frequency pipe-shell vibrations. The accelerometer sensor is used to measure the vibrations of noise leakage mostly in a plastic water pipeline by using different sensors to measure the accelerometer. These sensors have different sensitivities to record the vibration signals (acceleration) from leaks <sup>10</sup>.

### **2.3.6 Cable Hardware Base Method**

The cable method is widely used for the detection of leakage of liquid hydrocarbon fuels (such as liquefied petroleum gas). The main principle is to install special leak detection cables this cable can have some sort of physical or chemical reaction with the medium transported by the pipeline along the pipeline when the pipeline is installed. Once the leak occurs, the cable is degraded and converted into an electrical or optical signal output. The leak can be determined by a specific instrument <sup>11</sup>. The advantage of using the cable method is the detection speed is fast and the result is more accurate another benefit that, even small leaks can be detected.

## **2.4 Software Based Method**

### **2.4.1 Mass / Volume Balance Software Based Method**

According to the law of conservation of mass, when there is no leakage in the pipeline, the mass flow of fluid into the pipeline should equal the mass flow out of the pipeline. If a leak happens in the pipeline when the leakage reaches a certain amount, the outlet mass flow rate will decrease, and the inlet flow rate will increase. So, the detection of the input and output flow at multiple points of the pipeline, or the detection of the flow at the pump stations at both ends of the pipeline and the signals are aggregated to form a mass flow balance image<sup>11 7</sup>. Mass or volume balance method do not require to establish the mathematical model of the pipeline. The principle of detection is simple. But the accuracy to detect the small leak size is very less and can discover after a long time. The mass balance method is completely a software system relying on the existing pipeline instrumentation and SCADA system.

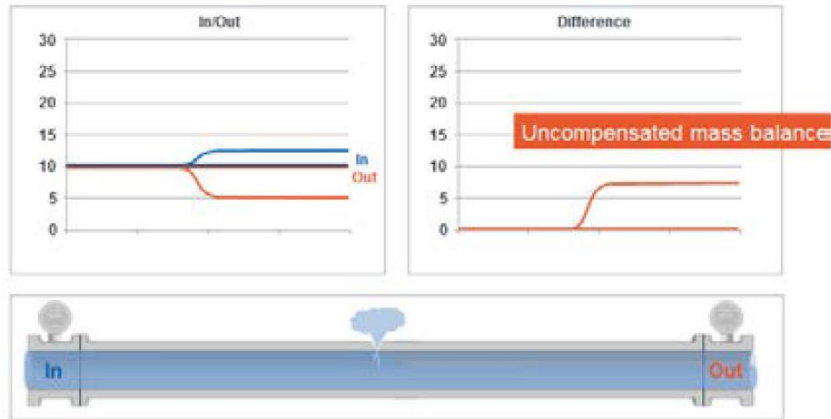


Figure 2. 6 Mass/ Volume Leak Detection Method<sup>7</sup>

#### 2.4.2 Real-Time Transient Monitoring (RTTM) Software Based Method

The main principle of this leak detection technique is based on pipe flow models which are constructed using three fundamental concepts, conservation of mass, conservation of momentum, and conservation of energy.

The difference between the measured value and the estimated value of the flow is used to determine the presence of leaks<sup>3</sup>. For setup, this model flow rate, pressure, and temperature measurements at both ends of the pipeline are necessary to measure. Also, to design a reliable system with minimum false alarm the noise level should be continuously inspected to modify the model<sup>5</sup>.

This method has been successfully applied in underwater environments and can be used to detect leaks of less than 1 percent of flow. Real-Time Transient Monitoring (RTTM) may be a good choice for multi-phase pipelines<sup>7</sup>.

**Conservation of Mass**

$$\frac{d\rho}{dt} + \rho \frac{\partial v}{\partial s} = 0$$

**Conservation of Momentum**

$$\frac{dv}{dt} + \frac{1}{\rho} \frac{\partial p}{\partial s} + f_s = 0$$

**Conservation of Energy**

$$\frac{dh}{dt} - \frac{1}{\rho} \frac{dp}{dt} - I_L = 0$$

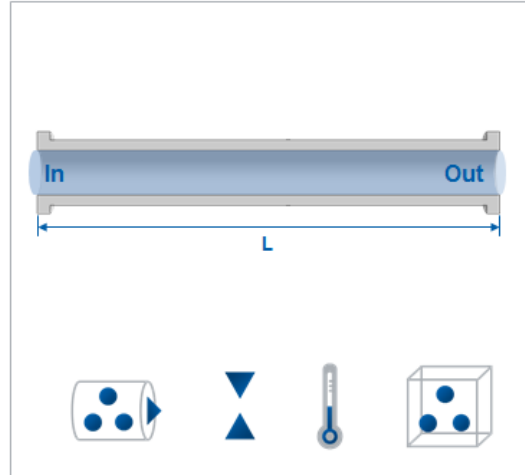


Figure 2. 7 Real-Time Transient Model RTTM <sup>7</sup>.

### 2.4.3 Negative Pressure Wave Software Based Method

Based on that when a pipeline leak happens, the fluid pressure drops suddenly at the position of the leak and creates a negative pressure wave, which propagates with a certain speed (speed of sound) in both pipeline direction.

The sensors located at both ends of the leakage point can detect the leakage location according to the change in the pressure signal and the time difference between the negative pressure wave generated by the leakage and the upstream and downstream waves <sup>11</sup>.

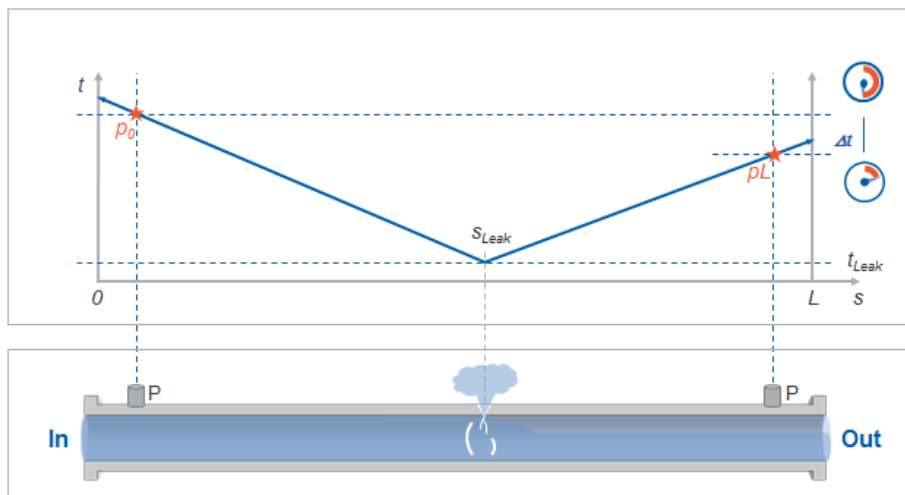


Figure 2. 8 Negative Pressure Wave<sup>7</sup>

To achieve better accuracy the Wave Propagation Method can be expanded by adding more than two pressure gauges as shown in the next figure. Once the leak happens, we obtain additional points in time at which the pressure wave reaches the sensors. By now taking into account the sensor sampling time and the actual fluid density / sound velocity profile the exact point in time at which the pressure wave reaches<sup>7</sup>.

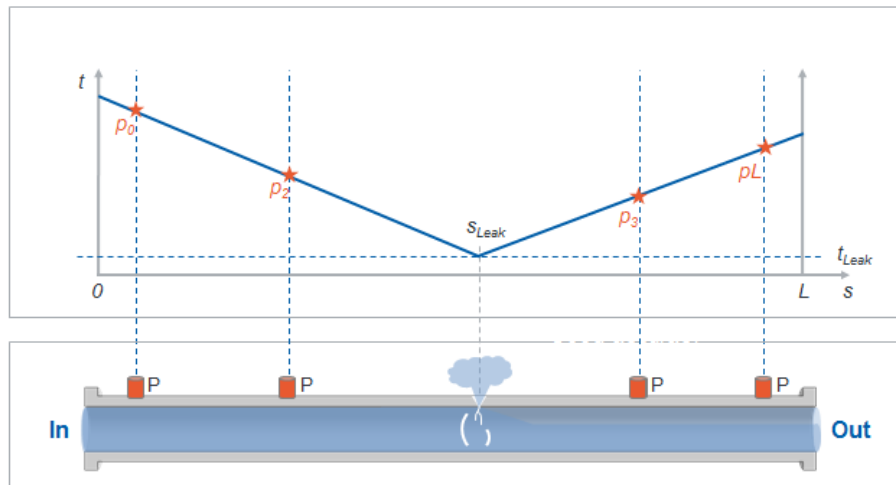


Figure 2. 9 Expanded Wave Propagation <sup>7</sup>

#### 2.4.4 Pressure Point Analysis (PPA) Software Based Method

This method used generally to detect leaks in gases, liquids, and certain multiphase flow pipes. The principle is to determine the rate of change of pressure and flow in pipelines. When the pipeline is in a steady-state, pressure, velocity, and density distributions do not change over time.

Based on the premise that the statistical property of a series of pressure measurements taken on a pipeline are different before and after a leak occurs. The Pressure Point Analysis leak detection system detects leak by comparing current pressure signals with the trend at a point along the pipeline<sup>7</sup>. This method has successfully applied in underwater environments but in the case of multiphase flow will act to dampen the propagation of pressure signals and create considerable background noise due to slugging and other internal flow structures.

#### 2.4.5 Statistical Analysis Software Based Method

The statistical leak detection system uses an advanced statistical technique to analyze the flow rate, pressure, and temperature measurements of a pipeline<sup>5</sup>. This method is

appropriate for complex pipe systems as it can be monitored continuously for continual changes in the line and flow/pressure instruments. Also, this technique could be used for leak localization. Variations generated by operational changes are registered and a leak alarm is generated only when a unique pattern of changes in flow and pressure exists <sup>12</sup>.

Using statistical analysis is also very easy and applicable to different pipeline systems by computer science. But there is some difficulty to detect the leak volume and cost with this method <sup>13</sup>.

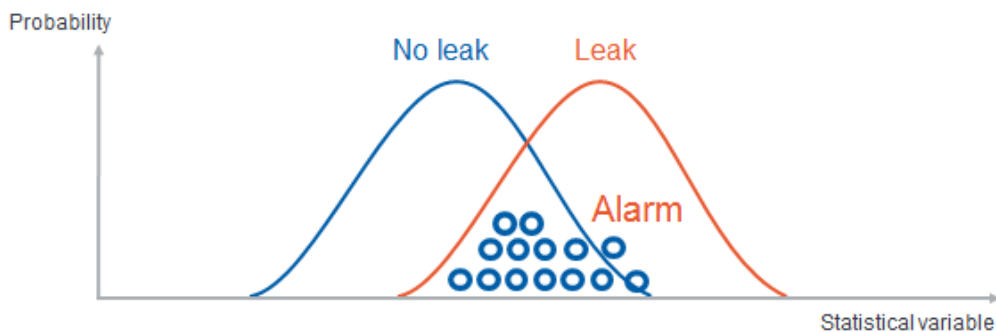


Figure 2. 10 Statistical Analysis <sup>7</sup>

#### 2.4.6 Digital Signal Processing Software Based Method

The principle for this method is based on digital signal processing techniques. The procedure of this method is that the response of the pipeline to a known input is measured over a period of time. Then, this response is compared with the later measurements. Based on a comparison of their signal's features such as frequency response or wavelet transform coefficients a leak alarm could be generated. It is considered more similar to statistical methods this technique does not need a pipeline model. The problem associated with using this method for leak detection is only leak occurrence could be detected not leak presence unless the size of the present leak increases considerably<sup>3</sup>.

#### 2.4.7 Dynamic Modeling Software Based Method

This method based on the mathematical models is formulated to represent the operation of a pipeline system based on physics principles. Dynamic modeling-based pipeline leak systems are gaining considerable attention as they appear to be a promising technique for

the detection of anomalies in both surface and subsea pipeline networks. The detection of leakages using this method is performed from two different points of views:

1. transient
2. statistical.

From the statistical point of view, the system utilizes decision theory based on the assumption that parameters associated with fluid flowing remain constant except in the presence of anomalies along the pipe.

Detection of leakage in pipelines mainly requires the formulation of a mathematical model using fluid flow equations. The equations of state for modeling fluid flow includes the equations of conservation of mass, conservation of momentum, conservations of energy and states of the fluid.

Transient point of view this method requires measurements of flow, temperature, pressure, and other parameters associated with fluid transport at the inlet and outlet of the pipeline or several points along the pipeline. The transient event or noise levels are continuously being monitored using a discrepancy between the measured values and simulated values to detect the occurrence of leakages <sup>14</sup>.

## **2.5 Comparison of Leak Detection Methods.**

The following table summarizes the recent pipeline leak detection method each method can use for specific work conditions such as single-phase flow or multiphase working fluid with the system accuracy and ability of leak method to localize the leak <sup>14111513</sup>.

**Table 2. 1 show the Performance comparison Metric**

Performance comparison Metric								
Technique	Internal or External Method	System Accuracy	Evaluation ability	Leak localization	False Alarm rate	Easy of usage	Cost	Application Working Fluid
Acoustic Sensor	External	High but sensitive with Noise	N/A	Yes	High	Yes	General	OL, GS, GS, OS, GU
Fiber Optical	External	High	Weak	Yes	General	Yes	High	OL, GS, GS, OS, GU
Accelerometer	External	N/A	Weak	N/A	General	Yes	General	GS, OS
Cable sensor	External	Good	Weak	N/A	Low	Yes	High	OL
Mass/ volume balance	Internal	Low, depended on leak size	Weak	No	High	Yes	Low	OL, GS, GS, OS, GU
Negative Pressure wave	Internal	Low	Weak	Yes	High	Yes	General	OL, GS, GS, OS, GU
Real Time Transient Modeling RTTM	Internal	Depend on Mathematical Model	N/A	Yes	Low	Complex need expert	High	N/A
Pressure Point Analysis PPA	Internal	Low	Weak	Yes	High	Yes	General	OL, GS, GS, OS, GU
Statistical	Internal	Medium	N/A	N/A	Low	Not easy	High	N/A
Dynamic	Internal	High, depends on Metaethical Model	N/A	Yes	General	No	N/A	N/A

## Chapter 3. Sensitivity Analysis

### 3. Flow Regimes for Horizontal Pipeline

There are many types of flow patterns/regimes that can happen in two-phase flow or three-phase flow, depending on the flow parameters that include pipe diameter, flow rate and velocity<sup>16</sup>. For flow regime analysis, several flow patterns maps have been proposed. *Taitel and Dukler* dimensionless flow regime map 1976.

#### Bubble Flow

It occurs at very low gas/liquid ratios where the gas forms bubbles at that the top of the pipe. However, when shear forces are dominant, the uniform distribution of bubbles might occur in the pipe.

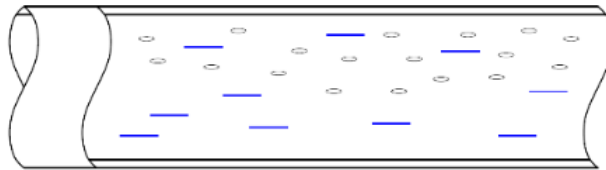


Figure 3. 1 Shows the bubble flow regime for horizontal pipeline<sup>17</sup>

#### Stratified Flow

The gas and liquid phases flow separately one on top of the other at low gas and liquid velocity. The liquid flows along the bottom of the pipe while the gas flows in the top section of the pipe.

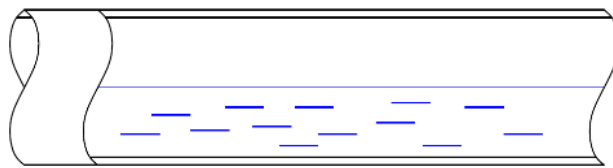


Figure 3. 2 Shows the stratified flow regime for horizontal pipeline<sup>17</sup>

#### Wavy Flow

The gas velocity increase in stratified flow creates a wave on the interface in the flow direction. The amplitude of the wave depends on the relative velocity (slip ratio) but it normally does not touch the upper side of the pipe wall.

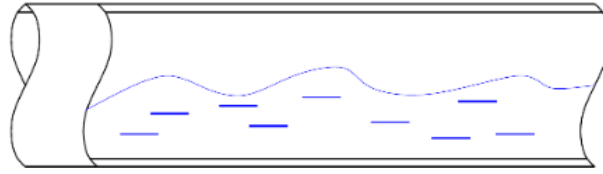


Figure 3. 3 Shows the wavy flow regime for horizontal pipeline<sup>17</sup>

### Slug Flow

Large amplitude waves or splashes of liquid occasionally pass through the upper side of the pipe when there is a high gas velocity than the average liquid velocity. Slug flow can cause sudden pressure pulses and vibrations in the pipelines.

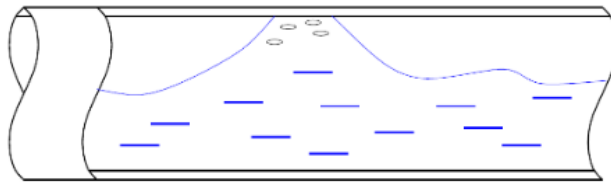


Figure 3. 4 Shows the slug flow regime for horizontal pipeline<sup>17</sup>

### Annular Flow

The liquid phase forms a continuous film around the inside wall of the pipe and the gas flows in the central core with higher velocity. Due to the effect of gravity, usually, the liquid film is thicker at the bottom of the pipe in horizontal flows.

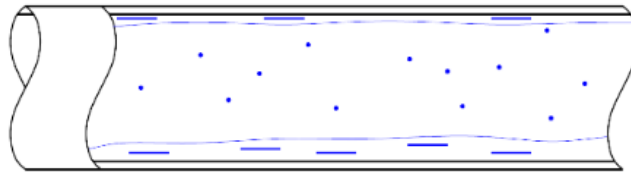


Figure 3. 5 Shows the Annular flow regime for horizontal pipeline<sup>17</sup>

Usually, at certain points, the flow regime transition can create unfavorable flow conditions when a slug of water travels at the high velocity of the gas stream. Slug flow should be avoided in the fluid transmission lines since it negatively impacts both the equipment and pipeline integrity. Slug flow may cause fatigue that can reduce pipe strength and cause severe damage in pipe support structures <sup>16</sup>.

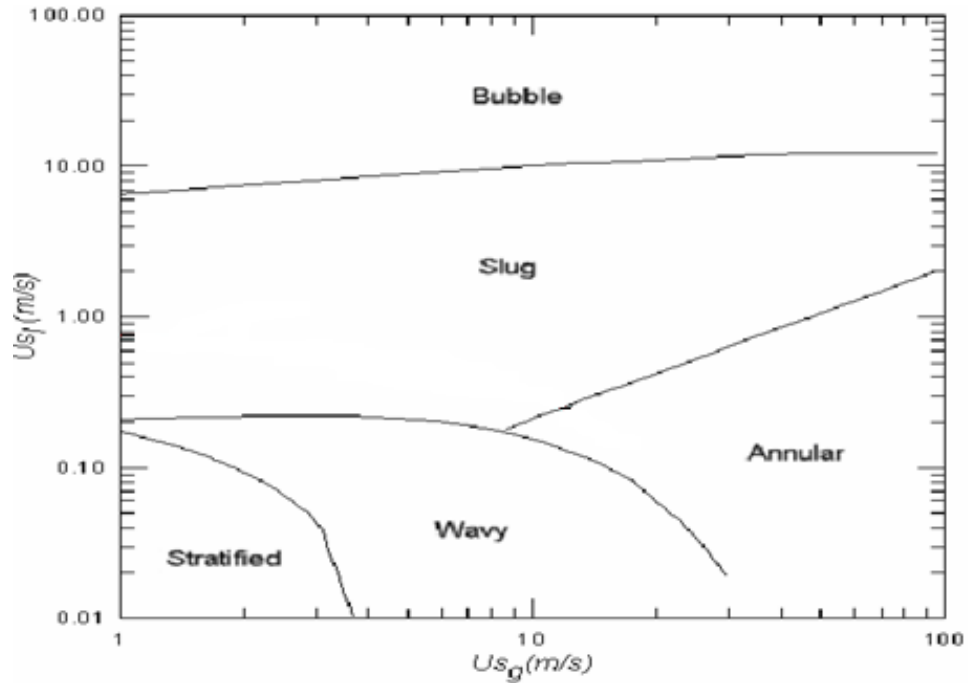


Figure 3. 6 Taitel and Dukler dimensionless flow regime map 1976 <sup>18</sup>

### 3.1 Entrance Length for Horizontal Pipeline

In the oil industry, complex multiphase mixtures consisting of oil, gas, water, and possibly precipitated solids and or formation sand may flow through the tubing with different flow regimes observed.

When uniform flow enters the circular tube, a boundary layer begins to develop along the pipe due to the effect of viscosity. The boundary layer thickness gradually grows to reach the completely sectional area of the pipe and then the flow is fully developed.

#### 3.1.1 Entrance Length for Single Phase Liquid

The length of the hydrodynamic entry region along the pipe is called the hydrodynamic entry length <sup>19</sup>. It is a function of Reynolds number of the flow. In the case of laminar flow, this length is given by:

$$L_e = 0.06 R_e D \quad \text{Eq (1)}$$

Where,  $R_e$  is Reynold's number and  $D$  is the diameter of the pipe

While in turbulent flow the equation changes as the following.

$$L_e = 4.4D R_e^{1/6} \quad \text{Eq (2)}$$

Thus, the entry length in turbulent flow is much shorter as compared to laminar one<sup>19</sup>. In most practical engineering applications, this entrance effect becomes insignificant beyond a pipe length of 10 times the diameter and hence it is approximated to be.

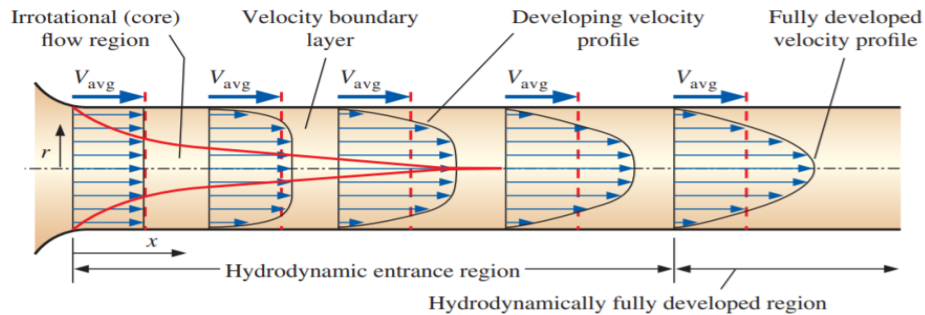


Figure 3. 7 The development of the velocity boundary layer in a pipe. (The developed average velocity profile is parabolic in laminar flow, as shown, but much flatter or fuller in a turbulent flow.)<sup>20</sup>

The speed of a fluid inside a pipe is distributed in a quadratic manner, where the maximum speed is in the center of the pipe and the minimum speed at the boundary to the pipe itself. Frictional forces slow down the molecules closest to the stationary pipe.

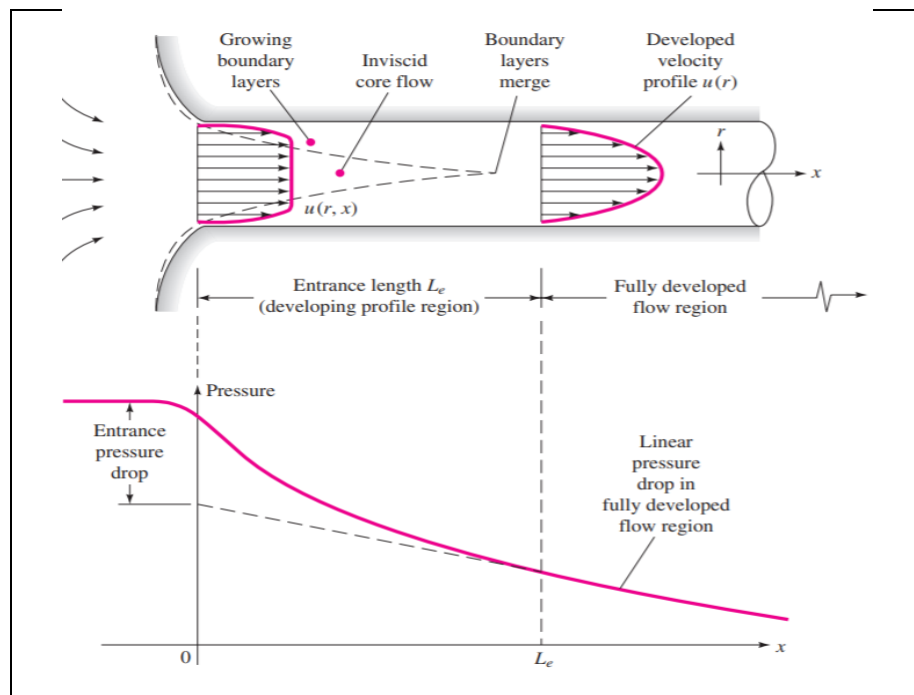


Figure 3. 8 Developing velocity profiles and pressure changes in the entrance of a duct flow<sup>19</sup>

### 3.1.2 Entrance Length for Single Phase Air

Since the very early time there have been a lot of efforts resulted in a variety of designs as pipe inserts to obtain fully developed flow in a short pipe length. This experimental work shows the tube bundle, a Laws' perforated plate, and an etoile were located at the entrance of a smooth circular pipe of inner diameter 26.6 mm. The laminar flow inside the pipe without an insert in the range of  $Re < 2450$  only<sup>21</sup>. The following formula shows the laminar equation has been used for this study.

$$L_e = 0.08 D Re + 0.70 D \quad \text{Eq (3)}$$

**Table 3. 1 shows the minimum required entrance lengths for fully developed laminar** <sup>21</sup>.

Reynold Number ( $R_e$ )	Entrance Length ( $L_e$ )	X/D
2000	4.27	160.70
938	2.01	75.56
704	1.52	57.14
547	1.18	44.36

### Calculation of the single-phase Air and Liquid as working fluid

The following calculation was performed for the different three proposed pipeline sizes 2,3 and 5.5 -inches. The working fluid is water single-phase then Air single-phase flow takes in consideration the calculation of Reynold number with different velocities according to Taitel & Dukler dimensionless flow regime map (1976) as a minimum and maximum velocities. The temperature and operation are constant <sup>22</sup>.

$$R_e = \frac{\text{Density} * \text{Velocity} * \text{Diamter}}{\text{Viscosity of Fluid}} \quad \text{Eq (4)}$$

If the Reynold number  $R_e > 4000$  the flow will be turbulent flow and  $R_e < 2000$  the flow is called laminar flow. The entrance length calculated by using equation (1) and (2) for turbulent and laminar flow.

**Table 3. 2 shows the entrance length summary for single-phase Air and Water**

<b>ID (inch)</b>	<b>ID (m)</b>	<b>Re</b>	<b>Velocity (m/s)</b>	<b>Density (kg/m<sup>3</sup>)</b>	<b>Le (inch)</b>	<b>Le (m)</b>
<b>Single-phase Air</b>						
2	0.051	2.6E+04	1	9.3476	45	1.14
3	0.077	4.0E+04	1	9.3476	72	1.84
4.5	0.114	5.9E+04	1	9.3476	115	2.92
5.5	0.140	7.2E+04	1	9.3476	145	3.68
<b>Single-phase Air</b>						
2	0.051	2.62E+05	10	9.3476	65	1.65
3	0.077	3.96E+05	10	9.3476	104	2.65
4.5	0.114	5.90E+05	10	9.3476	166	4.22
5.5	0.140	7.21E+05	10	9.3476	209	5.32
<b>Single-phase Air</b>						
2	0.051	1.3E+06	50	9.3476	84	2.13
3	0.077	2.0E+06	50	9.3476	135	3.43
4.5	0.114	2.95E+06	50	9.3476	215	5.45
5.5	0.140	3.6E+06	50	9.3476	271	6.88
<b>Single-phase Water</b>						
2	0.051	1.1E+03	0.02	996.7	27	0.69
3	0.077	1.7E+03	0.02	996.7	44	1.11
4.5	0.114	2.6E+03	0.02	996.7	69	1.77
5.5	0.140	3.1E+03	0.02	996.7	88	2.23
<b>Single-phase Water</b>						
2	0.051	5.7E+05	10	996.7	73	1.86
3	0.077	8.6E+05	10	996.7	118	3.00
4.5	0.114	1.3E+06	10	996.7	188	4.77
5.5	0.140	1.6E+06	10	996.7	237	6.02
<b>Single-phase Water</b>						
2	0.051	2.8E+06	50	996.7	95	2.41
3	0.077	4.3E+06	50	996.7	153	3.89
4.5	0.114	6.4E+06	50	996.7	243	6.17
5.5	0.140	7.8E+06	50	996.7	307	7.79

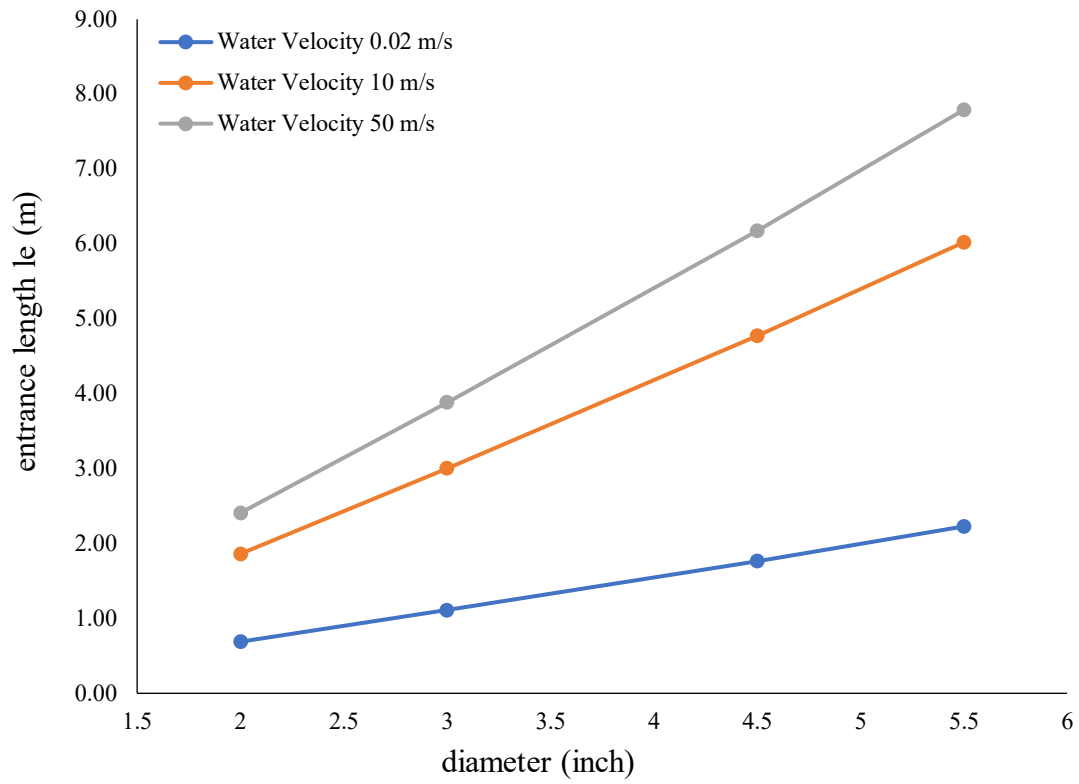


Figure 3. 9 shows the change in entrance of length with a diameter at different velocity for single-phase water

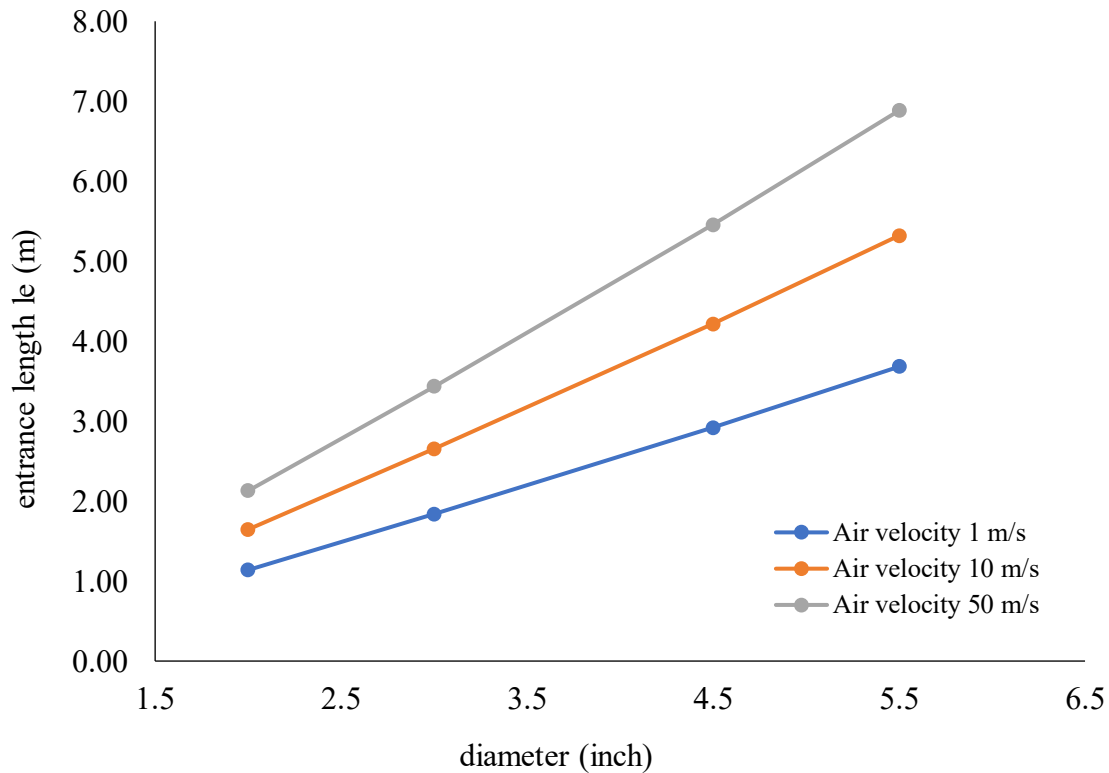


Figure 3. 10 shows the change in entrance of length with a diameter at different velocity for single-phase Air

Can conclude that the development entrance length ( $L_e$ ) increases with the increase of pipe diameter and decreases with the decrease in pipeline diameter. Also, can be noted that in the water flow when the Reynold number is between 2000 and 4000 in the transition zone the equation gives the wrong estimation for the length development calculation. Therefore, the Turbulent equation is used to calculate the Transition zone in this case because the laminar equation is not recommended here and gives the wrong estimation for  $L_e$ .

From the single-phase graphs air and water can conclude the following:

1. Velocity has a big impact on the entrance of length calculation for both air and water single-phase while the  $L_e$  increase with an increase in velocity of the fluid at all the diameter sizes.
2. The density has a minor effect on  $L_e$ . The change in entrance of length for both air and liquid is very small even after considering the change in velocity.
3. When pipeline diameter increases the entrance of length  $L_e$  increase as well.

**Table 3. 3 shows the entrance length summary for single-phase Air and Water with a change in air and water density.**

<b>ID (inch)</b>	<b>ID (m)</b>	<b>Re</b>	<b>Velocity (m/s)</b>	<b>Density (kg/m<sup>3</sup>)</b>	<b>L<sub>e</sub> (inch)</b>	<b>L<sub>e</sub> (m)</b>
<b>Single-phase Air</b>						
2	0.051	1.3E+04	1	4.5	40	1.01
3	0.077	1.9E+04	1	4.5	64	1.63
4.5	0.114	2.8E+04	1	4.5	102	2.59
5.5	0.140	3.5E+04	1	4.5	129	3.27
<b>Single-phase Air</b>						
2	0.051	1.26E+05	10	4.5	58	1.46
3	0.077	1.91E+05	10	4.5	93	2.36
4.5	0.114	2.84E+05	10	4.5	148	3.75
5.5	0.140	3.47E+05	10	4.5	186	4.73
<b>Single-phase Air</b>						
2	0.051	6.3E+05	50	4.5	75	1.89
3	0.077	9.5E+05	50	4.5	120	3.05
4.5	0.114	1.42E+06	50	4.5	191	4.85
5.5	0.140	1.7E+06	50	4.5	241	6.12
<b>Single-phase Water</b>						
2	0.051	1.4E+03	0.02	1200	28	0.71
3	0.077	2.1E+03	0.02	1200	45	1.14
4.5	0.114	3.1E+03	0.02	1200	72	1.82
5.5	0.140	3.8E+03	0.02	1200	90	2.30
<b>Single-phase Water</b>						
2	0.051	6.8E+05	10	1200	76	1.92
3	0.077	1.0E+06	10	1200	122	3.09
4.5	0.114	1.5E+06	10	1200	194	4.92
5.5	0.140	1.9E+06	10	1200	244	6.20
<b>Single-phase Water</b>						
2	0.051	3.4E+06	50	1200	98	2.48
3	0.077	5.2E+06	50	1200	158	4.00
4.5	0.114	7.7E+06	50	1200	250	6.36
5.5	0.140	9.4E+06	50	1200	316	8.03

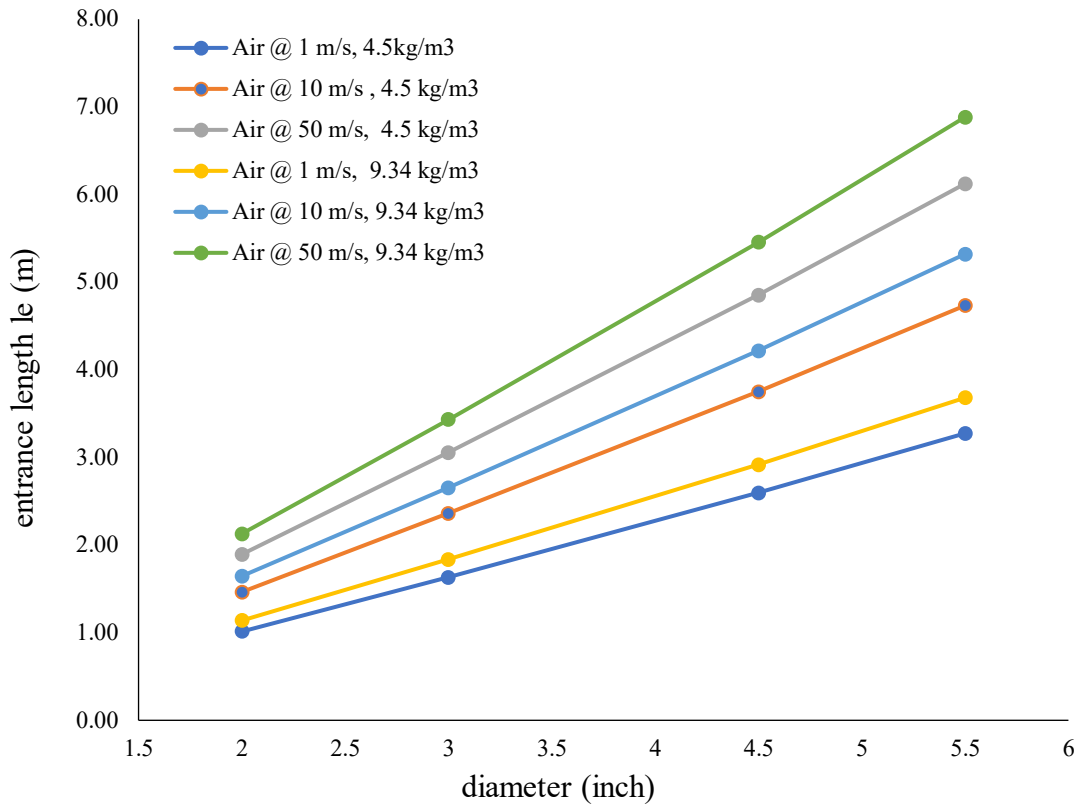


Figure 3. 11 shows the change in entrance of length with different air density

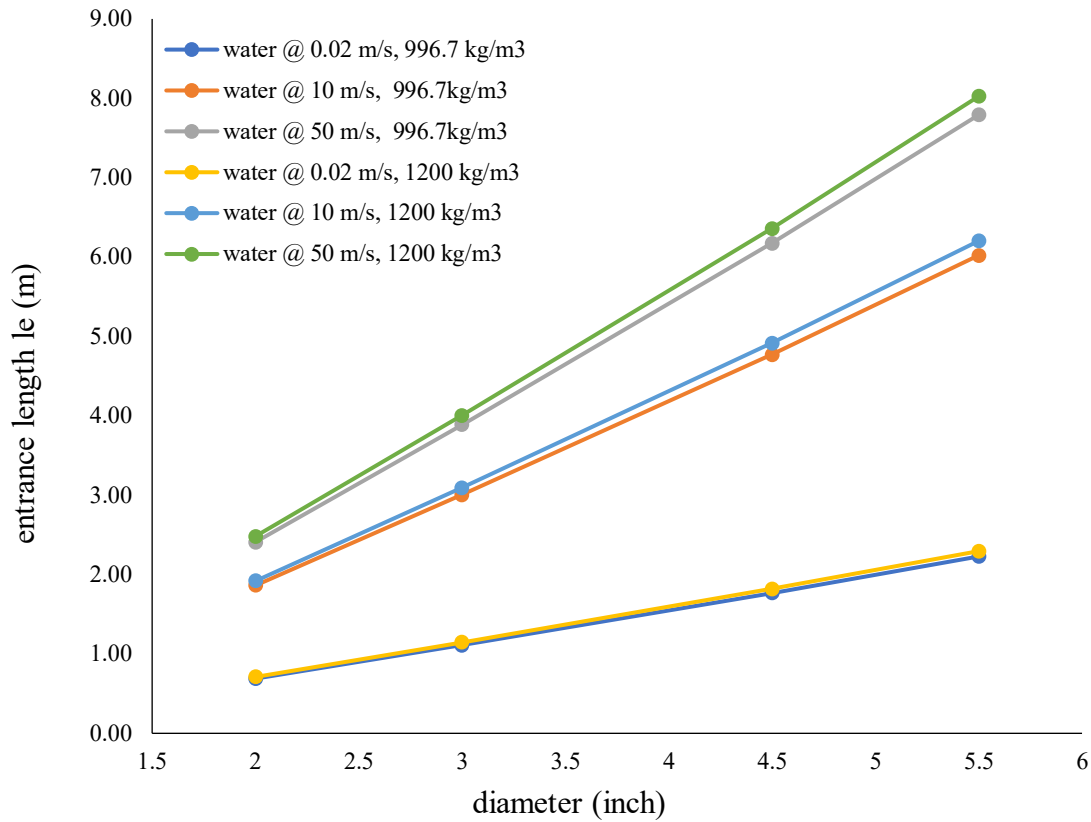


Figure 3. 12 shows the change in entrance of length with different water density

Table 3. 4 shows the entrance length summary for single-phase Air and Water with a change in air and water viscosity.

ID (inch)	ID (m)	Re	Velocity (m/s)	Viscosity (pa.s)	Le (inch)	Le (m)
<b>Single-phase Air</b>						
2	0.051	6.8E+05	1	9.00E-06	50	1.27
3	0.077	1.0E+06	1	9.00E-06	81	2.05
4.5	0.114	1.5E+06	1	9.00E-06	128	3.26
5.5	0.140	1.9E+06	1	9.00E-06	162	4.12
<b>Single-phase Water (996.7 kg/m3)</b>						
2	0.051	3.42E+06	10	9.00E-06	72	1.84
3	0.077	5.17E+06	10	9.00E-06	117	2.97
4.5	0.114	7.71E+06	10	9.00E-06	186	4.71
5.5	0.140	9.42E+06	10	9.00E-06	234	5.95
<b>Single-phase Water (1200 kg/m3)</b>						
2	0.051	0.0E+00	50	9.00E-06	94	2.38
3	0.077	0.0E+00	50	9.00E-06	151	3.84

4.5	0.114	0.00E+00	50	9.00E-06	240	6.10
5.5	0.140	0.0E+00	50	9.00E-06	303	7.70
<b>Single-phase Water</b>						
2	0.051	4.5E+00	0.02	5.40E-04	29	0.75
3	0.077	3.0E+00	0.02	5.40E-04	47	1.20
4.5	0.114	2.0E+00	0.02	5.40E-04	75	1.91
5.5	0.140	5.5E+00	0.02	5.40E-04	95	2.41
<b>Single-phase Air</b>						
2	0.051	6.8E+05	10	5.40E-04	79	2.02
3	0.077	7.7E-02	10	5.40E-04	128	3.25
4.5	0.114	5.1E-02	10	5.40E-04	203	5.17
5.5	0.140	1.4E-01	10	5.40E-04	257	6.52
<b>Single-phase Water</b>						
2	0.051	3.4E+06	50	5.40E-04	103	2.61
3	0.077	3.0E+06	50	5.40E-04	166	4.21
4.5	0.114	8.6E+05	50	5.40E-04	263	6.69
5.5	0.140	7.8E+06	50	5.40E-04	332	8.44

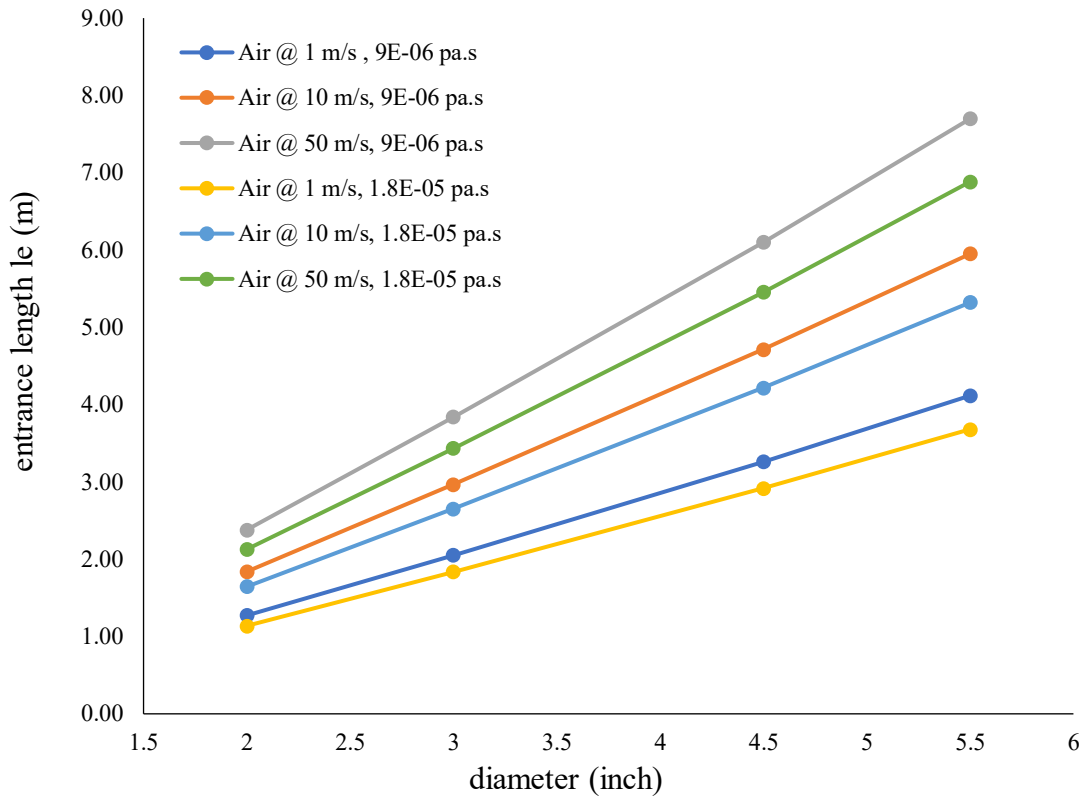


Figure 3. 13 shows the change in entrance of length with different air viscosity

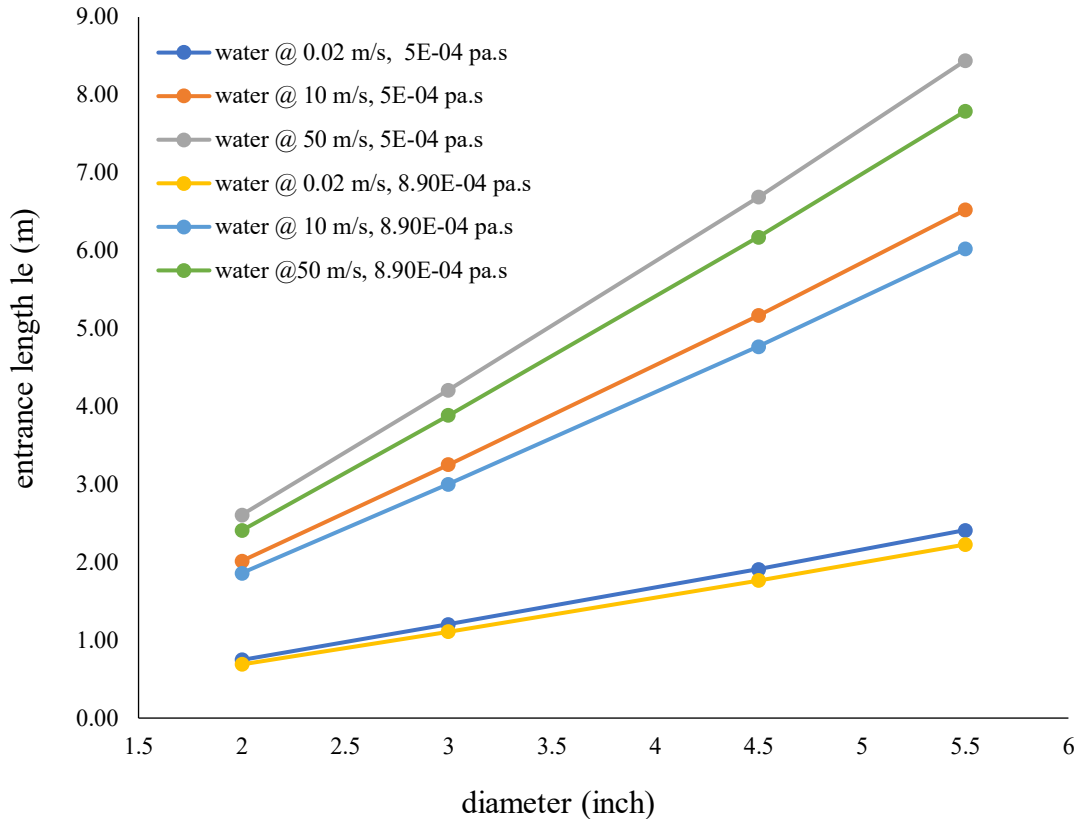


Figure 3. 14 shows the change in entrance of length with different water viscosity

### 3.2 Entrance Length for Two-Phase Flow

The two-phase flow can be water and air or water and solid. Transport of slurries through pipelines is been common throughout the world. Over the decades, the flow of slurries through pipelines had been a common practice for various industries such as oil and gas. Many factors affect the slurry behavior flow in the pipeline include particle size, velocity profile, frictional pressure loss, and concentration profile.

Since the last studies have suggested many empirical correlations to calculate the slurry flow behavior. Nonetheless, the capability of these correlations is limited to some data range and experimental setup especially the effect of length development<sup>23</sup>.

In this study will use the same equation (2) for the entrance of length calculation only for turbulent flow and consider the mixture viscosity effect and mixture density will be included as well to perform a sensitivity analysis.

### 3.2.1 Mixture Density

The density of slurry is a function of some variables: the density of the solid particles, the density of the liquid, the concentration of the solid phase by volume. The density of the slurry could be calculated with the following equation <sup>24</sup>.

$$\rho_m = C_{v,s} \rho_s + C_{v,f} \rho_f \quad \text{Eq (5)}$$

Where:

$C_v$ : Solids volume concentration (v/v).

$\rho_f$ : Fluid Density (kg/m<sup>3</sup>).

$\rho_s$ : Density of solid particles in mixture (kg/m<sup>3</sup>).

The density of the solid particles is determined through many experimental methods. For some materials, density also is a function of particle size, due to their packing ability. Due to the precipitation of particles in heterogeneous suspensions, the measurements of density are performed after intensive mixing. Otherwise, the results of the measurement will be incorrect <sup>23</sup>.

### 3.2.2 Mixture Viscosity

The shear stress is proportional to the shear rate and the constant of proportionality is the coefficient of viscosity, but it is only for Newtonian fluids.

Viscosity is a constant parameter if temperature and pressure are constant too. Non-Newtonian fluids do not obey this rule. Absolute (dynamic) viscosity for Newtonian slurries could be determined by using some equations given below.

*Absolute viscosity of mixtures with volume concentration smaller than 1%.* For these diluted slurries Einstein created the following equation for the viscosity of laminar slurry<sup>23</sup>:

$$\mu_m = \mu_L (1 + 2.5 C_v) \quad \text{Eq (6)}$$

Where:

$\mu_m$ : Absolute (dynamic) viscosity of the slurry mixture.

$\mu_L$ : Absolute viscosity of a liquid phase.

$\Phi$ : Total solid volume fraction ( $\phi = C_v / 100$ ).

$C_v$ : Solids concentration by volume (%).

This equation is based on the assumption that solid particles are sufficiently rigid and there is almost no interaction between them, due to dilute solution.

Absolute viscosity of mixtures with volume concentration smaller than 20%. To calculate the viscosity of more concentrated solutions of Newtonian slurries, it is possible to use a modified following Einstein equation<sup>25</sup>. In this equation, the interactions between solid particles in the solution were taken into account<sup>23</sup>.

$$\mu_m = \mu_L (1 + 2.5 \Phi + 14.1 \Phi^2) \quad \text{Eq (7)}$$

Absolute viscosity of mixtures with high volume concentration of solids. Thomas suggested the following equation with an exponential function for calculating the viscosity of slurry with a high concentration of solid particles<sup>26</sup>:

$$\mu_m = \mu_L (1 + 2.5 \Phi + 10.05 \Phi^2 + 0.00273 e^{16.6 \Phi}) \quad \text{Eq (8)}$$

### 3.3 Entrance Length for Multiphase Flow

The multiphase fluid flow development is important and has generated a lot of controversy in the literature. According to Brennen,<sup>1</sup> in single-phase flow, it is well established that an entrance length of 30D to 50D is necessary to create a fully developed flow for turbulent regime<sup>27</sup>.

Another estimation for the multiphase flow developing region calculation by using the same equation for a single-phase, but with mixture properties and consider different fractions for gas, liquid and solid.

$$Re_m = \frac{\rho_m U_m}{\mu_m} \quad \text{Eq (9)}$$

$$U_m = U_{sL} + U_{sg} \quad \text{Eq (10)}$$

$$\rho_m = \rho_l \lambda_L + \rho_g (1 - \lambda_L) \quad \text{Eq (11)}$$

$$\mu_m = \mu_l \lambda_L + \mu_g(1 - \lambda_L) \quad \text{Eq (12)}$$

Where:

$Re_m$ : mixture Reynold number

$\rho_m$ : mixture density

$U_m$ : mixture superficial velocity

$\mu_m$ : mixture Viscosity

$\lambda$ : Fraction of fluid

### 3.4 Entrance Length Calculation for Two-Phase (water and Air)

To perform the entrance of length for two-phase flow have to consider the mixture properties for both fluids. By using the mixture properties equation for Reynold number equation (9) and for mixture density using equation (11) and consider the mixture velocity and viscosity equations (10,12) respectively.

Table 3. 5 shows the original liquid and gas viscosity

water viscosity (pa.s)	Gas viscosity (pa.s)	Gas Fraction	Water Fraction	Mixture viscosity (pa.s)
8.90E-04	1.81E-05	0.3	0.7	6.28E-04
8.90E-04	1.81E-05	0.7	0.3	2.80E-04
8.90E-04	1.81E-05	0.5	0.5	4.54E-04
8.90E-04	1.81E-05	0.1	0.9	8.03E-04
8.90E-04	1.81E-05	0.9	0.1	1.05E-04

Table 3. 6 shows the original liquid and gas density

Water Density (kg/m <sup>3</sup> )	Gas Density (kg/m <sup>3</sup> )	Gas Fraction	Water Fraction	Mixture Density (kg/m <sup>3</sup> )
996.7	4.68	0.3	0.7	699.1
996.7	4.68	0.7	0.3	302.3
996.7	4.68	0.5	0.5	500.7
996.7	4.68	0.9	0.1	103.9
996.7	4.68	0.1	0.9	897.5

Table 3. 7 shows homogenous velocity for liquid and gas 20 m/s two-phase entrance length summary.

ID (inch)	ID (m)	Liquid Hold up	Gas Hold up	Mixture $R_e$	Velocity (m/s)	Mixture Density (kg/m <sup>3</sup> )	$L_e$ (inch)	$L_e$ (m)
<b>Two Phase Air and Water</b>								
2	0.051	0.7	0.3	1.1E+06	20	699.1	82	2.08
3	0.077	0.7	0.3	1.7E+06	20	699.1	132	3.35
4.5	0.114	0.7	0.3	2.5E+06	20	699.1	210	5.33
5.5	0.140	0.7	0.3	3.1E+06	20	699.1	265	6.72
<b>Two Phase Oil and Water</b>								
2	0.051	0.3	0.7	1.10E+06	20	302.3	81	2.07
3	0.077	0.3	0.7	1.66E+06	20	302.3	131	3.34
4.5	0.114	0.3	0.7	2.47E+06	20	302.3	209	5.30
5.5	0.140	0.3	0.7	3.02E+06	20	302.3	263	6.69
<b>Two Phase Gas and Water</b>								
2	0.051	0.5	0.5	1.1E+06	20	500.7	82	2.1
3	0.077	0.5	0.5	1.7E+06	20	500.7	132	3.3
4.5	0.114	0.5	0.5	2.52E+06	20	500.7	209	5.32
5.5	0.140	0.5	0.5	3.1E+06	20	500.7	264	6.71
<b>Two Phase Gas and Oil</b>								
2	0.051	0.9	0.1	1.1E+06	20	897.5	82	2.08
3	0.077	0.9	0.1	1.7E+06	20	897.5	132	3.36
4.5	0.114	0.9	0.1	2.6E+06	20	897.5	206	5.22
5.5	0.140	0.9	0.1	3.1E+06	20	897.5	265	6.73
<b>Two Phase Gas and Air</b>								
2	0.051	0.1	0.9	1.0E+06	20	103.9	80	2.04
3	0.077	0.1	0.9	1.5E+06	20	103.9	129	3.29
4.5	0.114	0.1	0.9	2.3E+06	20	103.9	206	5.22
5.5	0.140	0.1	0.9	2.8E+06	20	103.9	260	6.59

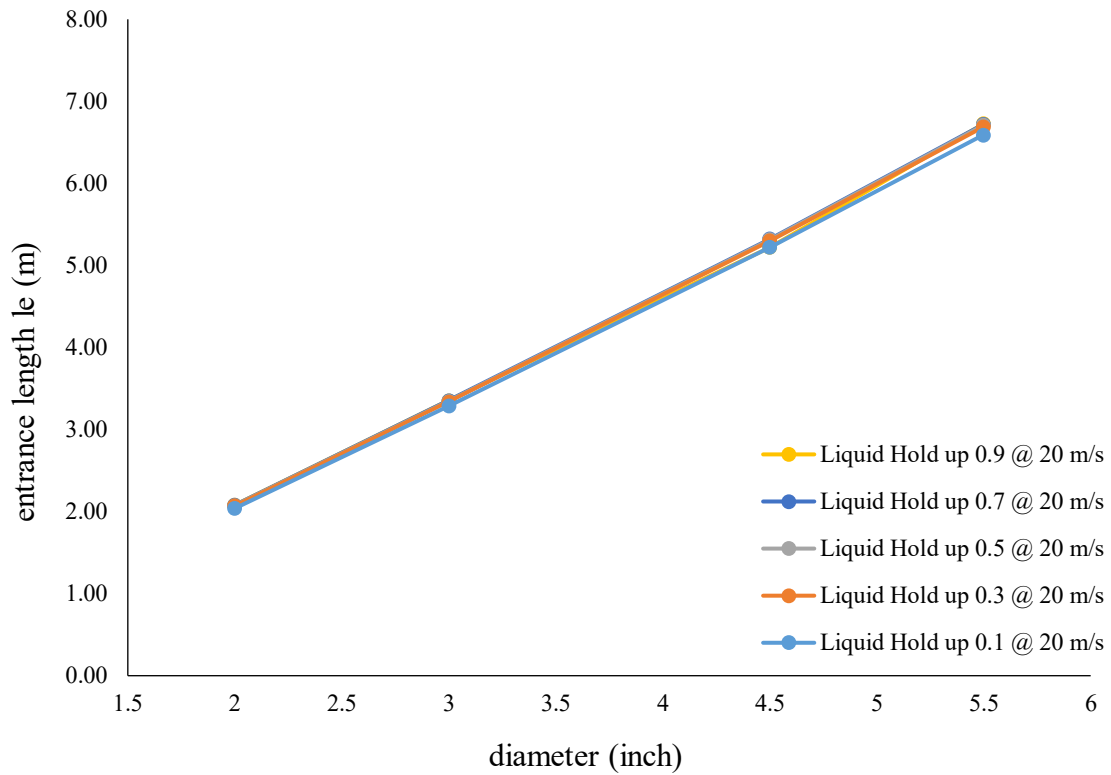


Figure 3. 15 shows a change in entrance of length with different liquid hold up at homogenous velocity 20 m/s

Table 3. 8 shows the change in velocity for two-phase with liquid and gas hold up 0.7, 0.3 respectively entrance length summary.

ID (inch)	ID (m)	Liquid Hold up	Gas Hold up	Mixture $R_e$	Velocity (m/s)	Mixture Density ( $kg/m^3$ )	$L_e$ (inch)	$L_e$ (m)
<b>Two-Phase Air and Water</b>								
2	0.051	0.7	0.3	2.3E+06	40	699.1	91	2.3
3	0.077	0.7	0.3	3.4E+06	40	699.1	147	3.7
4.5	0.114	0.7	0.3	5.09E+06	40	699.1	234	5.95
5.5	0.140	0.7	0.3	6.2E+06	40	699.1	296	7.51
2	0.051	0.3	0.7	2.2E+06	40	302.3	91	2.31
3	0.077	0.3	0.7	3.3E+06	40	302.3	147	3.73
4.5	0.114	0.3	0.7	4.9E+06	40	302.3	233	5.92
5.5	0.140	0.3	0.7	6.0E+06	40	302.3	294	7.48

2	0.051	0.7	0.3	4.5E+06	80	699.1	102	2.60
3	0.077	0.7	0.3	6.8E+06	80	699.1	165	4.19
4.5	0.114	0.7	0.3	1.0E+07	80	699.1	262	6.65
5.5	0.140	0.7	0.3	1.2E+07	80	699.1	330	8.39
2	0.051	0.3	0.7	4.4E+06	80	302.3	102	2.58
3	0.077	0.3	0.7	6.6E+06	80	302.3	164	4.17
4.5	0.114	0.3	0.7	9.9E+06	80	302.3	261	6.62
5.5	0.140	0.3	0.7	1.2E+07	80	302.3	329	8.35

Table 3. 9 shows the change in velocity for two-phase with liquid and gas hold up 0.9, 0.1 respectively entrance length  $L_e$  summary.

ID (inch)	ID (m)	Liquid Hold up	Gas Hold Up	Mixture $R_e$	Velocity (m/s)	Mixture Density (kg/m <sup>3</sup> )	$L_e$ (inch)	$L_e$ (m)
<b>Two-Phase Air and Water</b>								
2	0.051	0.9	0.1	2.3E+06	40	897.5	92	2.3
3	0.077	0.9	0.1	3.4E+06	40	897.5	148	3.7
4.5	0.114	0.9	0.1	9.02E+06	40	897.5	234	5.95
5.5	0.140	0.9	0.1	6.2E+06	40	897.5	290	7.37
2	0.051	0.1	0.9	2.0E+06	40	103.9	90	2.28
3	0.077	0.1	0.9	3.0E+06	40	103.9	145	3.67
4.5	0.114	0.1	0.9	4.5E+06	40	103.9	230	5.84
5.5	0.140	0.1	0.9	5.5E+06	40	103.9	290	7.37
2	0.051	0.9	0.1	4.5E+06	80	897.5	102	2.60
3	0.077	0.9	0.1	6.9E+06	80	897.5	165	4.19
4.5	0.114	0.9	0.1	1.0E+07	80	897.5	262	6.65
5.5	0.140	0.9	0.1	1.2E+07	80	897.5	331	8.40
2	0.051	0.1	0.9	4.0E+06	80	103.9	100	2.55
3	0.077	0.1	0.9	6.1E+06	80	103.9	162	4.11
4.5	0.114	0.1	0.9	9.0E+06	80	103.9	257	6.52
5.5	0.140	0.1	0.9	1.1E+07	80	103.9	324	8.23

**Table 3. 10 shows the change in velocity for two-phase with liquid and gas hold up 0.5, 0.5 respectively entrance length  $L_e$  summary.**

Two-Phase Air and Water								
2	0.051	0.5	0.5	2.24E+06	40	500.7	91	2.32
3	0.077	0.5	0.5	3.38E+06	40	500.7	147	3.74
4.5	0.114	0.5	0.5	5.04E+06	40	500.7	234	5.94
5.5	0.140	0.5	0.5	6.16E+06	40	500.7	295	7.50
2	0.051	0.5	0.5	4.5E+06	80	500.7	102	2.6
3	0.077	0.5	0.5	6.8E+06	80	500.7	165	4.2
4.5	0.114	0.5	0.5	1.01E+07	80	500.7	261	6.64
5.5	0.140	0.5	0.5	1.2E+07	80	500.7	330	8.38

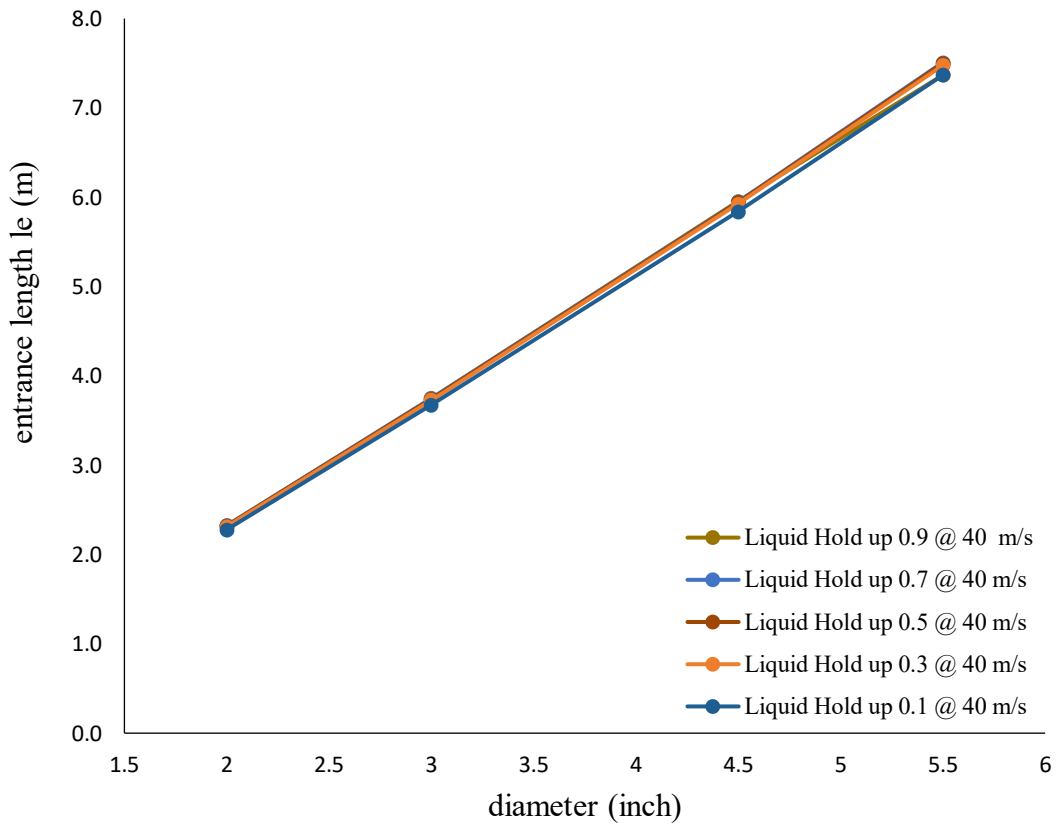


Figure 3. 16 shows change in entrance of length with different liquid hold up at velocity 40 m/s.

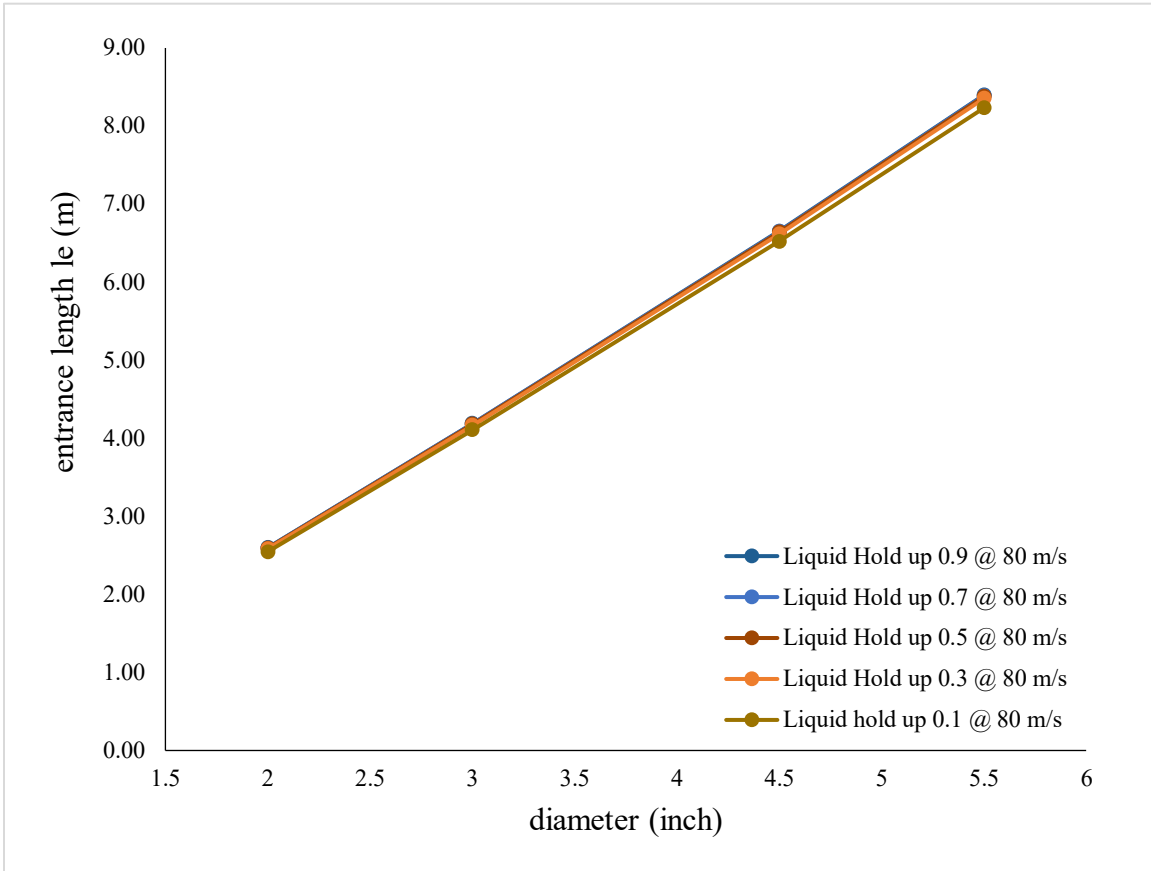


Figure 3. 17 shows change in entrance of length with different liquid hold up at velocity 80 m/s.

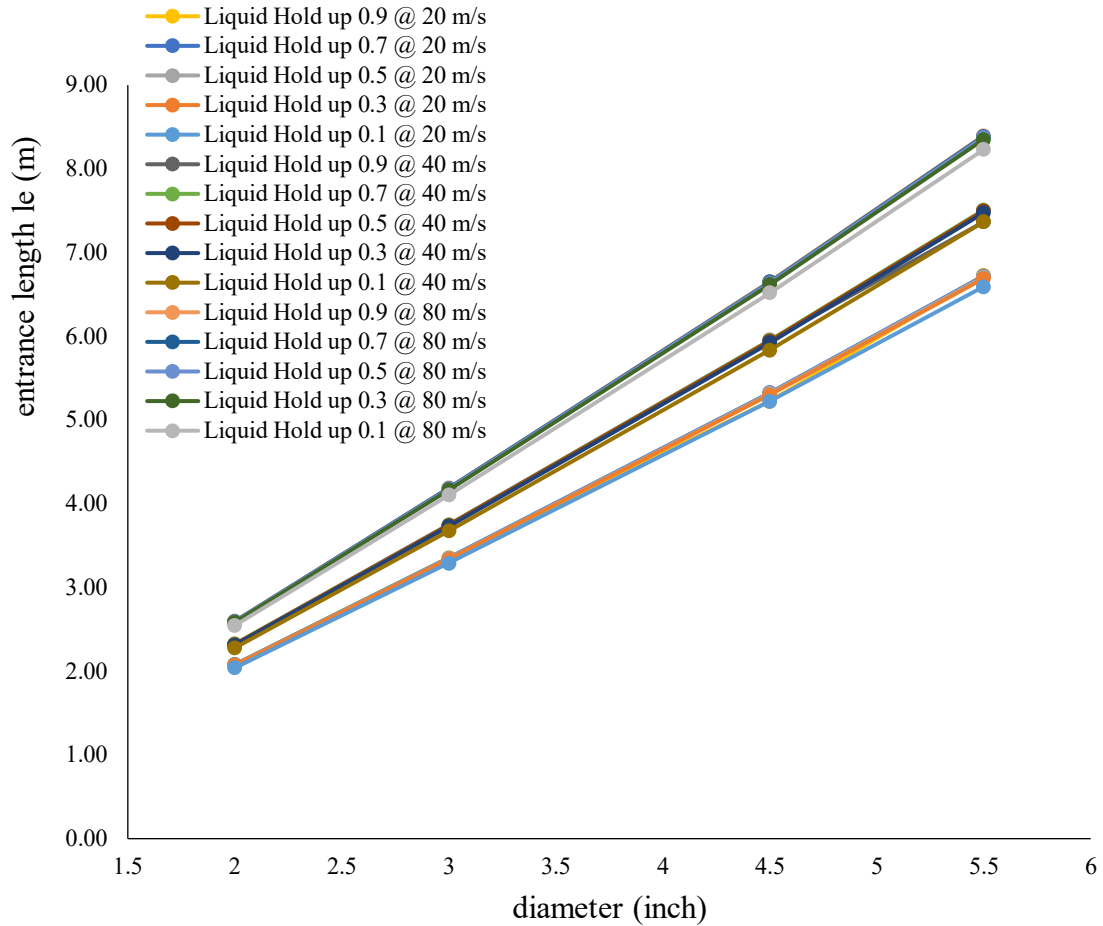


Figure 3. 18 shows the change in entrance of length with different liquid hold up at variable assumption velocities

From the previous graphs can conclude the following.

1. The change in gas and liquid hold up with constant (homogenous) velocity and different velocity shows as an increase with velocity the entrance of length will increase as well.
2. The increase in liquid hold up will increase the entrance of length at lower and higher velocities. When the liquid hold up is more than 0.5 the result of the entrance of length will be very close to each other in comparison with a lower liquid fraction such as 0.1 or 0.2.

Table 3. 11 shows the change in liquid (water) density

Water Density (kg/m <sup>3</sup> )	Gas Density (kg/m <sup>3</sup> )	Gas Fraction	Water Fraction	Mixture Density (kg/m <sup>3</sup> )
900	4.68	0.3	0.7	631.4
1100	4.68	0.7	0.3	333.3
1200	4.68	0.5	0.5	602.3
1300	4.68	0.9	0.1	134.2
1400	4.68	0.1	0.9	1260.5

Table 3. 12 shows a summary of the entrance of length with change in density at a homogenous velocity 20 m/s for liquid and gas.

ID (inch)	ID (m)	Liquid Hold up	Gas Hold Up	Mixture Re	Velocity (m/s)	Mixture Density (kg/m <sup>3</sup> )	L <sub>e</sub> (inch)	L <sub>e</sub> (m)
<b>Two-Phase Air and Water</b>								
2	0.051	0.7	0.3	1.0E+06	20	631.4	81	2.05
3	0.077	0.7	0.3	1.5E+06	20	631.4	130	3.30
4.5	0.114	0.7	0.3	2.5E+06	20	631.4	210	5.33
5.5	0.140	0.7	0.3	2.8E+06	20	631.4	260	6.61
<b>Two-Phase Water and Air</b>								
2	0.051	0.3	0.7	1.21E+06	20	333.3	83	2.10
3	0.077	0.3	0.7	1.83E+06	20	333.3	133	3.39
4.5	0.114	0.3	0.7	2.72E+06	20	333.3	212	5.38
5.5	0.140	0.3	0.7	3.33E+06	20	333.3	268	6.80
<b>Two-Phase Water and Gas</b>								
2	0.051	0.5	0.5	1.3E+06	20	602.3	84	2.1
3	0.077	0.5	0.5	2.0E+06	20	602.3	136	3.4
4.5	0.114	0.5	0.5	3.03E+06	20	602.3	216	5.48
5.5	0.140	0.5	0.5	3.7E+06	20	602.3	272	6.91
<b>Two-Phase Gas and Water</b>								
2	0.051	0.9	0.1	1.6E+06	20	1260.5	86	2.20
3	0.077	0.9	0.1	2.4E+06	20	1260.5	139	3.54
4.5	0.114	0.9	0.1	3.6E+06	20	1260.5	222	5.63
5.5	0.140	0.9	0.1	4.4E+06	20	1260.5	280	7.10
<b>Two-Phase Gas and Air</b>								
2	0.051	0.1	0.9	1.3E+06	20	134.2	84	2.12
3	0.077	0.1	0.9	2.0E+06	20	134.2	135	3.43
4.5	0.114	0.1	0.9	2.9E+06	20	134.2	214	5.44
5.5	0.140	0.1	0.9	3.6E+06	20	134.2	270	6.87

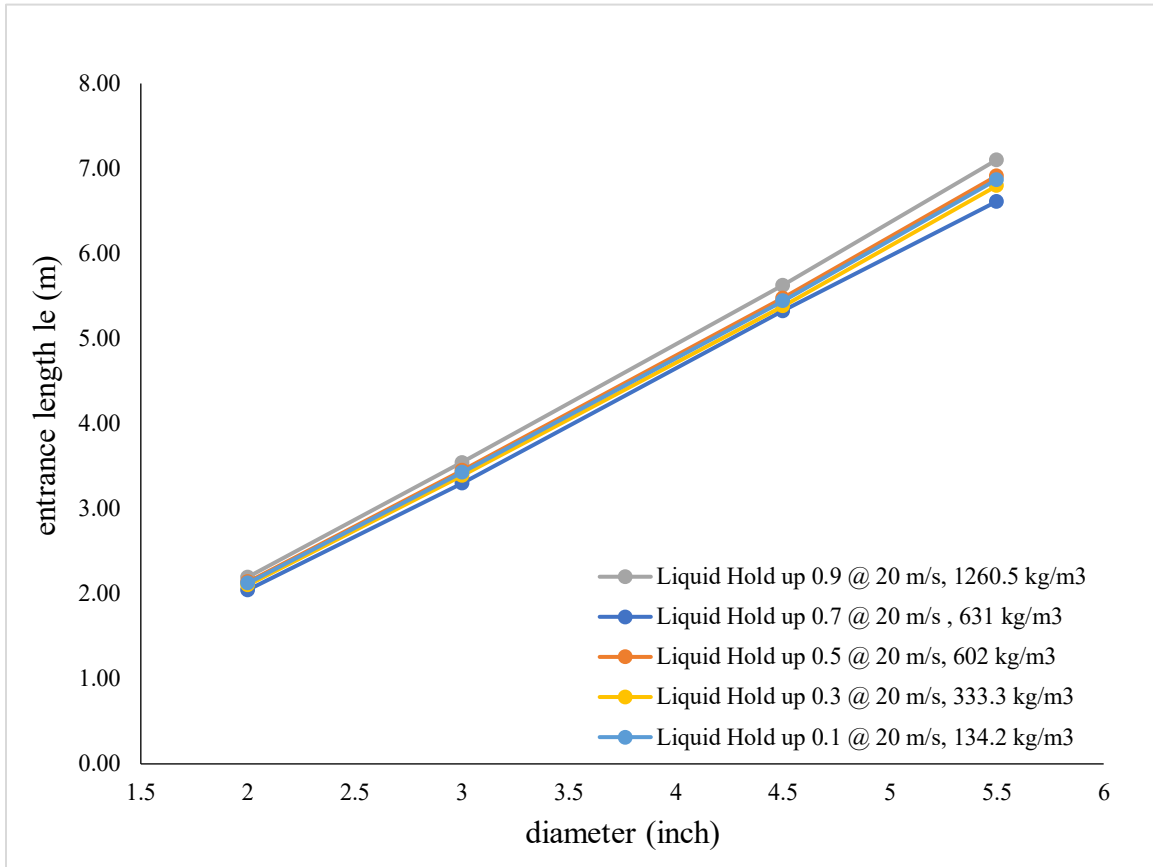


Figure 3. 19 shows the change in entrance of length with different liquid hold up at homogenous velocity 20 m/s and different density.

Table 3. 13 shows 2- phase summary entrance of length with change in density at different velocity with liquid and gas hold up 0.9, 0.1 respectively

ID (inch)	ID (m)	Liquid Hold up	Gas Hold up	Mixture $R_e$	Velocity (m/s)	Mixture Density (kg/m <sup>3</sup> )	$L_e$ (inch)	$L_e$ (m)
<b>Two-Phase Air and Water</b>								
2	0.051	0.9	0.1	3.2E+06	40	1260.5	97	2.5
3	0.077	0.9	0.1	4.8E+06	40	1260.5	156	4.0
4.5	0.114	0.9	0.1	7.18E+06	40	1260.5	248	6.29
5.5	0.140	0.9	0.1	8.8E+06	40	1260.5	312	7.94
2	0.051	0.1	0.9	2.6E+06	40	134.2	93	2.37
3	0.077	0.1	0.9	3.9E+06	40	134.2	151	3.83
4.5	0.114	0.1	0.9	5.8E+06	40	134.2	239	6.08
5.5	0.140	0.1	0.9	7.1E+06	40	134.2	302	7.67

2	0.051	0.9	0.1	6.4E+06	80	1260.5	108	2.74
3	0.077	0.9	0.1	9.6E+06	80	1260.5	174	4.42
4.5	0.114	0.9	0.1	1.4E+07	80	1260.5	277	7.02
5.5	0.140	0.9	0.1	1.8E+07	80	1260.5	349	8.87
2	0.051	0.1	0.9	5.2E+06	80	134.2	104	2.65
3	0.077	0.1	0.9	7.8E+06	80	134.2	168	4.28
4.5	0.114	0.1	0.9	1.2E+07	80	134.2	267	6.79
5.5	0.140	0.1	0.9	1.4E+07	80	134.2	338	8.58

**Table 3. 14 shows two-phase summary entrance of length with change in density at different velocity with liquid and gas hold up 0.7, 0.3 respectively**

ID (inch)	ID (m)	Liquid Hold up	Gas Hold up	Mixture $R_e$	Velocity (m/s)	Mixture Density (kg/m <sup>3</sup> )	$L_e$ (inch)	$L_e$ (m)
<b>Two-Phase Air and Water</b>								
2	0.051	0.7	0.3	2.0E+06	40	631.4	90	2.3
3	0.077	0.7	0.3	3.1E+06	40	631.4	145	3.7
4.5	0.114	0.7	0.3	4.59E+06	40	631.4	230	5.85
5.5	0.140	0.7	0.3	5.6E+06	40	631.4	291	7.39
2	0.051	0.3	0.7	2.4E+06	40	333.3	92	2.35
3	0.077	0.3	0.7	3.7E+06	40	333.3	149	3.79
4.5	0.114	0.3	0.7	5.4E+06	40	333.3	237	6.02
5.5	0.140	0.3	0.7	6.7E+06	40	333.3	299	7.59
2	0.051	0.7	0.3	4.1E+06	80	631.4	101	2.55
3	0.077	0.7	0.3	6.2E+06	80	631.4	162	4.12
4.5	0.114	0.7	0.3	9.2E+06	80	631.4	257	6.54
5.5	0.140	0.7	0.3	1.1E+07	80	631.4	325	8.25
2	0.051	0.3	0.7	4.8E+06	80	333.3	103	2.62
3	0.077	0.3	0.7	7.3E+06	80	333.3	167	4.23
4.5	0.114	0.3	0.7	1.1E+07	80	333.3	265	6.72
5.5	0.140	0.3	0.7	1.3E+07	80	333.3	334	8.48

Table 3. 15 shows two-phase summary entrance of length with change in density at different velocity with liquid and gas hold up 0.5, 0.5 respectively

Two-Phase Air and Water								
2	0.051	0.5	0.5	2.70E+06	40	602.3	94	2.39
3	0.077	0.5	0.5	4.07E+06	40	602.3	152	3.85
4.5	0.114	0.5	0.5	6.07E+06	40	602.3	241	6.12
5.5	0.140	0.5	0.5	7.41E+06	40	602.3	304	7.72
2	0.051	0.5	0.5	5.4E+06	80	602.3	105	2.7
3	0.077	0.5	0.5	8.1E+06	80	602.3	169	4.3
4.5	0.114	0.5	0.5	1.21E+07	80	602.3	269	6.84
5.5	0.140	0.5	0.5	1.5E+07	80	602.3	340	8.63

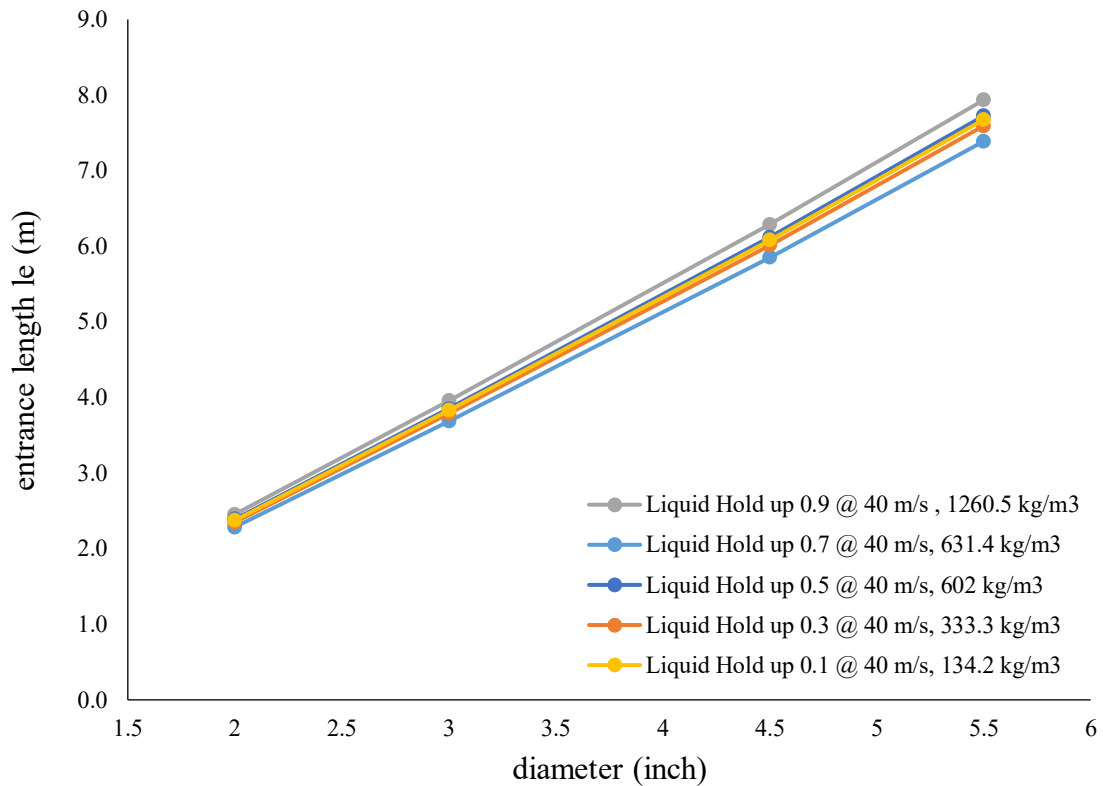


Figure 3. 20 Shows change in entrance of length with different liquid hold up at homogenous velocity 40 m/s and different density.

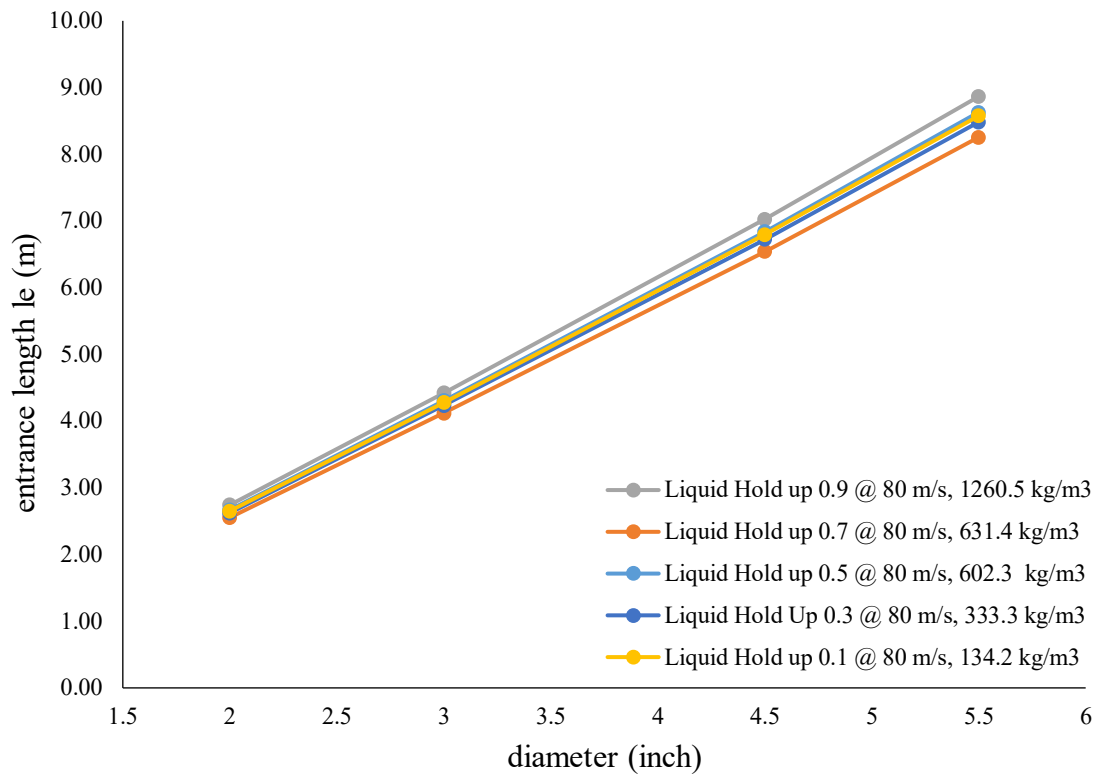


Figure 3. 21 shows the change in entrance of length with different liquid hold up at homogenous velocity 80 m/s and different density.

The previous two-phase flow graphs with a change in density can conclude the following.

1. The change in density effect on the entrance of length calculation. When the density decreases the entrance of length decrease as well for all different velocities and vice verse.
2. The liquid hold up helps to increase the entrance of length with an increase in density.

Table 3. 16 shows the change in liquid and gas viscosity

Water viscosity (pa.s)	Gas viscosity (pa.s)	Gas Fraction	Water Fraction	Mixture viscosity (pa.s)
1.78E-03	3.62E-05	0.3	0.7	1.26E-03
1.78E-03	3.62E-05	0.7	0.3	5.59E-04
1.78E-03	3.62E-05	0.5	0.5	9.08E-04
1.78E-03	3.62E-05	0.1	0.9	1.61E-03
1.78E-03	3.62E-05	0.9	0.1	2.11E-04

**Table 3. 17 shows homogenous velocity for two-phase with different liquid and gas hold up and change in viscosity.**

<b>ID (inch)</b>	<b>ID (m)</b>	<b>Liquid Hold up</b>	<b>Gas Hold up</b>	<b>Mixture Re</b>	<b>Velocity (m/s)</b>	<b>Mixture Density (kg/m<sup>3</sup>)</b>	<b>L<sub>e</sub> (inch)</b>	<b>L<sub>e</sub> (m)</b>	<b>Mixture Viscosity (pa.s)</b>
<b>Two-Phase Air and Water</b>									
2	0.051	0.7	0.3	5.7E+05	20	631.4	73	1.86	1.26E-03
3	0.077	0.7	0.3	8.5E+05	20	631.4	118	3.00	1.26E-03
4.5	0.114	0.7	0.3	1.3E+06	20	631.4	188	4.77	1.26E-03
5.5	0.140	0.7	0.3	1.6E+06	20	631.4	237	6.02	1.26E-03
<b>Two-Phase Water and Air</b>									
2	0.051	0.3	0.7	5.49E+05	20	333.3	73	1.85	5.59E-04
3	0.077	0.3	0.7	8.29E+05	20	333.3	118	2.99	5.59E-04
4.5	0.114	0.3	0.7	1.24E+06	20	333.3	187	4.74	5.59E-04
5.5	0.140	0.3	0.7	1.51E+06	20	333.3	236	5.99	5.59E-04
<b>Two-Phase Oil and Air</b>									
2	0.051	0.5	0.5	5.6E+05	20	602.3	73	1.9	9.08E-04
3	0.077	0.5	0.5	8.5E+05	20	602.3	118	3.0	9.08E-04
4.5	0.114	0.5	0.5	1.26E+06	20	602.3	187	4.76	9.08E-04
5.5	0.140	0.5	0.5	1.5E+06	20	602.3	237	6.01	9.08E-04
<b>Two-Phase Air and Oil</b>									
2	0.051	0.9	0.1	5.7E+05	20	1260.5	73	1.86	1.61E-03
3	0.077	0.9	0.1	8.6E+05	20	1260.5	118	3.00	1.61E-03
4.5	0.114	0.9	0.1	1.3E+06	20	1260.5	188	4.77	1.61E-03
5.5	0.140	0.9	0.1	1.6E+06	20	1260.5	237	6.02	1.61E-03
<b>Two-Phase Water and Oil</b>									
2	0.051	0.1	0.9	5.0E+05	20	134.2	72	1.83	2.11E-04
3	0.077	0.1	0.9	7.6E+05	20	134.2	116	2.94	2.11E-04
4.5	0.114	0.1	0.9	1.1E+06	20	134.2	184	4.68	2.11E-04
5.5	0.140	0.1	0.9	1.4E+06	20	134.2	232	5.90	2.11E-04

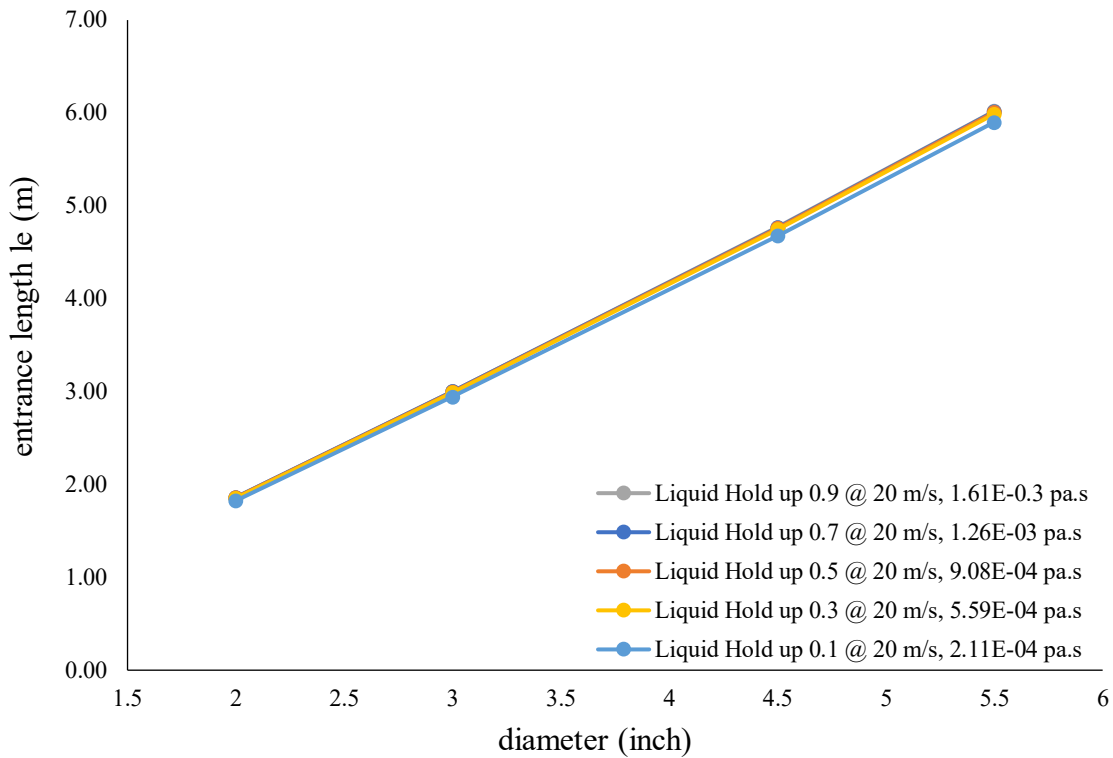


Figure 3. 22 shows the change in entrance of length with different liquid hold up at homogenous velocity 20 m/s and different viscosity.

Table 3. 18 shows a summary entrance of length with different velocity for two-phase with variable liquid and gas hold up and change in viscosity

ID (inch)	ID (m)	Liquid Hold up	Gas Hold up	Mixture $R_e$	Velocity (m/s)	Mixture Density ( $kg/m^3$ )	$L_e$ (inch)	$L_e$ (m)	Mixture Viscosity
<b>Two-Phase Air and Water</b>									
2	0.051	0.7	0.3	1.1E+06	40	631.4	82	2.1	1.26E-03
3	0.077	0.7	0.3	1.7E+06	40	631.4	132	3.4	1.26E-03
4.5	0.114	0.7	0.3	2.54E+06	40	631.4	210	5.33	1.26E-03
5.5	0.140	0.7	0.3	3.1E+06	40	631.4	265	6.72	1.26E-03
2	0.051	0.3	0.7	1.1E+06	40	333.3	81	2.07	5.59E-04
3	0.077	0.3	0.7	1.7E+06	40	333.3	131	3.34	5.59E-04
4.5	0.114	0.3	0.7	2.5E+06	40	333.3	209	5.30	5.59E-04
5.5	0.140	0.3	0.7	3.0E+06	40	333.3	263	6.69	5.59E-04

2	0.051	0.7	0.3	2.3E+06	80	631.4	91	2.32	1.26E-03
3	0.077	0.7	0.3	3.4E+06	80	631.4	147	3.75	1.26E-03
4.5	0.114	0.7	0.3	5.1E+06	80	631.4	234	5.95	1.26E-03
5.5	0.140	0.7	0.3	6.2E+06	80	631.4	296	7.51	1.26E-03
2	0.051	0.3	0.7	2.2E+06	80	333.3	91	2.31	5.59E-04
3	0.077	0.3	0.7	3.3E+06	80	333.3	147	3.73	5.59E-04
4.5	0.114	0.3	0.7	4.9E+06	80	333.3	233	5.92	5.59E-04
5.5	0.140	0.3	0.7	6.0E+06	80	333.3	294	7.48	5.59E-04

**Table 3. 19 shows a summary entrance of length with different velocity for two-phase with variable liquid and gas hold up and change in viscosity**

ID (inch)	ID (m)	Liquid Hold up	Gas Hold up	Mixture $R_e$	Velocity (m/s)	Mixture Density ( $kg/m^3$ )	$L_e$ (inch)	$L_e$ (m)	Mixture Viscosity
<b>Two-Phase Air and Water</b>									
2	0.051	0.9	0.1	1.1E+06	40	1260.5	82	2.1	1.61E-03
3	0.077	0.9	0.1	1.7E+06	40	1260.5	132	3.4	1.61E-03
4.5	0.114	0.9	0.1	2.56E+06	40	1260.5	210	5.33	1.61E-03
5.5	0.140	0.9	0.1	3.1E+06	40	1260.5	265	6.73	1.61E-03
2	0.051	0.1	0.9	1.0E+06	40	134.2	80	2.04	2.11E-04
3	0.077	0.1	0.9	1.5E+06	40	134.2	129	3.29	2.11E-04
4.5	0.114	0.1	0.9	2.3E+06	40	134.2	206	5.22	2.11E-04
5.5	0.140	0.1	0.9	2.8E+06	40	134.2	260	6.59	2.11E-04
2	0.051	0.9	0.1	2.3E+06	80	1260.5	92	2.32	1.61E-03
3	0.077	0.9	0.1	3.4E+06	80	1260.5	148	3.75	1.61E-03
4.5	0.114	0.9	0.1	5.1E+06	80	1260.5	234	5.95	1.61E-03
5.5	0.140	0.9	0.1	6.2E+06	80	1260.5	296	7.52	1.61E-03
2	0.051	0.1	0.9	2.0E+06	80	134.2	90	2.28	2.11E-04
3	0.077	0.1	0.9	3.0E+06	80	134.2	145	3.67	2.11E-04
4.5	0.114	0.1	0.9	4.5E+06	80	134.2	230	5.84	2.11E-04
5.5	0.140	0.1	0.9	5.5E+06	80	134.2	290	7.37	2.11E-04

**Table 3. 20** shows a summary entrance of length with different velocity two-phase with variable liquid and gas hold up and change in viscosity

Two-Phase Air and Water									
2	0.051	0.5	0.5	1.12E+06	40	602.3	82	2.08	9.08E-04
3	0.077	0.5	0.5	1.69E+06	40	602.3	132	3.35	9.08E-04
4.5	0.114	0.5	0.5	2.52E+06	40	602.3	209	5.32	9.08E-04
5.5	0.140	0.5	0.5	3.08E+06	40	602.3	264	6.71	9.08E-04
2	0.051	0.5	0.5	2.2E+06	80	602.3	91	2.3	9.08E-04
3	0.077	0.5	0.5	3.4E+06	80	602.3	147	3.7	9.08E-04
4.5	0.114	0.5	0.5	5.04E+06	80	602.3	234	5.94	9.08E-04
5.5	0.140	0.5	0.5	6.2E+06	80	602.3	295	7.50	9.08E-04

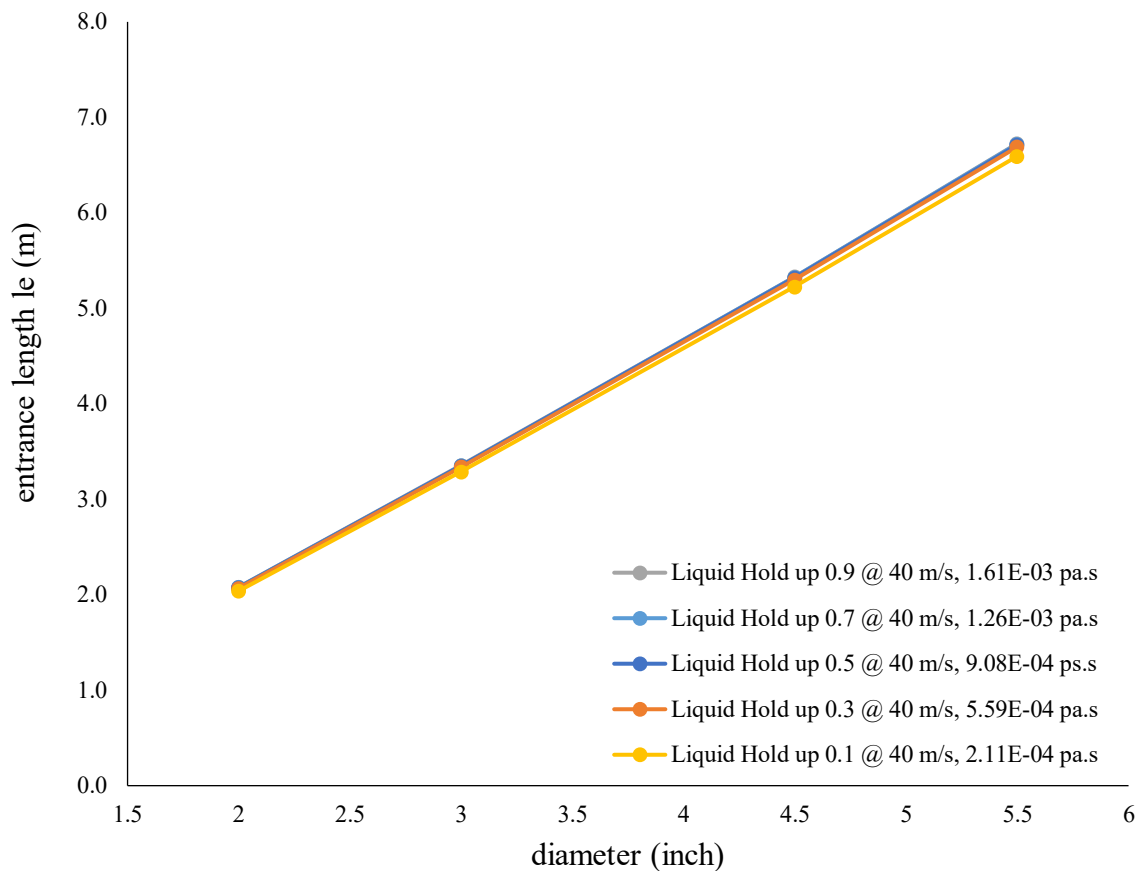


Figure 3. 23 shows the change in entrance of length with different liquid hold up at homogenous velocity 40 m/s and different viscosity.

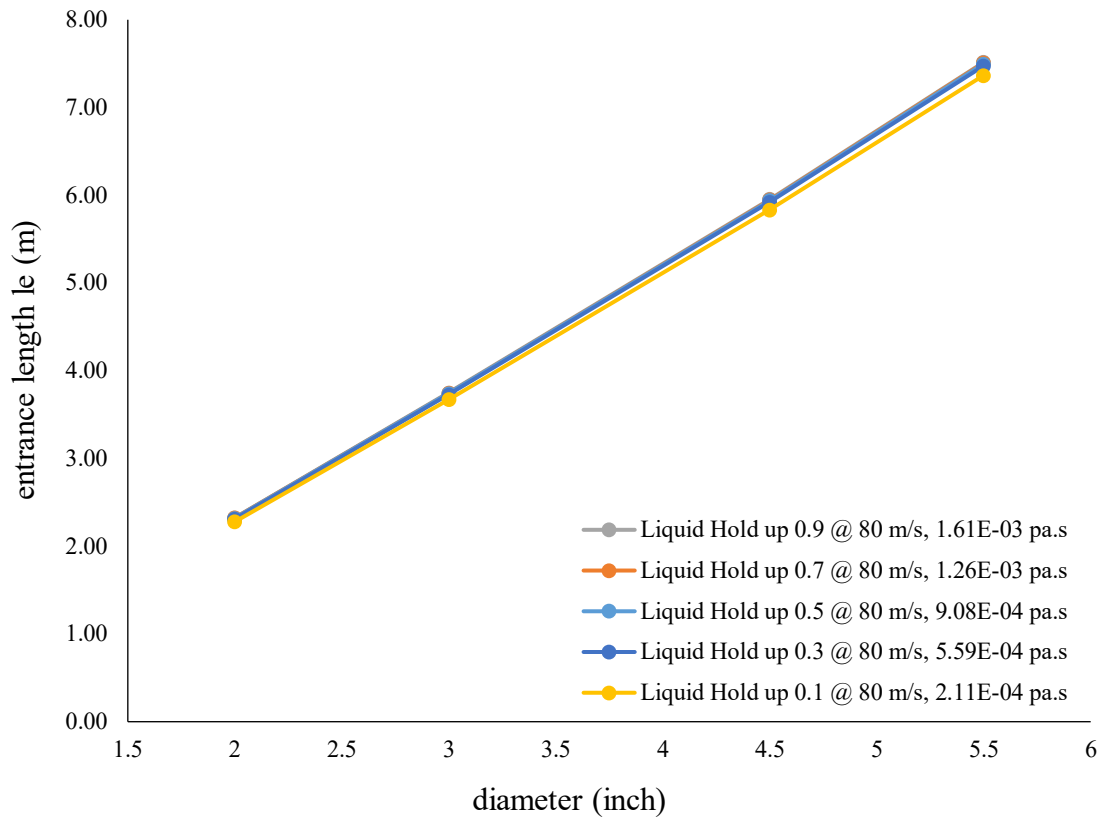


Figure 3. 24 Shows change in entrance of length with different liquid hold up at homogenous velocity 80 m/s and different viscosity.

From the previous two-phase flow graphs with a change in viscosity can conclude the following.

1. The change in viscosity effect on the entrance of length calculation. As viscosity increase the entrance of length increase, but it is depended on the liquid up.
2. The velocity effect in viscosity the same as in density. Increase in entrance of length with an increase in velocity.

### 3.5 Entrance of Length Calculation for Three-Phase (Water, Air, and Solid)

In multiphase flow can used water, air, and glass particle as a solid part to simulate the multiphase flow with a density of  $2.56 \text{ kg/m}^3$  <sup>28</sup>.

Using the same equation for two-phase mixture properties for calculation Reynold number by applying the equation (9) and for mixture, density using equation (5) and consider the solid concentration by using both equations (6,7).

**Table 3. 21 shows the water, air, and solid viscosity for 3-phase**

Water viscosity (pa.s)	Air Viscosity (pa.s)	Air and Water Viscosity (pa.s)	Solid Fraction	Water and Air Fraction	Mixture viscosity (pa.s)
8.90E-04	1.81E-05	4.54E-04	0.1	0.9	6.32E-04
8.90E-04	1.81E-05	4.54E-04	0.2	0.8	9.37E-04
8.90E-04	1.81E-05	4.54E-04	0.5	0.5	2.62E-03

**Table 3. 22 shows the water, air, and solid density for 3-phase**

Water Density (kg/m <sup>3</sup> )	Gas Density (kg/m <sup>3</sup> )	Solid Density kg/m <sup>3</sup>	Air & water Density	Solid Fraction	Fluid Fraction	Mixture Density (kg/m <sup>3</sup> )
996.7	9.35	2.56E-03	503	0.1	0.9	452.7
996.7	9.35	2.56E-03	503	0.2	0.8	402.4
996.7	9.35	2.56E-03	503	0.5	0.5	251.5

**Table 3. 23 shows the summary entrance of length with homogenous velocity 20 m/s for three-phase with variable liquid, air, and solid fraction**

ID (inch)	ID (m)	Liquid + Air Hold up	Solid Fraction	Mixture Re	Velocity (m/s)	Mixture Density (kg/m <sup>3</sup> )	L <sub>e</sub> (inch)	L <sub>e</sub> (m)	Mixture Viscosity pa.s
<b>3-Phase Air, Water and Solid</b>									
2	0.051	0.9	0.1	7.3E+05	20	452.7	76	1.94	6.32E-04
3	0.077	0.9	0.1	1.1E+06	20	452.7	123	3.12	6.32E-04
4.5	0.114	0.9	0.1	1.6E+06	20	452.7	195	4.96	6.32E-04
5.5	0.140	0.9	0.1	2.0E+06	20	452.7	247	6.26	6.32E-04
2	0.051	0.8	0.2	4.36E+05	20	402.4	70	1.79	5.59E-04
3	0.077	0.8	0.2	6.59E+05	20	402.4	113	2.88	5.59E-04
4.5	0.114	0.8	0.2	9.82E+05	20	402.4	180	4.57	5.59E-04
5.5	0.140	0.8	0.2	1.20E+06	20	402.4	218	5.55	5.59E-04
2	0.051	0.5	0.5	9.7E+04	20	251.5	55	1.4	2.62E-03
3	0.077	0.5	0.5	1.5E+05	20	251.5	89	2.3	2.62E-03
4.5	0.114	0.5	0.5	2.19E+05	20	251.5	142	3.60	2.62E-03
5.5	0.140	0.5	0.5	2.7E+05	20	251.5	179	4.54	2.62E-03

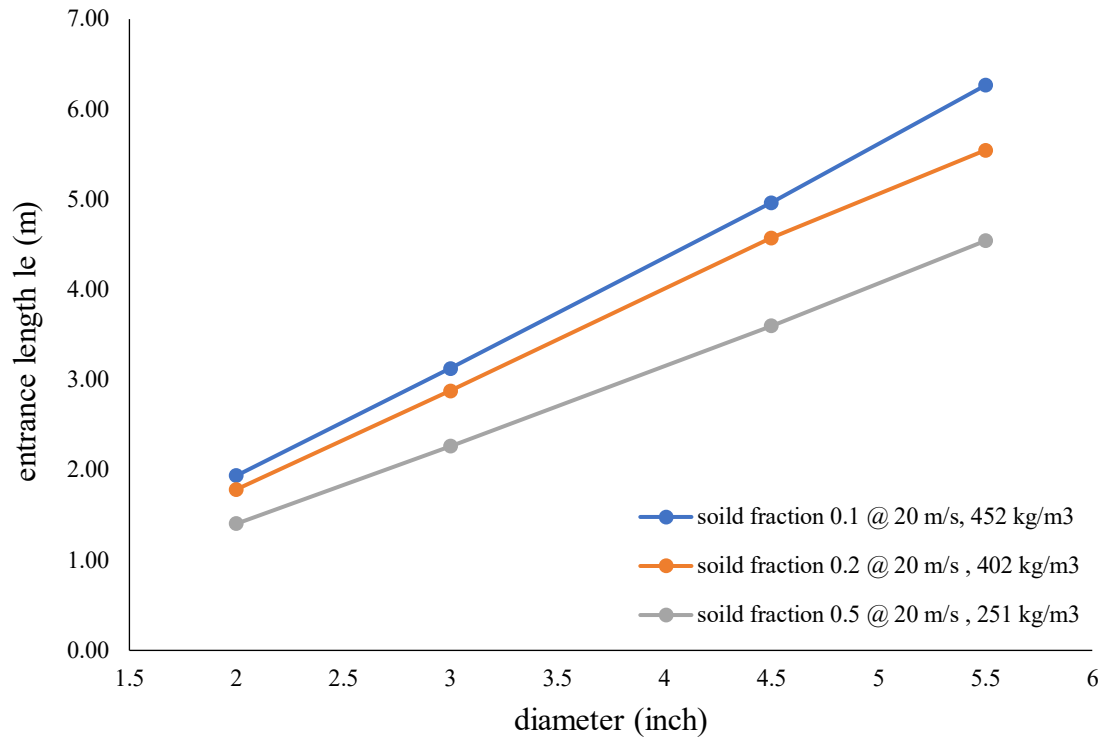


Figure 3. 25 shows the change in entrance of length for 3-phase flow with different solid fraction at a homogenous velocity 20 m/s

Table 3. 24 shows the summary entrance of length with homogenous velocity 40 m/s for three-phase with variable liquid, air, and solid fraction

ID (inch)	ID (m)	Liquid + Air Hold up	Solid Fraction	Mixture Re	Velocity (m/s)	Mixture Density (kg/m <sup>3</sup> )	Le (inch)	Le (m)	Mixture Viscosity pa.s
<b>3-Phase Air, Water and Solid</b>									
2	0.051	0.9	0.1	1.5E+06	40	452.7	85	2.16	6.32E-04
3	0.077	0.9	0.1	2.2E+06	40	452.7	137	3.49	6.32E-04
4.5	0.114	0.9	0.1	3.3E+06	40	452.7	218	5.55	6.32E-04
5.5	0.140	0.9	0.1	4.0E+06	40	452.7	276	7.00	6.32E-04
2	0.051	0.8	0.2	8.7E+05	40	402.4	79	1.99	9.37E-04
3	0.077	0.8	0.2	1.3E+06	40	402.4	127	3.22	9.37E-04
4.5	0.114	0.8	0.2	2.0E+06	40	402.4	201	5.11	9.37E-04
5.5	0.140	0.8	0.2	2.4E+06	40	402.4	254	6.45	9.37E-04
2	0.051	0.5	0.5	1.9E+05	40	251.5	62	1.6	2.62E-03
3	0.077	0.5	0.5	2.9E+05	40	251.5	100	2.5	2.62E-03
4.5	0.114	0.5	0.5	4.39E+05	40	251.5	158	4.02	2.62E-03
5.5	0.140	0.5	0.5	5.4E+05	40	251.5	200	5.07	2.62E-03

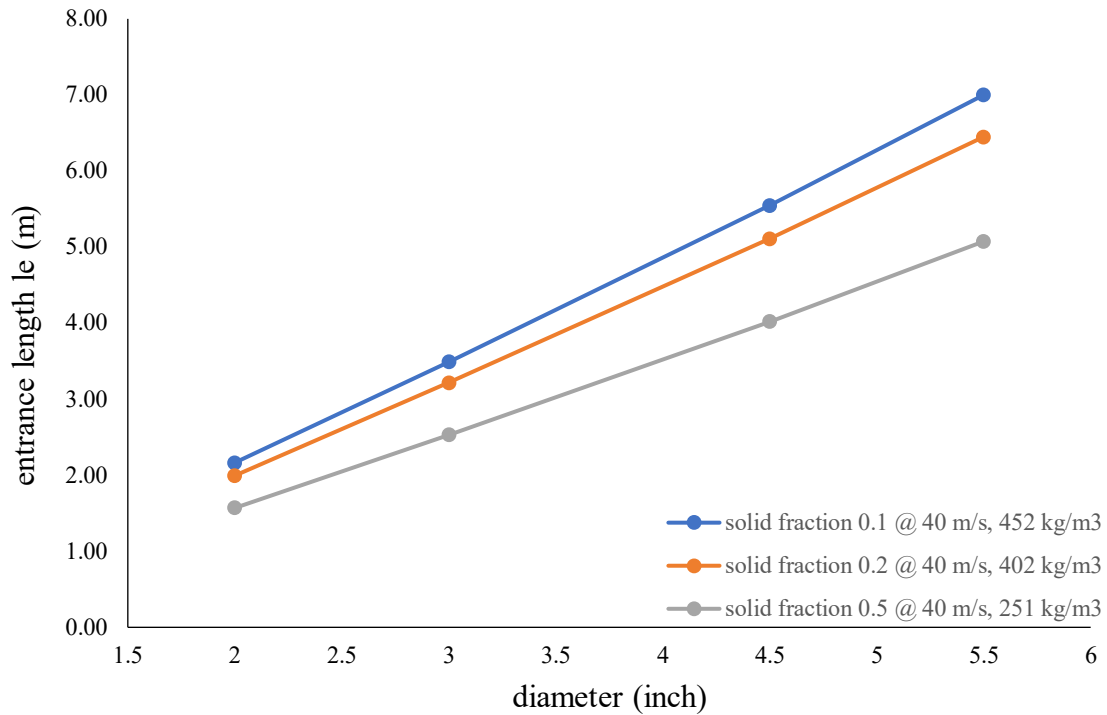


Figure 3. 26 shows the change in entrance of length for 3-phase flow with different solid fraction at a homogenous velocity 40 m/s

Table 3. 25 shows a summary for the entrance of length with homogenous velocity 80 m/s for three-phase with variable liquid, air, and solid fraction

ID (inch)	ID (m)	Liquid + Air Hold up	Solid Fraction	Mixture $R_e$	Velocity (m/s)	Mixture Density (kg/m <sup>3</sup> )	$L_e$ (inch)	$L_e$ (m)	Mixture Viscosity pa.s
<b>3-Phase Air, Water and Solid</b>									
2	0.051	0.9	0.1	2.9E+06	80	452.7	95	2.42	6.32E-04
3	0.077	0.9	0.1	4.4E+06	80	452.7	154	3.90	6.32E-04
4.5	0.114	0.9	0.1	6.6E+06	80	452.7	244	6.20	6.32E-04
5.5	0.140	0.9	0.1	8.0E+06	80	452.7	308	7.82	6.32E-04
2	0.051	0.8	0.2	1.75E+06	80	402.4	88	2.23	9.37E-04
3	0.077	0.8	0.2	2.63E+06	80	402.4	141	3.59	9.37E-04
4.5	0.114	0.8	0.2	3.93E+06	80	402.4	225	5.71	9.37E-04
5.5	0.140	0.8	0.2	4.80E+06	80	402.4	284	7.20	9.37E-04
2	0.051	0.5	0.5	3.9E+05	80	251.5	69	1.8	2.62E-03
3	0.077	0.5	0.5	5.9E+05	80	251.5	111	2.8	2.62E-03
4.5	0.114	0.5	0.5	8.77E+05	80	251.5	177	4.49	2.62E-03
5.5	0.140	0.5	0.5	1.1E+06	80	251.5	223	5.67	2.62E-03

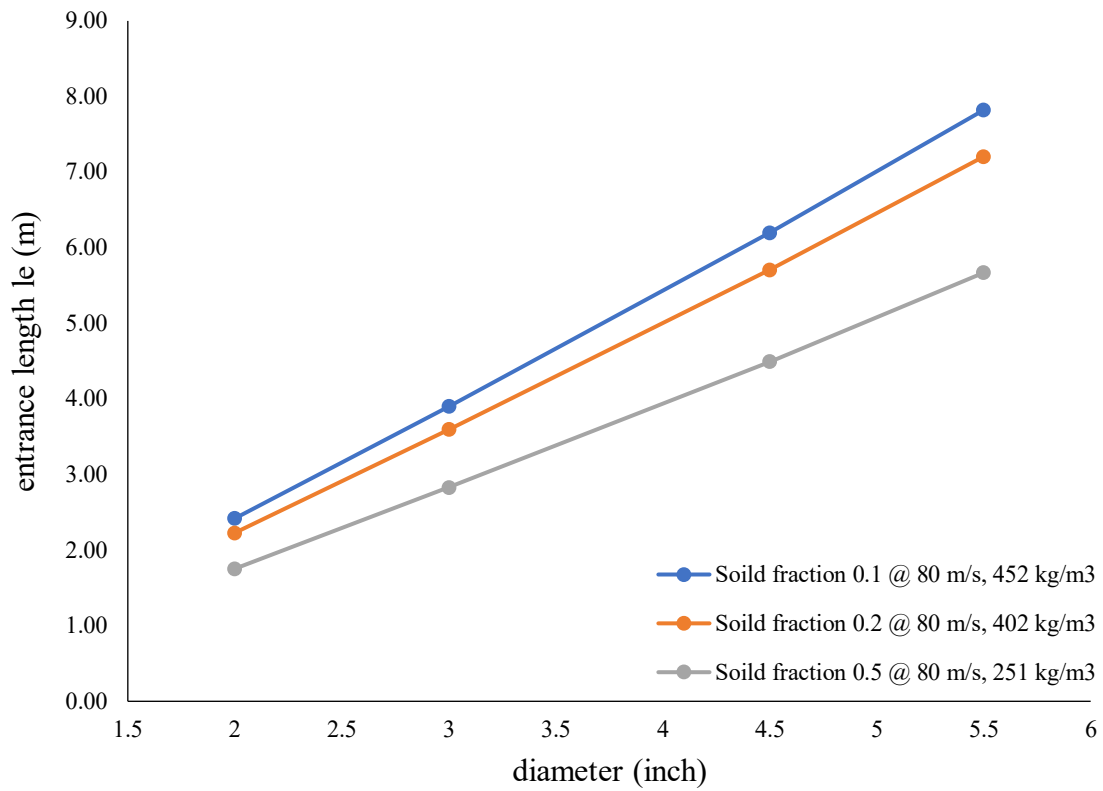


Figure 3. 27 shows the change in entrance of length for 3-phase flow with different solid fraction at a homogenous velocity 80 m/s

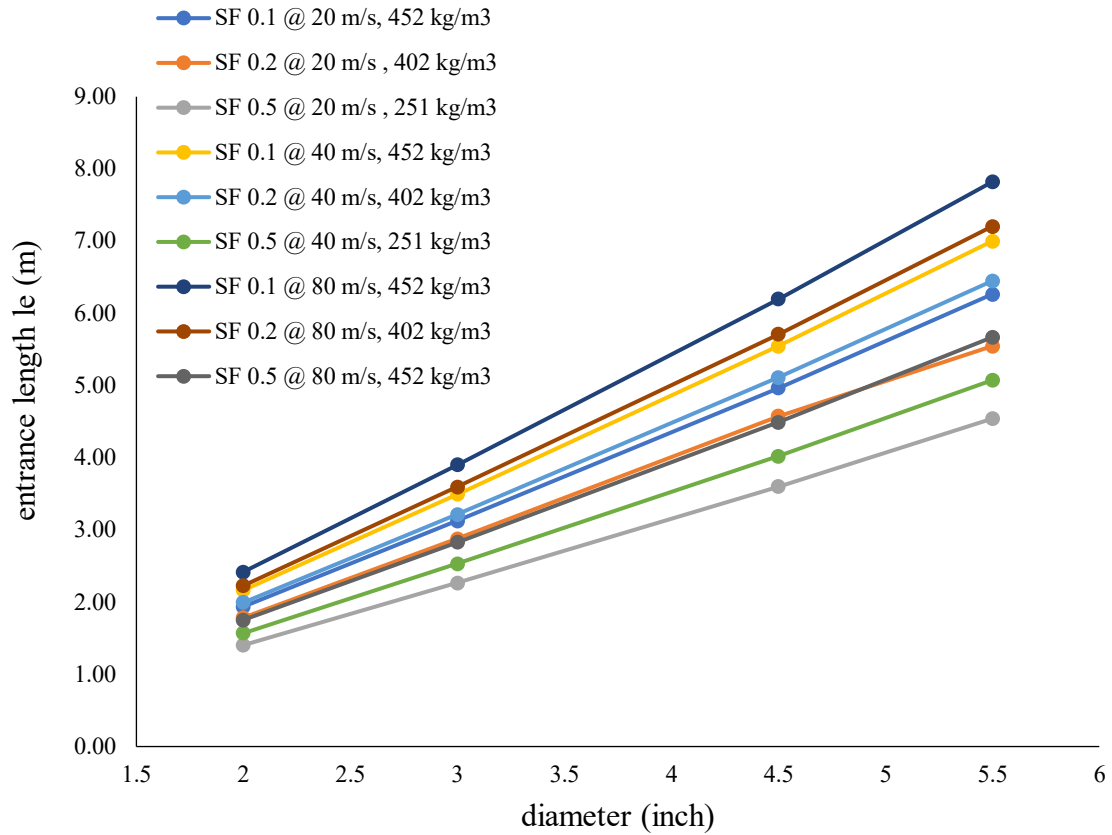


Figure 3. 28 shows the change in entrance of length for 3-phase flow with different solid fraction at variable velocities

From the previous three-phase flow entrance of length graphs with a change in solid fraction and velocity can conclude the following.

1. The increase of solid fraction the entrance of length will decrease for all velocities and vice versa.
2. When velocity increases the entrance of length will increase as well.

### 3.5.1 Entrance Length Calculation for Three-Phase (Water, Air, and Solid) Change in density

Table 3. 26 shows the water, air, and solid with a change in density for 3-phase

Water Density (kg/m <sup>3</sup> )	Gas Density (kg/m <sup>3</sup> )	solid Density (kg/m <sup>3</sup> )	Air & water Density	Solid Fraction	Fluid Fraction	Mixture Density (kg/m <sup>3</sup> )
700	7.35	1.56E-03	354	0.1	0.9	318.3
700	7.35	1.56E-03	354	0.2	0.8	282.9
700	7.35	1.56E-03	354	0.5	0.5	176.8

Table 3. 27 shows the summary entrance of length with homogenous velocity 20 m/s for three-phase with variable liquid, air, and solid fraction and different density

ID (inch)	ID (m)	Liquid + Air Hold up	Solid Fraction	Mixture Re	Velocity (m/s)	Mixture Density (kg/m <sup>3</sup> )	L <sub>e</sub> (inch)	L <sub>e</sub> (m)	Mixture Viscosity pa.s
<b>3-Phase Air, Water and Solid</b>									
2	0.051	0.9	0.1	5.1E+05	20	318.3	72	1.83	6.32E-04
3	0.077	0.9	0.1	7.7E+05	20	318.3	116	2.95	6.32E-04
4.5	0.114	0.9	0.1	1.2E+06	20	318.3	185	4.69	6.32E-04
5.5	0.140	0.9	0.1	1.4E+06	20	318.3	233	5.92	6.32E-04
2	0.051	0.8	0.2	3.07E+05	20	282.9	66	1.69	9.37E-04
3	0.077	0.8	0.2	4.63E+05	20	282.9	107	2.72	9.37E-04
4.5	0.114	0.8	0.2	6.90E+05	20	282.9	170	4.32	9.37E-04
5.5	0.140	0.8	0.2	8.44E+05	20	282.9	215	5.46	9.37E-04
2	0.051	0.5	0.5	6.9E+04	20	176.8	52	1.3	2.62E-03
3	0.077	0.5	0.5	1.0E+05	20	176.8	84	2.1	2.62E-03
4.5	0.114	0.5	0.5	1.54E+05	20	176.8	134	3.40	2.62E-03
5.5	0.140	0.5	0.5	1.9E+05	20	176.8	169	4.29	2.62E-03

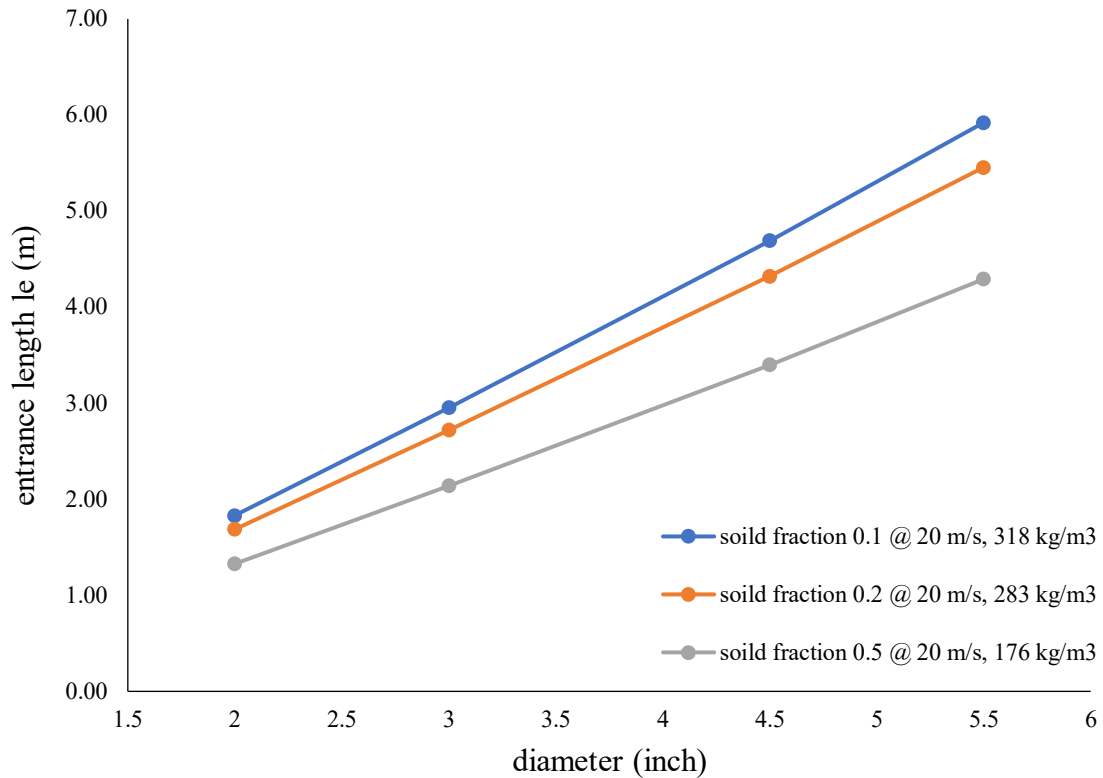


Figure 3. 29 shows a change in entrance of length for 3-phase flow with different solid fractions and different density at a homogenous velocity 20 m/s.

Table 3. 28 shows the summary entrance of length with homogenous velocity 40 m/s for three-phase with variable liquid, air, and solid fraction and different density

ID (inch)	ID (m)	Liquid + Air Hold up	Solid Fraction	Mixture $Re$	Velocity (m/s)	Mixture Density ( $kg/m^3$ )	$L_e$ (inch)	$L_e$ (m)	Mixture Viscosity pa.s
<b>3-Phase Air, Water and Solid</b>									
2	0.051	0.9	0.1	1.0E+06	40	318.3	81	2.05	6.32E-04
3	0.077	0.9	0.1	1.5E+06	40	318.3	130	3.30	6.32E-04
4.5	0.114	0.9	0.1	2.3E+06	40	318.3	206	5.24	6.32E-04
5.5	0.140	0.9	0.1	2.8E+06	40	318.3	260	6.62	6.32E-04
2	0.051	0.8	0.2	6.1E+05	40	282.9	74	1.89	9.37E-04
3	0.077	0.8	0.2	9.3E+05	40	282.9	120	3.04	9.37E-04
4.5	0.114	0.8	0.2	1.4E+06	40	282.9	190	4.83	9.37E-04
5.5	0.140	0.8	0.2	1.7E+06	40	282.9	240	6.10	9.37E-04

2	0.051	0.5	0.5	1.4E+05	40	176.8	58	1.5	2.62E-03
3	0.077	0.5	0.5	2.1E+05	40	176.8	94	2.4	2.62E-03
4.5	0.114	0.5	0.5	3.08E+05	40	176.8	150	3.80	2.62E-03
5.5	0.140	0.5	0.5	3.8E+05	40	176.8	189	4.80	2.62E-03

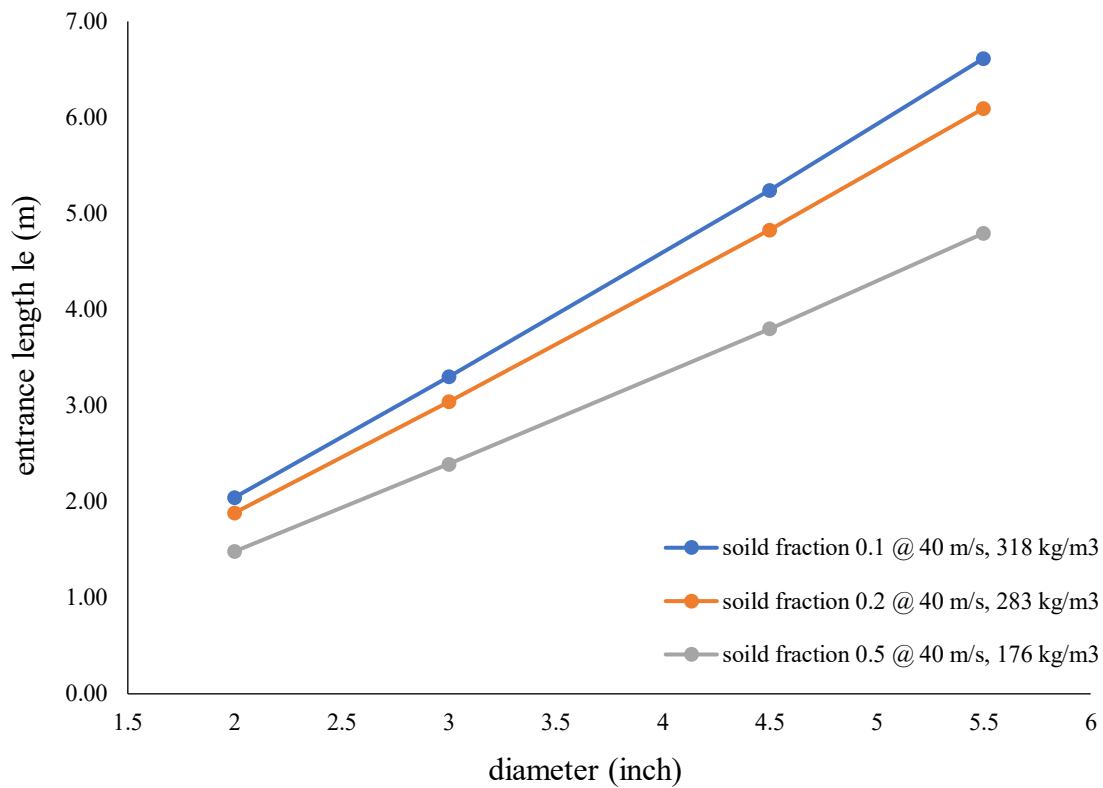


Figure 3. 30 shows a change in entrance of length for 3-phase flow with different solid fractions and different density at a homogenous velocity 40 m/s.

Table 3. 29 shows the summary entrance of length with homogenous velocity 80 m/s for three-phase with variable liquid, air, and solid fraction and different density

ID (inch)	ID (m)	Liquid + Air Hold up	Solid Fraction	Mixture $R_e$	Velocity (m/s)	Mixture Density (kg/m <sup>3</sup> )	$L_e$ (inch)	$L_e$ (m)	Mixture Viscosity pa.s
<b>3-Phase Air, Water and Solid</b>									
2	0.051	0.9	0.1	2.0E+06	80	318.3	90	2.29	6.32E-04
3	0.077	0.9	0.1	3.1E+06	80	318.3	145	3.69	6.32E-04
4.5	0.114	0.9	0.1	4.6E+06	80	318.3	231	5.86	6.32E-04
5.5	0.140	0.9	0.1	5.6E+06	80	318.3	291	7.39	6.32E-04
2	0.051	0.8	0.2	1.23E+06	80	282.9	83	2.11	9.37E-04

3	0.077	0.8	0.2	1.85E+06	80	282.9	134	3.40	9.37E-04
4.5	0.114	0.8	0.2	2.76E+06	80	282.9	212	5.40	9.37E-04
5.5	0.140	0.8	0.2	3.37E+06	80	282.9	268	6.81	9.37E-04
2	0.051	0.5	0.5	2.7E+05	80	176.8	65	1.7	2.62E-03
3	0.077	0.5	0.5	4.1E+05	80	176.8	105	2.7	2.62E-03
4.5	0.114	0.5	0.5	6.17E+05	80	176.8	167	4.25	2.62E-03
5.5	0.140	0.5	0.5	7.5E+05	80	176.8	211	5.36	2.62E-03

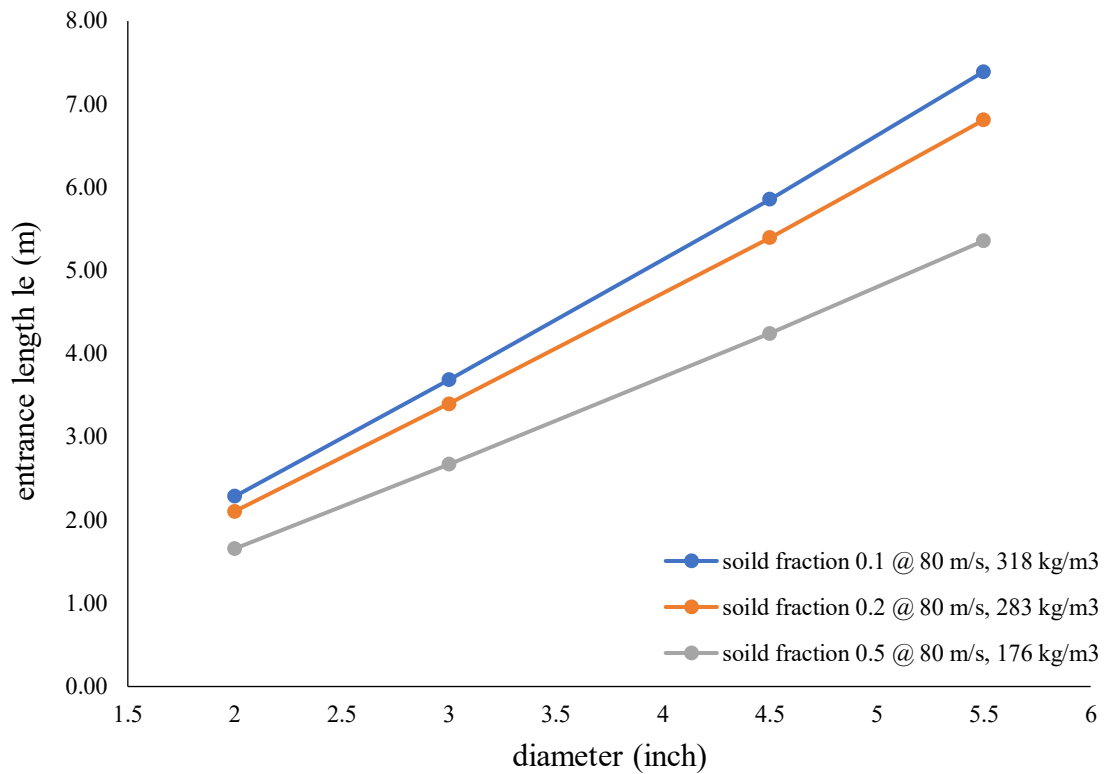


Figure 3. 31 shows a change in entrance of length for 3-phase flow with different solid fractions and different density at a homogenous velocity 80 m/s.

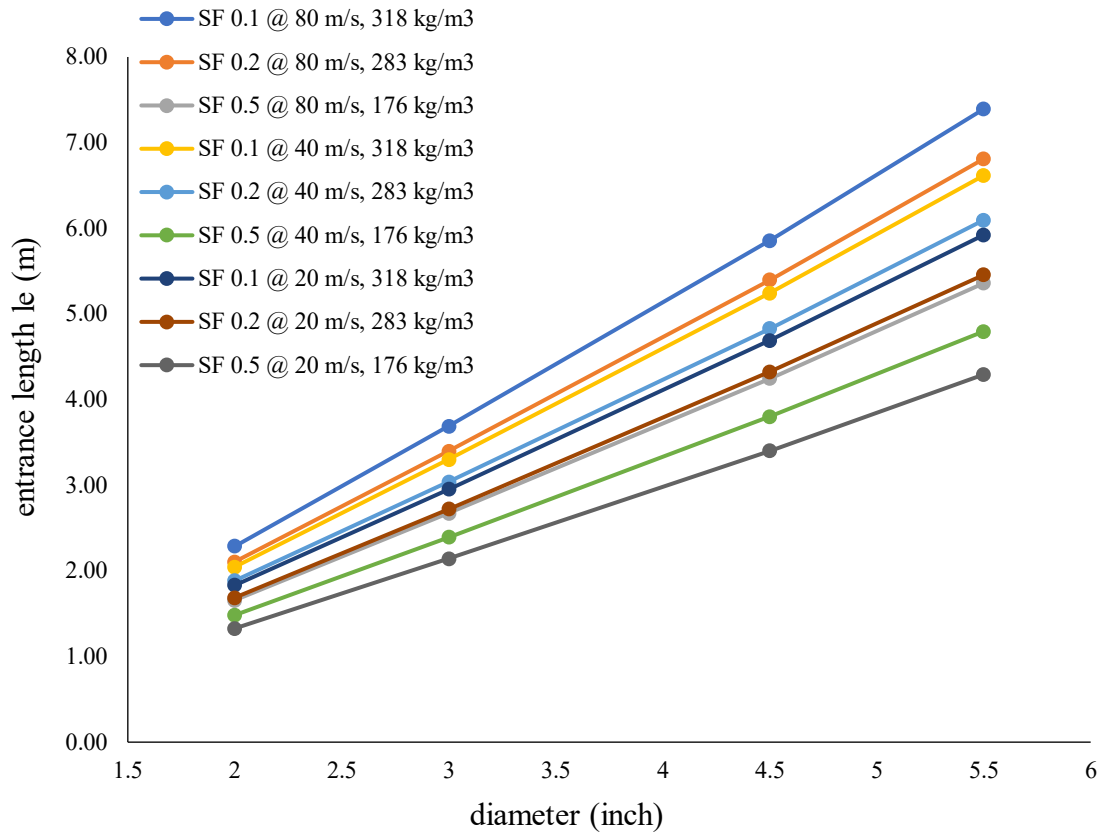


Figure 3. 32 shows a change in the entrance of length for 3-phase flow with different solid fractions and different density at variable velocities.

From the previous three-phase flow entrance of length graphs with a change in solid fraction, velocity and density can conclude the following.

1. The increase of solid fraction the entrance of length will decrease for all velocities and vice verse.
2. When the density decreases the entrance of length will decrease as well with different velocities.

### 3.5.2 Entrance Length Calculation for Three-Phase (Water, Air and Solid) with Change in Viscosity

Table 3. 30 shows the water, air, and solid with a change in viscosity for 3-phase

water viscosity (pa.s)	Air Viscosity (pa.s)	Air and Water Viscosity (pa.s)	Solid Fraction	Water & Air Fraction	Mixture viscosity (pa.s)
4.45E-04	9.00E-06	2.27E-04	0.1	0.9	3.16E-04
4.45E-04	9.00E-06	2.27E-04	0.2	0.8	4.69E-04
4.45E-04	9.00E-06	2.27E-04	0.5	0.5	1.31E-03

Table 3. 31 shows the summary entrance of length with homogenous velocity 20 m/s for three-phase with variable liquid, air, and solid fraction and different viscosity

ID (inch)	ID (m)	Liquid + Air Hold up	Solid Fraction	Mixture $R_e$	Velocity (m/s)	Mixture Density (kg/m <sup>3</sup> )	$L_e$ (inch)	$L_e$ (m)	Mixture Viscosity pa.s
<b>3-Phase Air, Water and Solid</b>									
2	0.051	0.9	0.1	1.5E+06	20	452.7	85	2.16	3.16E-04
3	0.077	0.9	0.1	2.2E+06	20	452.7	137	3.49	3.16E-04
4.5	0.114	0.9	0.1	3.3E+06	20	452.7	218	5.55	3.16E-04
5.5	0.140	0.9	0.1	4.0E+06	20	452.7	276	7.00	3.16E-04
2	0.051	0.8	0.2	8.73E+05	20	402.4	79	1.99	4.69E-04
3	0.077	0.8	0.2	1.32E+06	20	402.4	127	3.22	4.69E-04
4.5	0.114	0.8	0.2	1.96E+06	20	402.4	201	5.11	4.69E-04
5.5	0.140	0.8	0.2	2.40E+06	20	402.4	254	6.45	4.69E-04
2	0.051	0.5	0.5	1.9E+05	20	251.5	62	1.6	1.31E-03
3	0.077	0.5	0.5	2.9E+05	20	251.5	100	2.5	1.31E-03
4.5	0.114	0.5	0.5	4.39E+05	20	251.5	158	4.02	1.31E-03
5.5	0.140	0.5	0.5	5.4E+05	20	251.5	200	5.07	1.31E-03

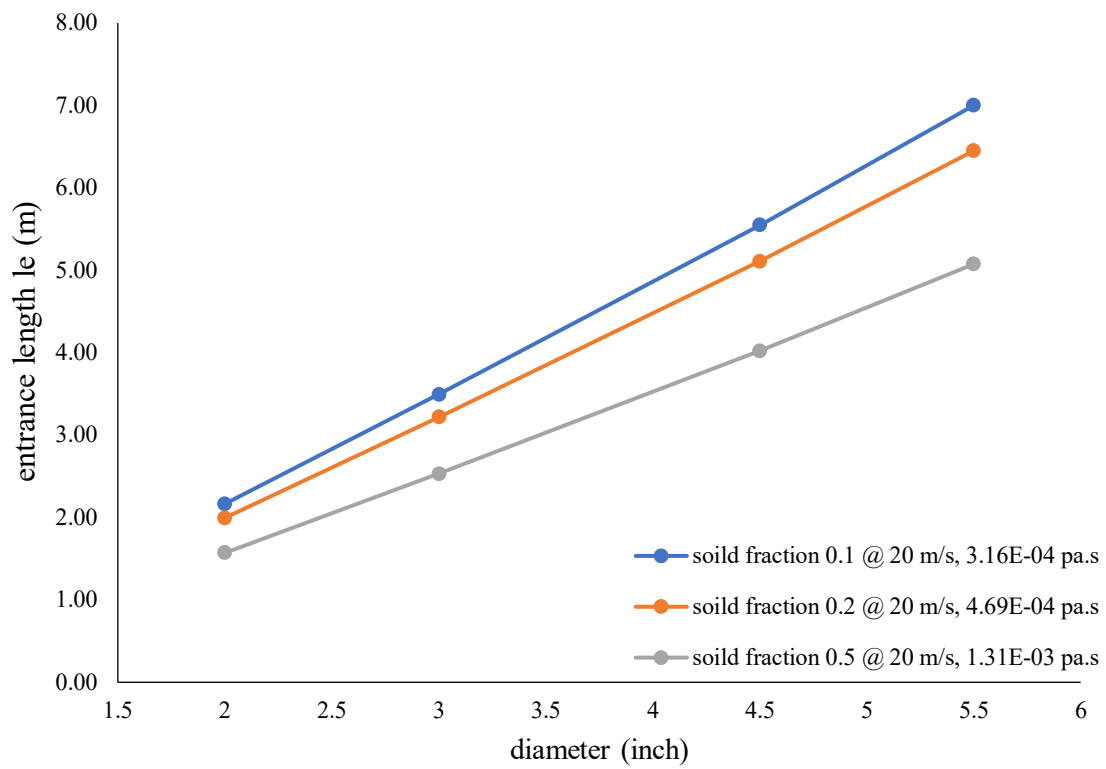


Figure 3. 33 shows a change in entrance of length for 3-phase flow with different solid fractions and different viscosity at a homogenous velocity 20 m/s.

Table 3. 32 shows the summary entrance of length with homogenous velocity 40 m/s for three-phase with variable liquid, air and solid fraction and different viscosity

ID (inch)	ID (m)	Liquid + Air Hold up	Solid Fraction	Mixture $R_e$	Velocity (m/s)	Mixture Density ( $kg/m^3$ )	$L_e$ (inch)	$L_e$ (m)	Mixture Viscosity pa.s
<b>3-Phase Air, Water and Solid</b>									
2	0.051	0.9	0.1	2.9E+06	40	452.7	95	2.42	3.16E-04
3	0.077	0.9	0.1	4.4E+06	40	452.7	154	3.90	3.16E-04
4.5	0.114	0.9	0.1	6.6E+06	40	452.7	244	6.20	3.16E-04
5.5	0.140	0.9	0.1	8.0E+06	40	452.7	308	7.82	3.16E-04
2	0.051	0.8	0.2	1.7E+06	40	402.4	88	2.23	4.69E-04
3	0.077	0.8	0.2	2.6E+06	40	402.4	141	3.59	4.69E-04
4.5	0.114	0.8	0.2	3.9E+06	40	402.4	225	5.71	4.69E-04
5.5	0.140	0.8	0.2	4.8E+06	40	402.4	284	7.21	4.69E-04
2	0.051	0.5	0.5	0.0E+00	40	251.5	69	1.8	1.31E-03
3	0.077	0.5	0.5	0.0E+00	40	251.5	111	2.8	1.31E-03
4.5	0.114	0.5	0.5	0.0E+00	40	251.5	177	4.49	1.31E-03
5.5	0.140	0.5	0.5	0.0E+00	40	251.5	223	5.67	1.31E-03

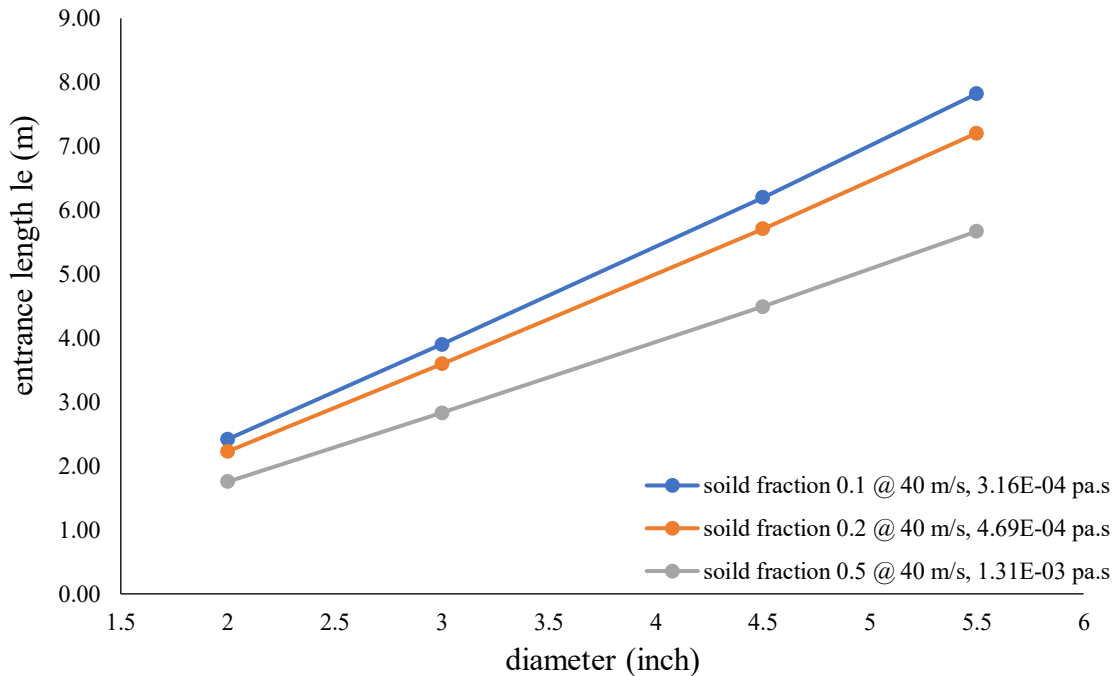


Figure 3. 34 shows a change in entrance of length for 3-phase flow with different solid fractions and different viscosity at a homogenous velocity 40 m/s.

Table 3. 33 shows the summary entrance of length with homogenous velocity 80 m/s for three-phase with variable liquid, air and solid fraction and different viscosity

ID (inch)	ID (m)	Liquid + Air Hold up	Solid Fraction	Mixture $R_e$	Velocity (m/s)	Mixture Density ( $kg/m^3$ )	$L_e$ (inch)	$L_e$ (m)	Mixture Viscosity pa.s
<b>3-Phase Air, Water and Solid</b>									
2	0.051	0.9	0.1	5.8E+06	80	452.7	106	2.70	3.16E-04
3	0.077	0.9	0.1	8.8E+06	80	452.7	172	4.36	3.16E-04
4.5	0.114	0.9	0.1	1.3E+07	80	452.7	273	6.92	3.16E-04
5.5	0.140	0.9	0.1	1.6E+07	80	452.7	344	8.74	3.16E-04
2	0.051	0.8	0.2	3.49E+06	80	402.4	98	2.49	4.69E-04
3	0.077	0.8	0.2	5.27E+06	80	402.4	158	4.02	4.69E-04
4.5	0.114	0.8	0.2	7.85E+06	80	402.4	251	6.38	4.69E-04
5.5	0.140	0.8	0.2	9.60E+06	80	402.4	317	8.05	4.69E-04
2	0.051	0.5	0.5	7.8E+05	80	251.5	77	2.0	1.31E-03
3	0.077	0.5	0.5	1.2E+06	80	251.5	124	3.2	1.31E-03
4.5	0.114	0.5	0.5	1.75E+06	80	251.5	198	5.02	1.31E-03
5.5	0.140	0.5	0.5	2.1E+06	80	251.5	249	6.33	1.31E-03

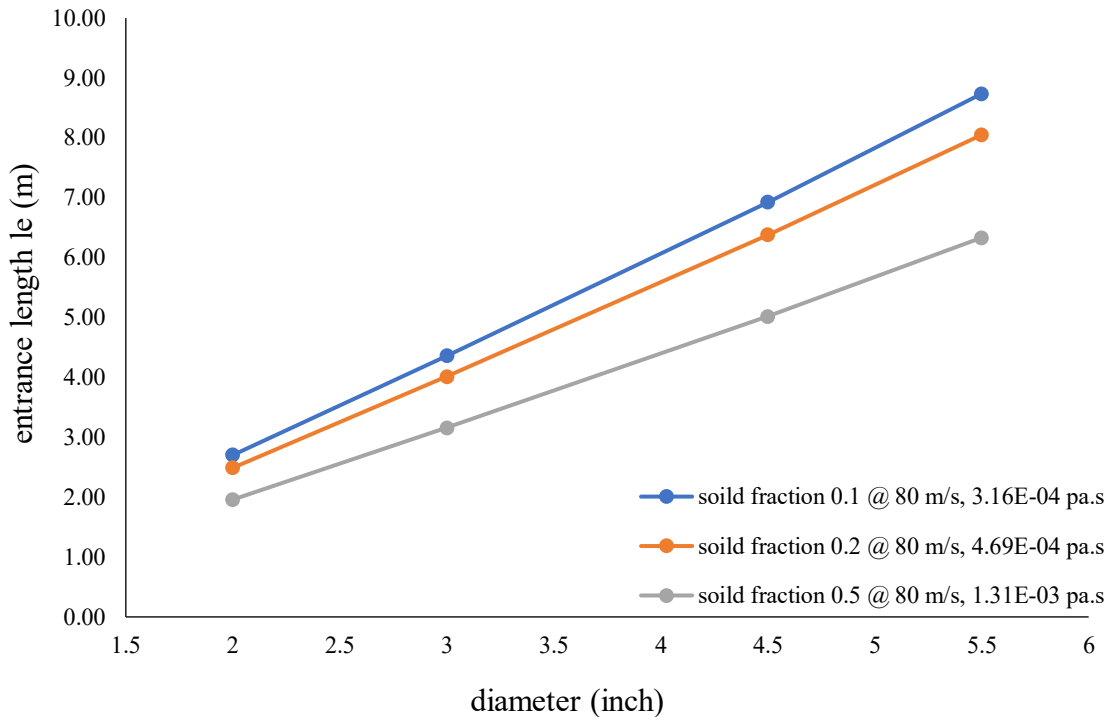


Figure 3. 35 shows a change in entrance of length for 3-phase flow with different solid fractions and different viscosity at a homogenous velocity 80 m/s.

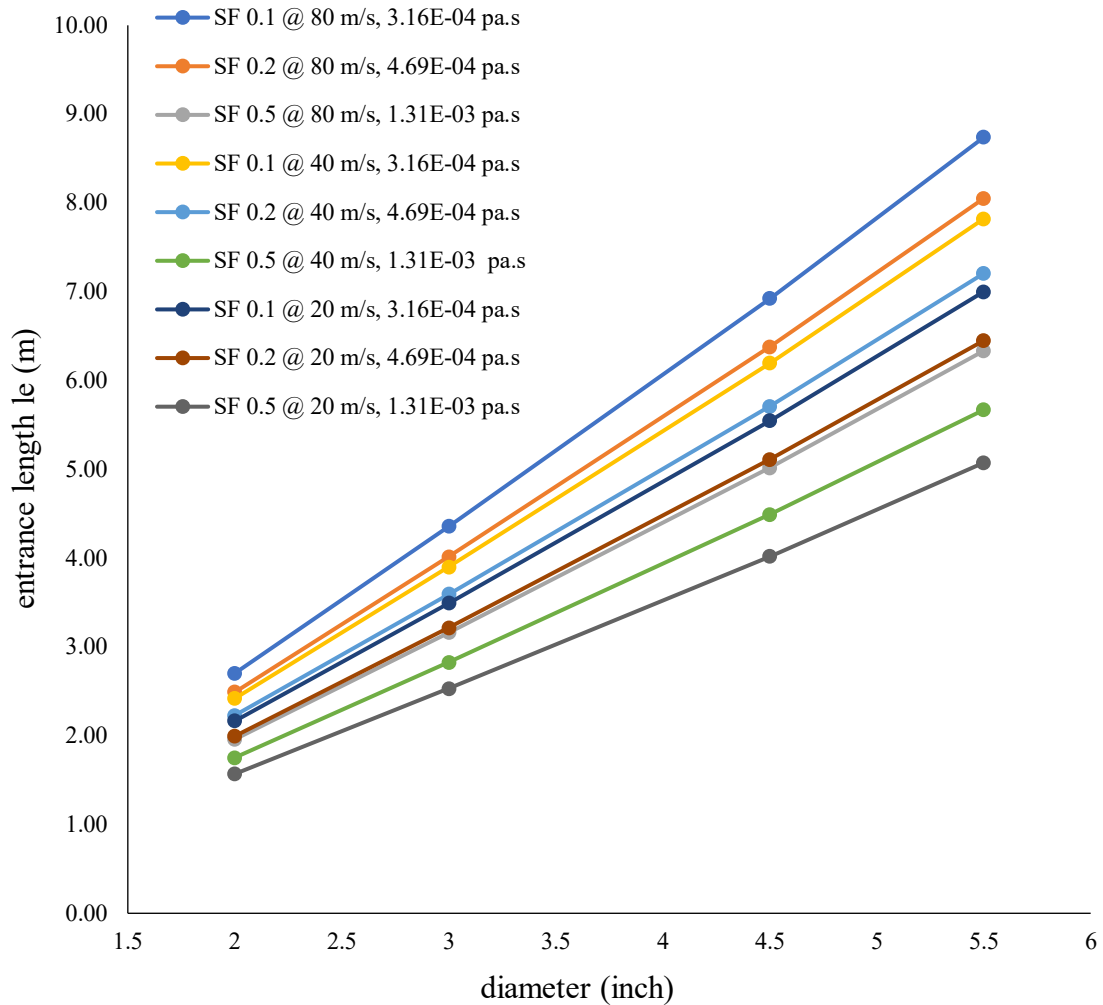


Figure 3. 36 shows a change in the entrance of length for 3-phase flow with different solid fractions and different viscosity at variable velocities.

From the previous three-phase flow entrance of length graphs with a change in solid fraction, velocity and viscosity can conclude the following.

1. The increase of solid fraction the entrance of length will decrease for all velocities and vice versa.
2. The main observed here is that when the viscosity increase as a result of an increase in solid fraction, the entrance of length will decrease for all velocities.

## Chapter 4. Literature Background

### 4. Recent studies for single and Multiphase flow loop with Technical Specifications and Fluids.

In experimental study need to select an appropriate instrumental to perform the experiment with less risk and more accuracy. The selection depended on different criteria for different devices including the pressure and flow rate in the pipeline.

This chapter shows the recent studies for the single-phase and multiphase experiment leak detection. Including the name, technical, and kind of instrument that has been used.

The main idea is to know the kind of sensors and gauges that are used before so, it will help to know the configuration of our experiment setup and how the modification for the exits flow loop at Texas A&M – Qatar can modify to be leak detection flow loop.

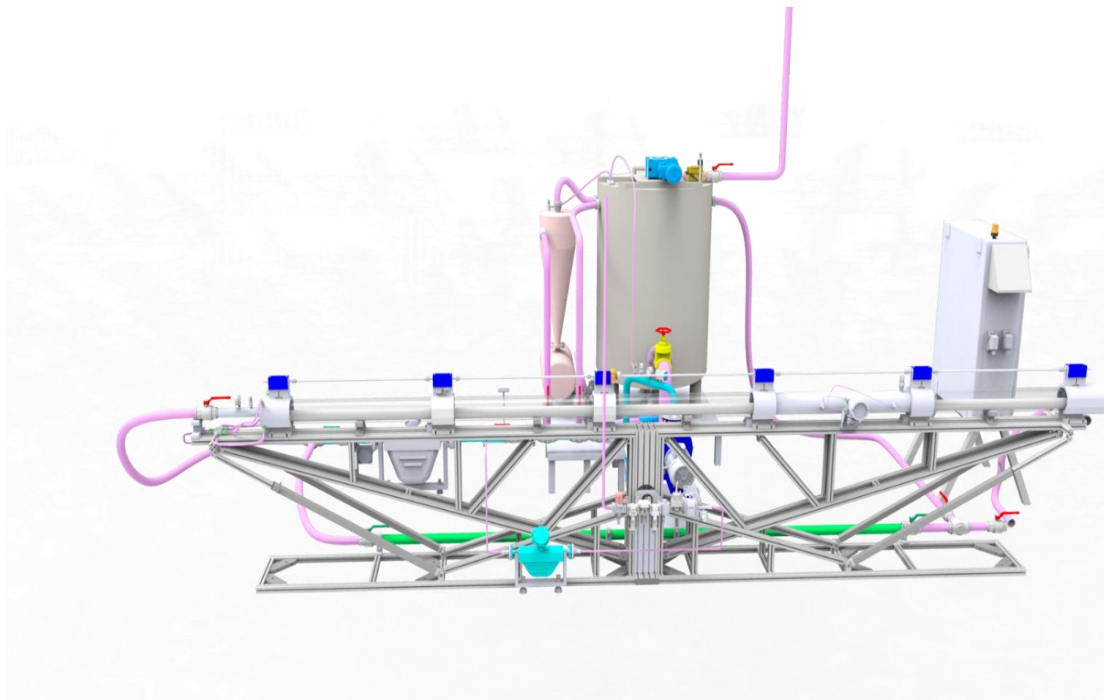


Figure 4. 1 Current Multiphase flow loop At Texas A&M University – Qatar (ant3Dlab)

#### **4.1 Single Phase Experiments.**

In the presented paper, using a single phase the potential of fiber-optic Distributed Acoustic Sensing (DAS) for the detection of small gas pipeline leaks (<1%) is investigated. The fiber -optic distribution is not directly through the pipeline it is in Helical wrapping of the sensing fiber directly around the pipeline is used to increase the system sensitivity for detection of weak leak-induced vibrations. Used accelerometer measurement as a reference to analyze the nature of recorded vibration signals in the leaking segment. <sup>29</sup>

The experiment performed with pressure buffer was firstly pumped up to 25–30 bars. When the desired buffer pressure level was reached, the valve between the buffer and the main pipeline was opened. After a brief period, pressures in the buffer and the pipeline equalized and a relatively steady leak from the holey adapter was achieved on the leak size starting with 1 mm to 8 mm.

Finally, the results reveal that (DAS) measurement using direct helical fiber application is capable of detecting pipeline natural vibration modes induced by the broadband leak-noise excitation. Comparison with reference accelerometer data indicates that pipeline vibrations with acceleration values down to single micro are detectable in the performed experiment. <sup>29</sup>

However, the fiber application approach increases instrumentation complexity and decreases the system's ultimate monitoring range.

The increase of pipeline pressure at constant leak size was shown to lead to an increase of the magnitude of the induced signal while its general spectral content remains relatively stable. On the other hand, leaking through holes of increasing sizes leads to the excitation of vibrational modes with higher frequencies.

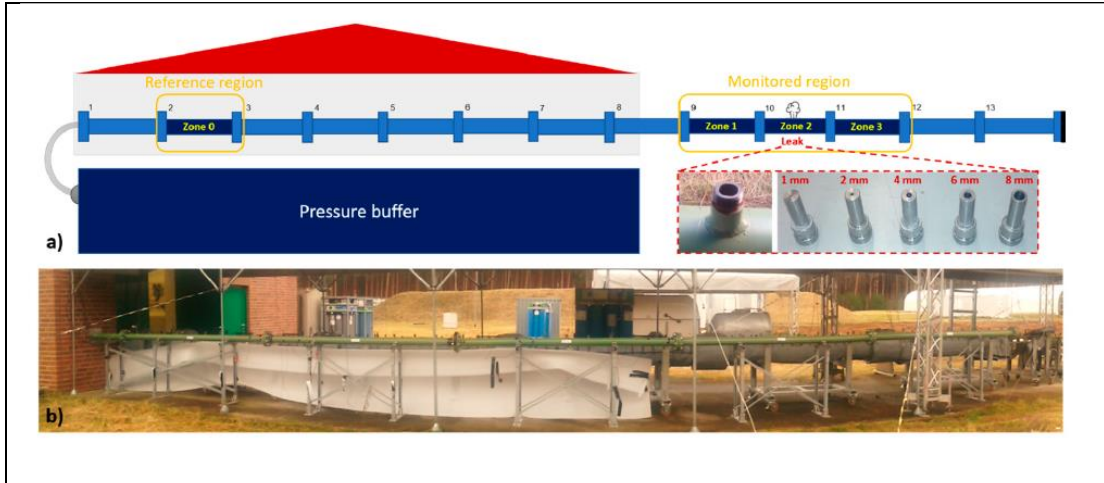


Figure 4. 2 Experimental Set-Up for Single phase <sup>29</sup>

#### 4.1.1 Single-Phase Flow

This experimental design is similar to our multiphase design especially in the pressure-temperature and acoustic sensors configuration but, the authors have not written any information related to the technical details. The configuration of instruments gives more ideas to build up the current multiphase leak detection loop.

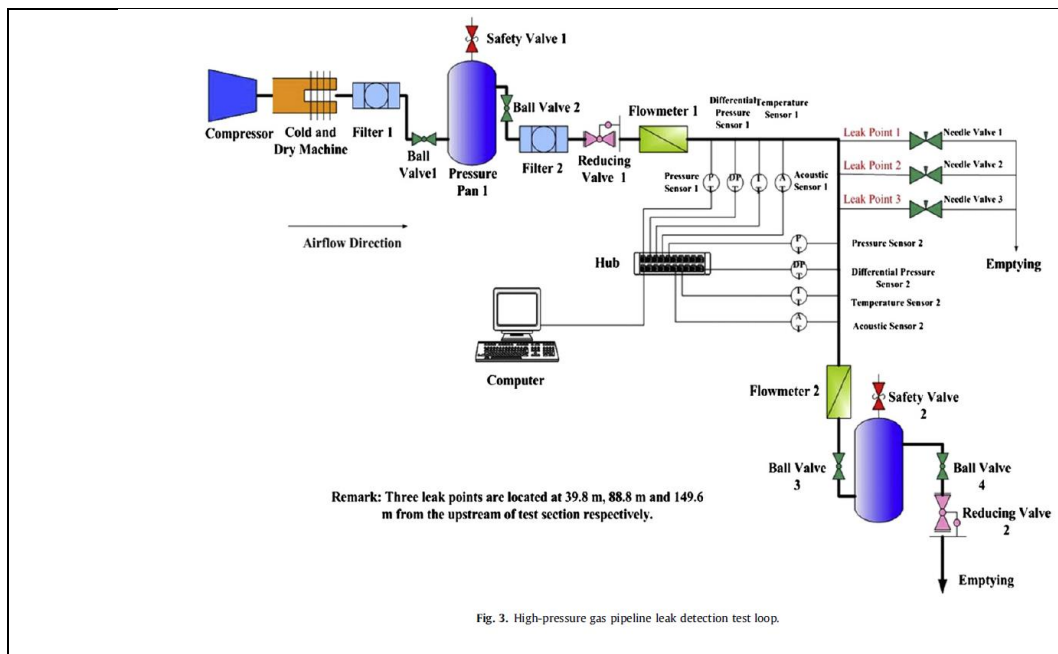


Figure 4. 3 Experimental Set-Up for Single phase <sup>30</sup>

### 4.1.2 Single-Phase Flow

Most of the recent experimental study used external sound acoustic sensors in this paper presented an experimental investigation that addressed the feasibility and potential of in-pipe acoustic measurements for leak detection. An experimental test rig was constructed to simulate a water transmission pipeline and permits different leak sizes, flow rates, and pressure

A test section of the experimental simulates by two leak sizes the large size is 2.5-cm (1-in) and the small leak size is 0.635-cm (1/4-in). The leak sizes simulate a valve located in the middle of the test section so the leak flow rate is controllable and measured at this time.

The leak flow rate has been addressed and indicates in the following table.

**Table 4. 1 shows the leak flow rate with a change in leak size at different pressure**

<b>Pressure Gauge Kpa</b>	<b>Leak Size</b>	<b>Leak Flow Rate</b>
100	Small 1/4-in	0.082 L/s
200	Small 1/4-in	0.192 L/s
300	Small 1/4-in	0.266 L/s
100	Large 1 in	4.54 L/s
200	Large 1 in	10.74 L/s

### Observation

- 1- The frequency recorded by sensors and hydrophones at the leak, upstream leak, and downstream leak shows that the leak acoustic signature may vary for the same pipe setup depending on the leak size.
- 2- When the pressure increases the leak -signature strength increase as well.
- 3- The acoustic energy of the leak signal at the leak port drops to a lower value in the downstream side of the port.

Using a swimming hydrophone. The leak acoustic signature is more observable at the leak port and downstream of the leak port.

The last observation is consistent with the reported experimental finding by Hunaidi et al. (2004), in which they observed that it is difficult to detect leaks in pipes having pressures less than 100-kPa (15 psi) <sup>31</sup>. In this experimental report agree that The acoustic signal of the leak signal becomes noticeable for line pressures above 1 bar. <sup>32</sup>



Figure 4. 4 Shows the instrument test rig <sup>32</sup>

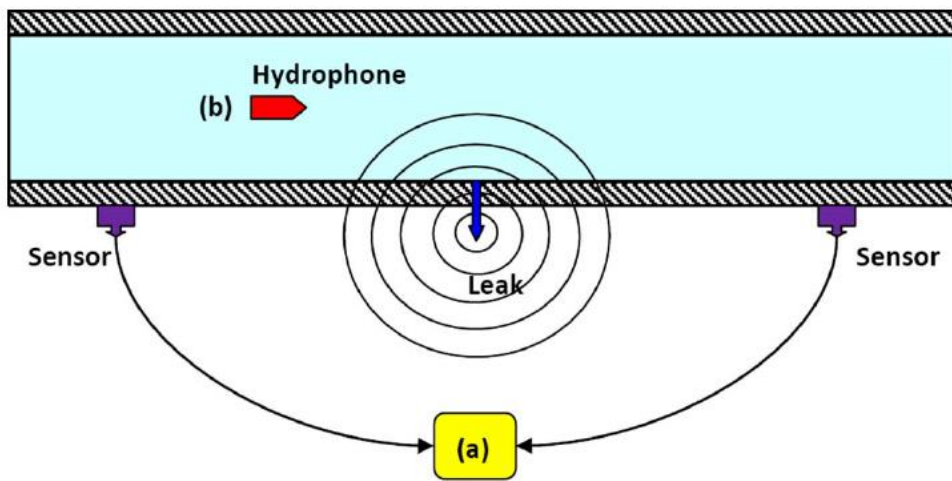


Figure 4. 5 shows the leak sound source (a) external correlation technique (b) in-pipe measurement technique <sup>32</sup>

### 4.1.3 Single-Phase Flow

Dynamic simulation models can be used along with flow and pressure measurements, for on-line leak detection and identification in gas pipeline networks. In this paper, the first part of the study is a methodology proposed for detecting and localizing leaks occurring in the gas pipeline. The proposed method is shown. The online leak detection and identification method consists of the following objectives: (a) detection of the time at which a leak has occurred by continually monitoring the measured pressures and flows (b) identification of the pipe segment or branch where the leak has occurred; and (c) estimation of the leak location and magnitude. The second part of the paper is using experiments with compressed air on a laboratory scale network. The on-line applicability of the proposed methodology was demonstrated through field level leak detection tests carried out on a 204.7km long pipeline in India, supplying natural gas to a power plant. The laboratory and field tests demonstrated that the proposed methodology can be used for quick on-line detection of leaks, and locating the leaks reasonably accurately. What is interest in this paper is the long of the pipeline and the kind of instrument that has been used to perform the experiment.

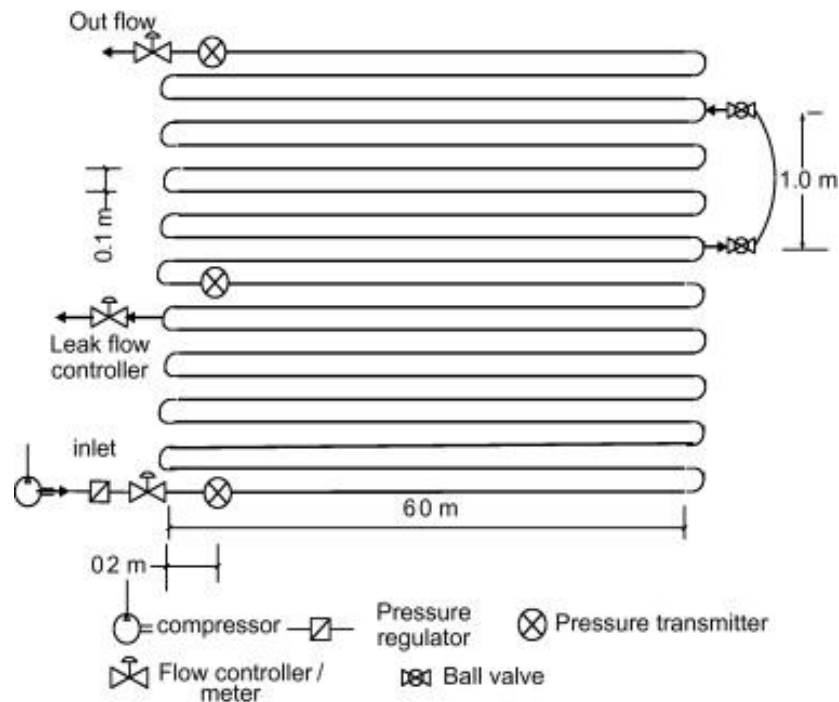


Figure 4. 6 shows the experimental set-up<sup>33</sup>

#### 4.1.4 Single-Phase Flow

Gas pipeline is key transportation equipment in the gas and petrochemical industry, and to ensure safe operation of the gas pipeline, the pipeline system needs a real-time monitor. Pipeline leakage needs alarm timely and locates accurately, in this paper they presented the new sound pressure capture method based on acoustic technology. This method taking the theory of aeroacoustics into the sound pressure calculative model solves the difficulty of the gas pipeline leakage detection.<sup>34</sup>

The vibration model of gas pipeline leakage is constructed based on harmonic analysis, and the paper proposes that the collection and the installation of the sensor should make it more sensible to the radial vibration signal. Also, the corresponding frequency to the vibration maximum amplitude near the leak hole should be reserved in the signal collection.<sup>34</sup>

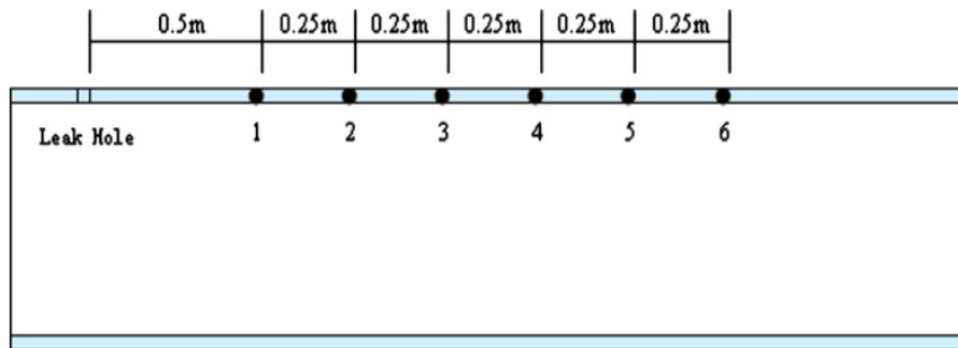


Figure 4. 7 shows the nodes schematic diagram

The vibration of the pipeline wall is analyzed with the harmonic analysis technology of the ANSYS software when the leaking wall bears broadband harmonic sound pressure.

#### 4.2 Multiphase Flow Experiments

Most of the current literature available only analyze leak detection for systems that contain single-phase flow. The earliest work that provides a comprehensive review of the different techniques, and also discusses if they are capable of detecting leaks in systems that contain multiphase flow was provided in (Scott and Barrufet 2003).<sup>35</sup>

Start with (Siebenaler 2017) paper. The main idea of this paper is to investigating underwater acoustic signatures of pipeline leaks in multiphase flow, specifically slug flow,

to determine the applicability of fiber-optic distributed acoustic sensing (DAS) technology for multiphase subsea pipeline leak detection.<sup>36</sup>

1. determine whether acoustic energy present in the multiphase leaks would be sufficiently high for detection by distributed acoustic sensing (DAS) technology.
2. compare acoustic signatures from multiphase leaks with single-phase leaks that were benchmarked in an earlier joint industry project (Siebenaler et al., 2015 and Siebenaler et al., 2016).

In this paper were generated using hydrophones, which are point-measurement instruments. DAS systems are distributed measurement technologies so, while there is not a direct comparison between results, it is assumed that the results from the hydrophones can be used to infer similar trends from distributed systems.<sup>36</sup>

Finally, they concluded that the distribution of acoustic content as a function of frequency is the same for multiphase flow as it is for single-phase flow. As part of There is acoustic energy at least there is much acoustic in slug flow as the corresponding single-phase flow cases.

The amplitude of the gas pocket leak signal is greater than the amplitude of the slug leak signal at lower frequencies (up to approximately 500 Hz) but, after 500 Hz the slug leak signal is more than the gas leak signal.

The choice of gas or liquid thresholds for sizing purposes will depend on the frequency range utilized by a particular vendor. For example, if a particular vendor is looking at the acoustic energy produced by gas leaks at low frequencies, the detection threshold should be higher than if the vendor is looking at the energy produced at high frequencies. The opposite is true for liquid leaks.<sup>36</sup>

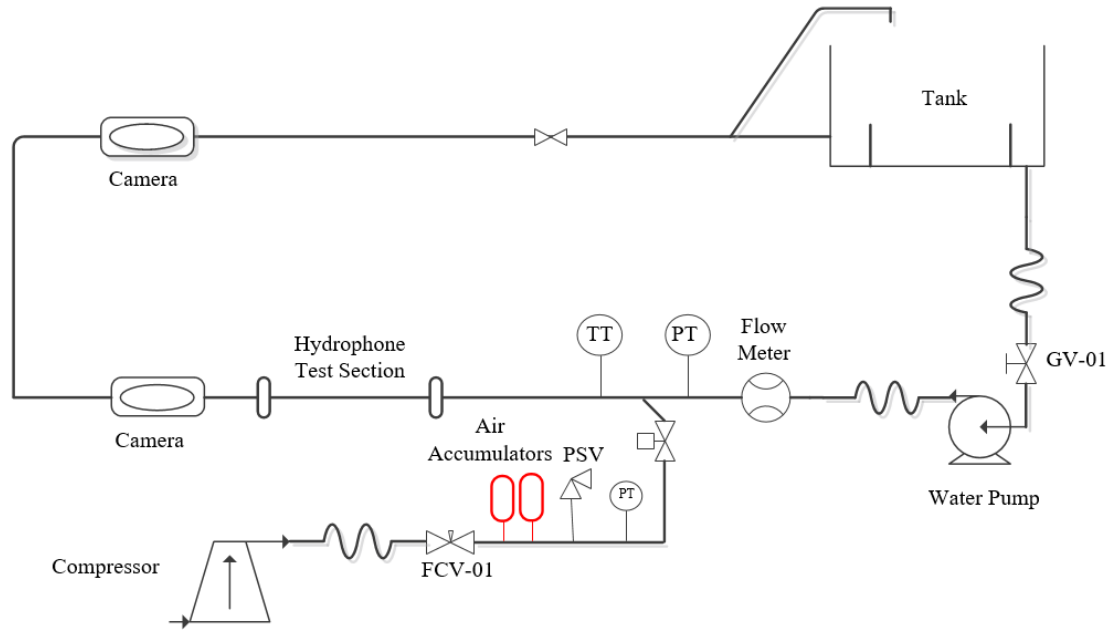


Figure 4. 8 shows a sketch of the experimental set-up<sup>36</sup>

Volume fraction calculation in the presented paper used two pairs of conductivity probes were placed at the inlet of the test section to measure impedance, which provided an indirect measure of the liquid fraction in the gas-liquid mixture.<sup>36</sup> The following table 3.3 shows all the components that have been used in the experimental work including the name of the model, type, and range.

#### 4.2.1 Two-phase Flow

Many traditional methods of signal processing are used in the early study, such as the signal mean, average amplitude, signal variance, and mean square value. But under a three-flow pattern, the change of acoustic characteristics of leakage signal is not obvious by traditional methods. In this research, it is found that the Empirical Mode Decomposition (EMD) correlation can effectively analyze the signals of leakage acoustic.

The key of EMD technology is empirical pattern decomposition. It decomposes complex signals into finite intrinsic mode function (IMF). The IMF components contain the characteristics of signals at different timescales of the original signal. The foundation of EMD technology is separate from the Fourier transform technology, which processes no stationary signals always resulting in false signals and redundant signal components.<sup>37</sup>

In this study, conducted an acoustic leakage detection experiment in gas-liquid, two-phase pipelines. Acoustic leakage detection is based on the leakage acoustics of signals generated when leakage occurs. The leakage rate is estimated by the amplitude of the acoustic wave, and it increases with the increase of the amplitude of acoustic signals.<sup>37</sup>

In this study used the Mandhane flow pattern to select the range of gas-liquid flow rates for different flow patterns in horizontal pipelines. Stratified, wave and slug flow

**Table 4. 2 shows the flow regime perform with specific gas and liquid flow rates**

Flow Regime	Gas Flow Rate m <sup>3</sup> /h	Liquid Flow Rate m <sup>3</sup> /h
Stratified	10 m <sup>3</sup> /h	0.1 m <sup>3</sup> /h
Wave	25 m <sup>3</sup> /h	3.5 m <sup>3</sup> /h
slug	15 m <sup>3</sup> /h	0.6 m <sup>3</sup> /h

Finally, EMD-based acoustic signature analyses could successfully recognize the leakage signatures based on verified experimental data.

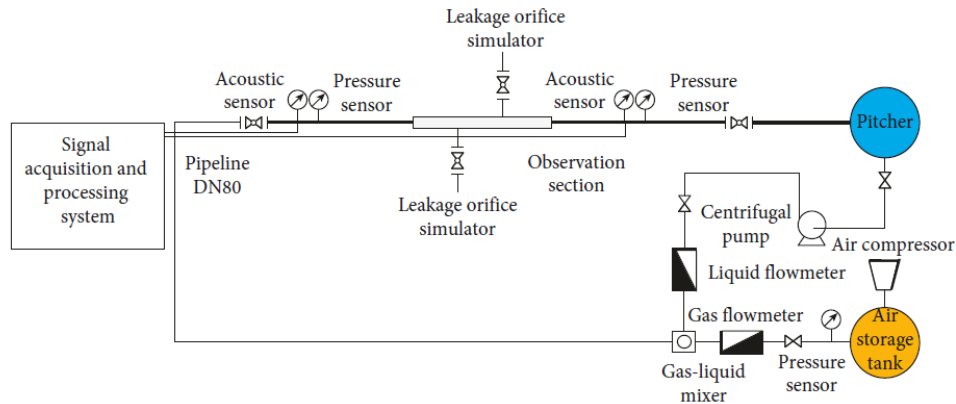


Figure 4. 9 shows the flow chart of the acoustic leakage experimental<sup>37</sup>

**Table 4. 3 show the experimental component details**

Experimental Technique			Fluid & Flow Regime	Geometry Diameter & Material	Leak Size	Experimental Result	Limitation
<b>Stajanca et al., 2018</b>	Pressure	Range to <b>30 bars</b>	Single-phase Air Horizontal flow	Overall length 38m Pipe OD 114.3 mm (4.5- in) (DN100)	1,2,4,6,8 mm	fiber application approach relying on direct fiber wrapping around the pipeline is used to detect weak leak-induced pipeline vibration and it is successes to indicate small leak vibration signals	Applied from medium to short pipeline gas.  the particular geometry of the leak influences generated vibration signals.
	Single-mode optical fiber	SMF-28e, Corning, cable					
	accelerometer	KS95B.100, MMF, Radebeul, Germany) 200 kHz acquisition rate					
	Distribution acoustic sensor DAS	(Helios DAS, Fotech Solutions, Church Crookham, UK) Specification 200 ns laser pulse length and 80 kHz pulse repetition rate					
<b>Yuxing, L et al, 2012</b>	Acoustic Sensor	Range 0/57.3 Kpa sensitivity sensor 43.5 mV/kpa	Air flow Horizontal flow	ID 10mm (0.39 -in) test pipeline 200.8	0.45 & 0.5 mm (0.017–0.019 -in)		
	Operation pressure	8 Mpa (1160 psi)					
<b>Khulief, Y et al, 2012</b>	Pressure	300 Kpa – 3 bar	Water flow Horizontal flow	4-in ID Plastic pipeline	Large leak is (1-in) Small leak (0.25 -in)	Mainly make a comparison between the acoustic spectrum in pipeline of the leak – free and	The hydrophone is fixed inside the pipeline. If the hydrophone is in movement along the pipeline how
	Pump	10-hp centrifugal pump ( <b>Goulds 21/2 × 3-in</b> )					
	Hydrophone	Brüel & Kjør hydrophone <b>type 8103</b> frequency range 0.1 Hz to 180 kHz with a receiving					

		sensitivity of -211 dB re 1 V/ $\mu$ Pa.				that with same pipeline with an induced leak. To carry out the in-pipe hydrophone measurement technique in field applications	can investigate the leak signal and location when collection the data from traversed hydrophone
	Five-channel data acquisition system	<b>B&amp;K PULSE</b> type 3560-B PULSE software type 7707					
	Flow meter	Standard 10.15-cm 4-in stainless steel orifice					
	Tank size	1 m <sup>3</sup> plastic tank					
<b>Reddy, H. P. et al , 2011</b>	Pipeline	Perspex tubes	Air flow Pipeline with U bends	ID 12 mm (0.47 -in) & OD 18 mm (0.70-in) 120-meter total length	According to flow rate range from 0-30 SLPM (Standard liter per minute)	Study the leak detection and location used change in pressure through the pipeline after leak and change in mass flow rate after leak ass well make clear to identify noise leak location	
	Compressor	AirEquip, Chennai max pressure 12kg/cm <sup>2</sup> and tank size was 160l					
	Pressure sensor	Tecsis make (Forbes Marshall)					
	Mass flow meter/controllers	Cole Parmer, United States) <b>Range 2.5–250 SLPM</b> (standard liters per minute).					
<b>Liang et al, 2013</b>	Pressure	0.4 Mpa	Gas Flow	ID 0.05 m	1 to 5 mm	CFD Result not Experimental	
<b>Siebenaler et al , 2017</b>	High speed camera	S-PRI 130421-11 500 frames/sec.	slug flow air & water	5 -in O.D 127 mm	(0.125-0.375 -in)	Study the power spectrum signal	

	Geophone	The hydrophones Bruel & Kjaer (B&K) Model Type 8104, (frequency range of <b>0.1 Hz to 120 kHz.</b> )	Horizontal Flow			of different leak size and position in gas phase and slug phase by using the geophone signal record outside the pipeline and close to the leak location  Distribution of acoustic content as a function of frequency is the same for multiphase flow as it is for single-phase flow.	The data included in this paper are based on hydrophone measurements and no DAS data are included
	Density measure	Nuclear gamma densitometers S-TEC Model DT-9315 150-mCu Cs-137 sources					
	Gas compressor	Gas compressor with a maximum capacity of 350 <b>scfm at 300 psig.</b>					
	Manual Ball valve flow control	Model FCV 01					
	PVC FLANGE	Connection with acrylic pipe					
<b>Ji, J. et al, 2018</b>	Pressure sensor	MPM480	Gas-liquid, two-phase Horizontal flow	80 mm (3.14 -in) DN 80	3,4,5,6 mm Result only on 5 mm (0.19-in)	Using of Empirical Mode Decomposition EMD with acoustic leak signal and identify the leakage signature	
	dynamic pressure	<b>PCB106B</b> Range ( <b>-57.2 kPa to 57.2 kPa</b> ) sensitivity is 43.5 mv/kPa.					

## Chapter 5. Experimental Setup

### 5.1 Current Experimental Design Goal

Design and development of an experimental setup capable of collecting sensor measurements to examine the potential of using statistical monitoring techniques to determine if a leak has occurred early or not. The ability to detect a micro-leak is also of interest. The current modified setup will be initially designed to be used with air and water as the working fluid then solid part as multiphase flow.

### 5.2 Eventual Experimental Design Goal

An eventual plan for this project is to perform the multiphase loop for leak detection. A second eventual goal is to simulate subsea conditions by developing an aquarium to submerge the pipeline under so that leak behavior can be observed and studied under these conditions.

This report will primarily serve to cover updates regarding the progress of the current experimental design goal.

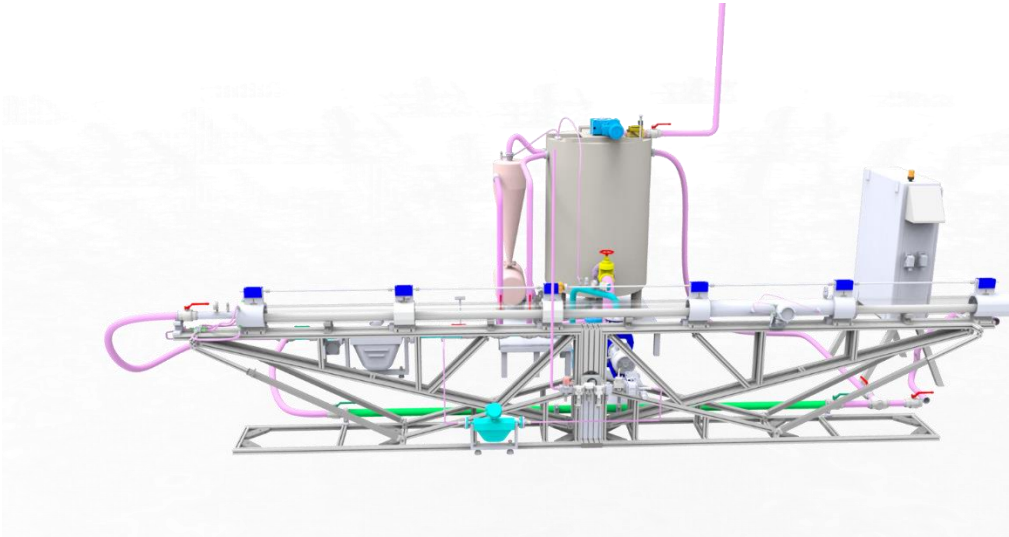


Figure 5. 1 Show the current multiphase flow loop at Texas A&M University – Qatar (ant3Dlab)

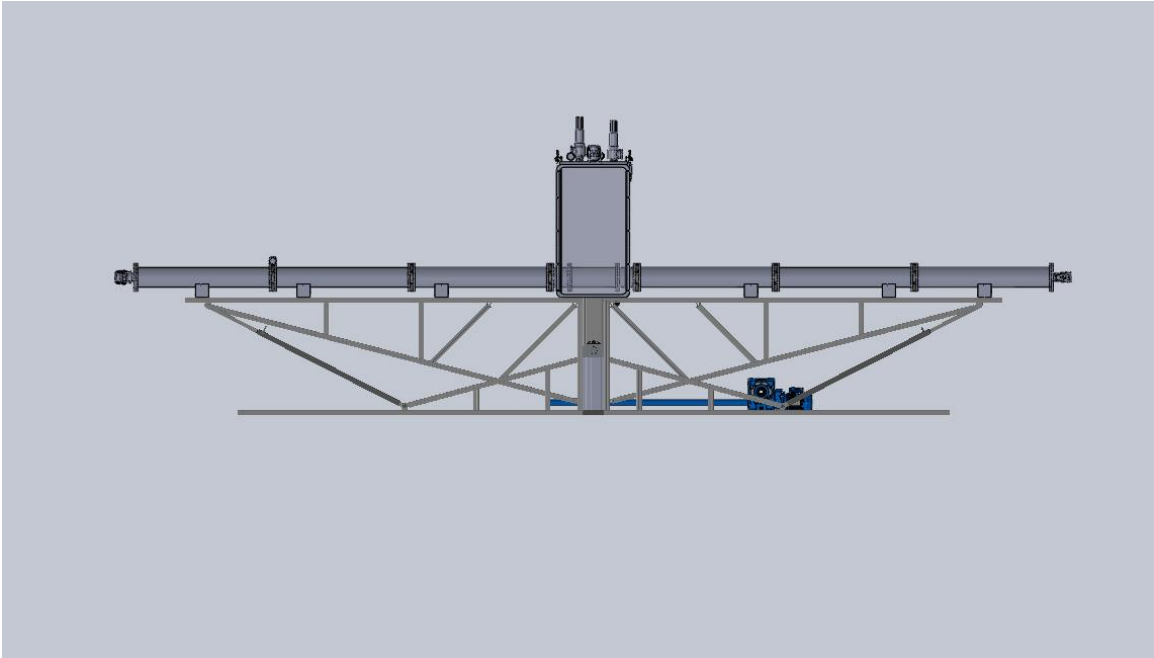


Figure 5. 2 Shows the modified multiphase flow loop leak detection 2D Drawing (ant3Dlab)

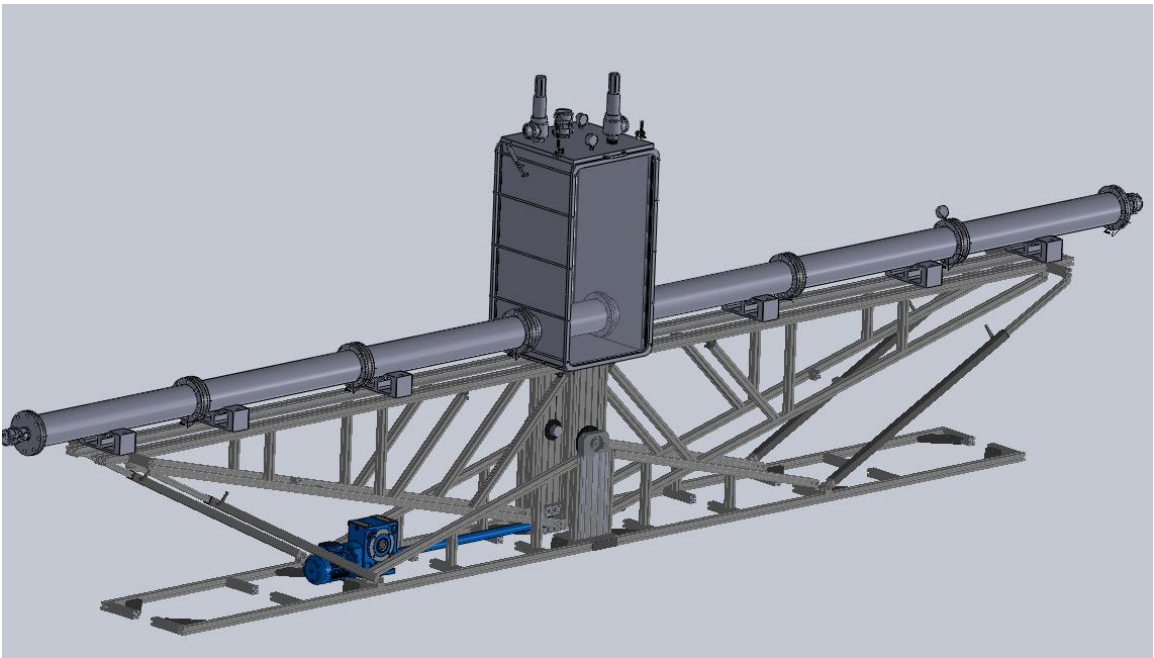


Figure 5. 3 Shows the modified multiphase flow loop leak detection 3D Drawing (ant3Dlab)

**Table 5. 1 show the Modification for the multiphase flow loop to leak detection**

<b>Equipment</b>	<b>Change</b>	<b>Not Change</b>	<b>New Proposed</b>	<b>Specification</b>
Pipeline			√	Using stainless steel instead of Acrylic
Pump		√		-
Slurry pump		√		-
Structure frame			√	Proposed a new structural support frame
Compressor			√	Proposed a new compressor
Control panel		√		-
Annular pipe	√			Removed the annular pipe
Leak valve			√	Modeling leak valve
Submersed tank			√	Proposed a new subsea condition tank bath
Camera			√	Proposed a new Camera
Hydro cyclone		√		-
Water tank		√		-
Refractive Index Matching box	√			Removed
Differential Pressure	√		√	Proposed a new differential pressure
Pressure Regulator and Oil Filter			√	Proposed a new oil filter
Dynamic Pressure Transducer			√	Proposed a new dynamic pressure gauge
Acoustic data acquisition			√	Proposed a new hydrophone for acoustic acquisition
Electric Resistance Tomography ERT		√		-

## 5.3 Equipment Selection

### 5.3.1 Pipeline

Pressure drop calculations for a stainless-steel pipeline 4.5-inch internal diameter need to be assessed under the following conditions:

- Operating pressures: 8 bars.

**Volumetric flow rate:** It is the multiphase flow air and water in this case to calculate the volumetric flow rate you need to calculate the mass flow rate and velocity as well before calculation. According to the non-dimensionless map flow chart (Taitel and Dukler 1949) with different superficial velocity for both air and water at 4.5 -inch diameter the volumetric flow rate calculation shows as the following.

- Volumetric flow rate for air: 30 to 500 L/s
- Volumetric flow rate for Liquid: 0.3 to 600 L/s

### Selection of pipeline material

There is a variety of pipeline material could use to perform the experimental, such as brass, copper, and stainless. The stainless is more appropriate material to obtain the result that matching the subsea condition.

Changing in the pipeline as the current flow loop pipeline material is Acrylic which has the ability to working under maximum pressure 2 bars and the new proposed working pressure is 8 bars. Pipeline material needs to change from Acrylic to stainless steel that can work at high pressure.

The pipeline inner diameter is computed as follows.

Pipeline Inner Diameter ID = Pipeline Outer Diameter (OD) – (2 x Tube Wall Thickness)

$$\begin{aligned}\text{Pipeline ID} &= 5 \text{ in} - (2 \times 0.250 \text{ inch}) \\ &= 4.5 \text{ inch}\end{aligned}$$

## Pipeline Connection

The total flow loop length is 6.5 meters each section 1 meter separate except the tank aquarium 0.5 m. A decision to be each 1-meter separate connected with flange to make is easy for assembling and for installation the gauges another reason for future planning might be required to change one section for visualization or other reasons.

### 5.3.2 Acrylic pipeline material

The multiphase flow in the pipeline consider as complex kind of fluids so to capture the behavior of fluid in the pipeline (3.28 ft) of the total pipeline length will be acrylic glass pipe to allow capturing the picture and film the movement of fluids inside the pipeline during the run of experimental.

### 5.3.3 Differential Pressure Transducer Availability

The pressure drop will be measured across a length of **3.28 ft**. The length of the pipeline is directly proportional to the expected pressure drop i.e. a longer length will correspond to a higher pressure drop.

To select an appropriate differential pressure transducer for the current experimental it is required to work in parallel with the current pipeline dimensions 4.5 inches. A list of the available differential pressure transducers and their ranges are provided in the following table with (Pa and mbar).

**Table 5. 2 show the availability of the pressure gauge ranges**

Range					Choice	
0	25	mbar	0	2500	pa	A
0	70	mbar	0	7000	Pa	B
0	170	mbar	0	17000	Pa	C
350		mbar	35000		Pa	D
1		mbar	100000		Pa	E
2		mbar	200000		Pa	F
3.5		mbar	350000		Pa	G
7		mbar	700000		Pa	H

10	mbar	1000000	Pa	I
17.5	mbar	1750000	Pa	J
35	mbar	3500000	Pa	K
50	mbar	5000000	Pa	L
70	mbar	7000000	Pa	M

In our experimental design, we have two flow air and liquid to calculate the pressure drop for two- phases in a horizontal pipeline Lockhart Martinelli correlation have been used here<sup>38</sup>. Starting with calculating the pressure drop for each single-phase air and water using the fanning equation by applying for the Reynold number with superficial velocity then perform Lockhart Martinelli method to calculate the two-phase pressure drop.

$$R_e = \frac{\text{Density} * \text{Velocity} * \text{Diamter}}{\text{Viscosity of Fluid}} \quad \text{Eq 4.1}$$

Fanning equation:

$$dP = \frac{f \rho v^2}{2D'} \quad \text{Eq 4.2}$$

Where:

f: fraction factor

$\rho$ : fluid density (kg/m<sup>3</sup>)

v: Fluid velocity (m/s)

D: pipeline diameter (m)

### 5.3.3.1 Lockhart–Martinelli Correlation.

In 1949, Proposed Correlation of Data for Isothermal Two-Phase Flow, Two-Component Flow in Pipes, In the correlation the assumption made is no volume fraction generation is needed. The pressure drop in single-phase is the same as in two-phase flow pressure drop multiple by some multiplier.

$$\left[ \frac{dP}{dL} \right]_{2-p} = \phi^2_G \left[ \frac{dP}{dL} \right]_{s-p} \quad \text{Eq 4.3}$$

If you know how to calculate  $\phi_L^2$  or  $\phi_G^2$  then you can calculate pressure drop for two phases.

The **Lockhart–Martinelli** parameter  $X^2$

$$X^2 = \frac{\phi_G^2}{\phi_L^2} \quad \text{Eq 4.4}$$

$$X = \sqrt{\frac{\left[\frac{dP}{dL}\right]_{SL}}{\left[\frac{dP}{dL}\right]_{SG}}} \quad \text{Eq 4.5}$$

Where:

SL: Single Phase Liquid

SG: Single Phase Gas

Another correlation is needed to calculate the  $\phi_L^2$  or  $\phi_G^2$

$$\phi_G^2 = 1 + Cx + X^2 \quad \text{Eq 4.6}$$

$$\phi_L^2 = 1 + \frac{C}{X} + \frac{1}{X^2} \quad \text{Eq 4.7}$$

Based on the Reynold number the constant C can be estimated according to the following table.

**Table 5. 3 shows Lockhart–Martinelli constant**

<b>Liquid</b>	<b>Gas</b>	<b>C</b>
Turbulent	Turbulent	20
Laminar	Turbulent	12
Turbulent	Laminar	10
Laminar	Laminar	5

In addition, the three-phase flow has been calculated with air, water, and solid. An example for solid Polypropylene considers with a maximum solid concentration 15%. By using the modified Lockhart Martinelli correlation<sup>39</sup>. Base on two and three-phase the pressure differential gauge has been chosen to use for purpose of two and three-phase flow.

### 5.3.3.2 Modified Lockhart Martinelli correlation

Using the Modified **Lockhart Martinelli correlation** parameter to calculate the pressure drop for three phases fluid.

$$\left[ \frac{dP}{dL} \right]_{fs} = \frac{4\tau_w}{D} \quad \text{Eq 4.8}$$

$$\tau_w = \frac{j_{fs}^2}{8} (\rho_f f_f + \rho_s f_s) \quad \text{Eq 4.9}$$

Where  $D$  is the diameter. In Eq. 4.9  $j_{fs}$  is the slurry superficial velocity,  $\rho_f$  and  $\rho_s$  are the liquid and particle densities,  $f_f$  is the Darcy – Weisbach friction factor for the liquid flowing at the slurry velocity <sup>39</sup>.

Finally,  $f_s$  is the particle friction factor, it increases the Fraction Pressure Gradient (FPG) accounting the friction caused by the particle-particle and particle-wall collisions, and it can be computed using Eq. 4.10, as a function of the linear concentration  $\lambda$  (Eq. 4.11), and the dimensionless particle diameter  $d^+$  (Eq. 4.12) to the shortest distance between neighboring particles. In Eq. 4.11,  $C_{\max}$  is the maximum package concentration of the solid phase, this is the maximum volume fraction of solid objects obtained when they are packed randomly, and  $C_s$  is the in-situ volumetric solid concentration for calculation they are taken from literature.

$$F_s = 0.00132 \cdot \lambda^{1.25} [0.15 + e^{-0.1d^+}] \quad \text{Eq 4.10}$$

$$\lambda = \left[ \left( \frac{C_{\max}}{C_s} \right)^{1/3} - 1 \right]^{-1} \quad \text{Eq 4.11}$$

$$d^+ = \frac{d \cdot j_{fs} \sqrt{\frac{f_f}{8}}}{v_f} \quad \text{Eq 4.12}$$

$$x^2 = \frac{\left[ \frac{dP}{dL} \right]_{fs}}{\left[ \frac{dP}{dL} \right]_g} \quad \text{Eq 4.13}$$

Here  $(dP/dL)_{fs}$  is calculated following Eqs. (4.8 – 4.12). Then, the multi-phase multiplier  $(\mathcal{O}^2_{fs})$  is calculated with Eq 4.7, and finally, the Fraction Pressure Gradient (FPG) for three-phase flows is obtained by modifying Eq 4.3.

$$\left[ \frac{dP}{dL} \right]_{gfs} = \phi^2_{fs} \left[ \frac{dP}{dL} \right]_{fs} \quad \text{Eq 4.14}$$

The expected pressure drops for two-phase water and air using equation 4.3 with operating pressures 8 bars are shown in the following Tables.

**Table 5. 4 shows pressure drop for different flow regime**

<b>Water Calculation for Two-Phase</b>						
		<b>Stratified</b>	<b>Wavy</b>	<b>Annular</b>	<b>Slug</b>	<b>Bubble</b>
Volumetric Flow Rate	(L/s)	0.3	1.0	3.1	51.3	103
Reynolds Number		2.56E+03	1.28E+04	3.84E+04	6.40E+05	1.28E+06
Operation Pressure	(bar)	8				
Water Density	kg/m <sup>3</sup>	996.7				
Diameter	(m)	0.1143				
Mass Flow Rate	kg/min	18	61	184	3068	6136
Fluid Velocity	m/s	0.02	0.1	0.3	5	10
Friction Factor	f	0.04	0.04	0.04	0.04	0.04
Delta P	pa	0.07	2	16	4493	17973

**Table 5. 5 shows a two-phase pressure drop for different flow regime**

<b>Air Calculation for Two-Phase</b>						
		<b>Stratified</b>	<b>Wavy</b>	<b>Annular</b>	<b>Slug</b>	<b>Bubble</b>
Volumetric Flow Rate	(L/s)	20	40	102	51	80
Reynolds Number		1.18E+05	2.36E+05	5.90E+05	2.95E+05	4.72E+05
Operation Pressure	(bar)	8				
Air Density At 8 Bars	kg/m <sup>3</sup>	9.3476				
Diameter	(m)	0.1143				
Mass Flow Rate	kg/min	11	23	57	29	46
Fluid Velocity	m/s	2	4	5	8	10
Friction Factor	f	0.015	0.015	0.015	0.015	0.015
Delta P	pa	7	27	169	42	108
<b>Multiphase Delta P for Two - Phase (pa)</b>		<b>21</b>	<b>168</b>	<b>1229</b>	<b>13237</b>	<b>45927</b>

The expected pressure drops for three-phase water, air, and solid using equation 4.14 with operating pressures 8 bars are shown in the following Tables.

**Table 5. 6 shows a three-phase pressure drop for different flow regime**

<b>Water Calculation for – Three Phase</b>						
		<b>Stratified</b>	<b>Wavy</b>	<b>Annular</b>	<b>Slug</b>	<b>Bubble</b>
Volumetric Flow Rate	(L/s)	0.2	1.0	3.0	51.0	102
Reynolds Number		2.56E+03	1.28E+04	3.84E+04	6.40E+05	1.28E+06
Operation Pressure	(bar)	8				
Water Density	kg/m <sup>3</sup>	996.7				
Diameter	(m)	0.1143				
Mass Flow Rate	kg/min	18	61	184	3068	6136
Fluid Velocity	m/s	0.02	0.1	0.3	5	10
Friction Factor	f	0.04	0.04	0.04	0.04	0.04
Delta P	pa	0.07	1.74	16	4360	17440

**Table 5. 7 shows a three-phase pressure drop for different flow regime**

<b>Air Calculation for – Three Phase</b>						
		<b>Stratified</b>	<b>Wavy</b>	<b>Annular</b>	<b>Slug</b>	<b>Bubble</b>
Volumetric Flow Rate	(L/s)	20	40	102	51	80
Reynolds Number		1.18E+05	2.36E+05	5.90E+05	2.95E+05	4.72E+05
Operation Pressure	(bar)	8				
Air Density At 8 Bars	kg/m <sup>3</sup>	9.3476				
Diameter	(m)	0.1143				
Mass Flow Rate	kg/min	11	23	57	29	46
Fluid Velocity	m/s	2	4	10	5	8
Friction Factor	f	0.015	0.015	0.015	0.015	0.015
Delta P	pa	2.45	9.81	61.34	15.33	39.26

**Table 5. 8 shows the three-phase pressure drop**

<b>Solid Polypropylene</b>						
Operation Pressure	(bar)	8				
Water Density	kg/m <sup>3</sup>	866				
Diameter	(m)	0.1143				
Solid Velocity	m/s	0.02	0.1	0.3	5	10
Friction Factor	f	2.00E-03	2.02E-03	2.03E-03	2.03E-03	2.03E-03
Delta P	pa	0.0031	0.08	0.69	192.50	770.02
<b>Multiphase Delta P for Three - Phase (Pa)</b>		<b>11</b>	<b>96</b>	<b>711</b>	<b>9852</b>	<b>35158</b>

### **5.3.4 Pressure Drop with Inclination**

Another calculation has been considered with the inclination pipeline to decide the proper differential pressure. Following the Same procedure and equations Lockhart Martinelli

correlation for two-phase and Modified – Lockhart Martinelli correlation for three phases with considering the static elevation for the pipeline. Angle has to consider in this case with different maximum angles that the structural frame can do 15° and 20°.

Starting with calculating the pressure drop for each single-phase air and water using the fanning equation plus the static elevation by applying for the Reynold number with superficial velocity then perform Lockhart Martinelli method.

### 5.3.4.1 Pressure Drop with Inclination Two-Phase

Table 5. 9 shows a two-phase pressure drop for different flow regime at an angle 20°

<b>Water Two-Phase Inclination 20°</b>						
		<b>Stratified</b>	<b>Wavy</b>	<b>Annular</b>	<b>Slug</b>	<b>Bubble</b>
Volumetric Flow Rate	(L/s)	0.3	1.0	3.1	51.3	103
Reynolds Number		2.56E+03	1.28E+04	3.84E+04	6.40E+05	1.28E+06
Operation Pressure	(bar)	8				
Water Density	kg/m <sup>3</sup>	996.7				
Diameter	(m)	0.1143				
Mass Flow Rate	kg/min	18	61	184	3068	6136
Fluid Velocity	m/s	0.02	0.1	0.3	5	10
Friction Factor	f	0.04	0.04	0.04	0.04	0.04
Delta P	pa	13390	13391	13406	17883	31363

Table 5. 10 shows a two-phase pressure drop for different flow regime at an angle 20°

<b>Air Two-Phase Inclination 20°</b>						
		<b>Stratified</b>	<b>Wavy</b>	<b>Annular</b>	<b>Slug</b>	<b>Bubble</b>
Volumetric Flow Rate	(L/s)	20	40	102	51	80
Reynolds Number		1.18E+05	2.36E+05	5.90E+05	2.95E+05	4.72E+05
Operation Pressure	(bar)	8				
Air Density At 8 Bars	kg/m <sup>3</sup>	9.3476				
Diameter	(m)	0.1143				
Mass Flow Rate	kg/min	11	23	57	29	46
Fluid Velocity	m/s	2	4	10	5	8
Friction Factor	f	0.04	0.015	0.015	0.015	0.015
Delta P	pa	132	153	294	168	233
<b>Multiphase Delta P</b>		<b>40044</b>	<b>41776</b>	<b>52073</b>	<b>52687</b>	<b>86168</b>

Table 5. 11 shows a two-phase pressure drop for different angles 15° and 20°

<b>Two-phase (Air and Water) Inclination 15°</b>		
<b>Pipeline Diameter (m)</b>	<b>velocity (m/s)</b>	<b>Multiphase Pressure Drops (pa)</b>
0.1143	2	29110
0.1143	4	31882
0.1143	5	41337
0.1143	8	72832
0.1143	10	45676
<b>Two-phase (Air and Water) Inclination 20°</b>		
0.1143	2	40044
0.1143	4	41776
0.1143	5	52687
0.1143	8	86168
0.1143	10	52073

### 5.3.4.2 Pressure Drop with Inclination Three – Phase

Table 5. 12 shows three-phase pressure drop for different flow regime at angle 20°

<b>Water Three Phase Inclination 20°</b>						
		<b>Stratified</b>	<b>Wavy</b>	<b>Annular</b>	<b>Slug</b>	<b>Bubble</b>
Volumetric Flow Rate	(L/s)	0.2	1.0	3.0	51.0	102
Reynolds Number		2.56E+03	1.28E+04	3.84E+04	6.40E+05	1.28E+06
Operation Pressure	(bar)	8				
Water Density	kg/m <sup>3</sup>	996.7				
Diameter	(m)	0.1143				
Mass Flow Rate	kg/min	18	61	184	3068	6136
Fluid Velocity	m/s	0.02	0.1	0.3	5	10
Friction Factor	f	0.04	0.04	0.04	0.04	0.04
Delta P	pa	13390	13391	13405	17750	30830

Table 5. 13 shows a three-phase pressure drop for different flow regime at an angle 20°

<b>Air Three Phase Inclination 20°</b>						
		<b>Stratified</b>	<b>Wavy</b>	<b>Annular</b>	<b>Slug</b>	<b>Bubble</b>
Volumetric Flow Rate	(L/s)	20	40	102	51	80
Reynolds Number		1.18E+05	2.36E+05	5.90E+05	2.95E+05	4.72E+05
Operation Pressure	(bar)	8 bars				
Air Density At 8 Bars	kg/m <sup>3</sup>	9.3476				
Diameter	(m)	0.1143				
Mass Flow Rate	kg/min	11	23	57	29	46
Fluid Velocity	m/s	2	4	10	5	8
Friction Factor	f	0.015	0.015	0.015	0.015	0.015
Delta P	pa	128.03	135.39	186.91	140.91	164.83

Table 5. 14 shows a three-phase pressure drop for different flow regime at an angle 20°

<b>Solid Polypropylene Three Phase Inclination 20°</b>						
Operation Pressure	(bar)	8				
Water Density	kg/m <sup>3</sup>	866				
Diameter	(m)	0.1143				
Mass Flow Rate	kg/min	61362	61	184	3068	24500
Solid Velocity	m/s	0.02	0.1	0.3	5	10
Friction Factor	f	2.03E-03	2.03E-03	2.03E-03	2.03E-03	2.03E-03
Delta P	pa	11634	11634	11635	11826	12404
<b>Multiphase Delta P</b>		<b>189</b>	<b>451</b>	<b>1310</b>	<b>20712</b>	<b>53025</b>

Table 5. 15 shows a two-phase pressure drop for different angles 15° and 20°

<b>Three-phase (Air, Water and Solid) Inclination 15°</b>		
<b>Pipeline Diameter (m)</b>	<b>velocity (m/s)</b>	<b>Multiphase pressure drops (pa)</b>
0.1143	0.02	144
0.1143	0.1	370
0.1143	0.3	1161
0.1143	5	18471
0.1143	10	48957
<b>Three-phase (Air, Water and Solid) Inclination 20°</b>		
0.1143	0.02	189
0.1143	0.1	451
0.1143	0.3	1310
0.1143	5	20712
0.1143	10	53025

### 5.3.5 Differential Pressure Transducer

By calculation pressure drop with different velocity to perform different flow regimes. The outcome is maximum and minimum pressure drop that is expected to occur doing experimentally. The maximum pressure drops calculated for the safety reason and the minimum pressure drop calculated to help the select of the differential pressure sensor in between them to confirm the sensor can record the minimum and maximum pressure drop that exposure during the experimental.

From the multiphase pressure drop calculation for two phases and three phases a decision to purchase choice E for the differential pressure sensor was made using Table 1. Choice E covers a working pressure range of 0 to 100000 Pa, which will cover experimental runs for up to 600 L/s at 8 bar operating pressure.

The proposed differential pressure sensor **Omega** model number for the selected product will be **PXM409-001BGUSBH**.

### 5.3.6 Dynamic Pressure Transducer

In addition to the differential pressure measurements, obtaining dynamic pressure measurements on either side of the pipeline leak is of interest, to examine if these readings can also be utilized to determine if a micro-leak has occurred. Dynamic pressure sensors take high-frequency pressure measurements (in the range of kHz).

At Texas A&M University has used the (**Sensors One**) company product to calculate the dynamic pressure transducer before for other flow loop and it is very simple and easy to connect with USB port. Sensors ONE / Stork Solutions was able to provide a catalog of the products that they have. The product that meets our specifications (working pressure) and is designed for a working pressure of (0 to 16 bars, 0 to 1600000 Pa ) with NPT fitting just need a converter from ¼ inch to 4.5 inches for fitting or can connect directly with a pipeline using welding.

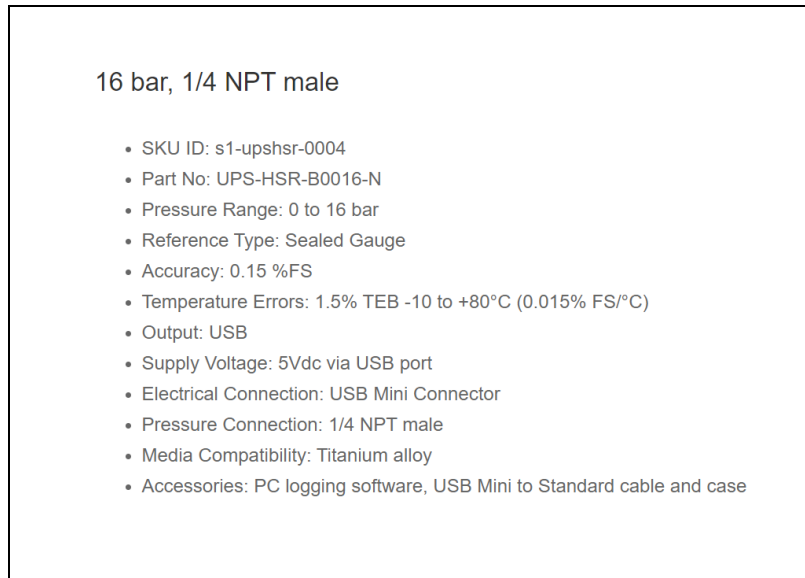


Figure 5. 4 Shows the Dynamic Pressure Transducer specification

### 5.3.7 Leak Modeling

There were two initial suggestions provided by the PI in charge of experimental design. The initial suggestion to model the leak was to create a hole in the pipeline using a 1mm drill-bit. However, several concerns arise with this method. Without a means of closing the hole, it is impossible to obtain sensor measurements under no leak conditions. A suggestion was then provided to cap the 1 mm hole using a screw cap. Unfortunately, these do not exist. It is also difficult to obtain measurements from a transient stage from a leak to no leak conditions in this hypothetical scenario.

As the recent studies (Siebenaler 2017)<sup>36</sup> performed a leak modeling with different sizes of orifices that can open and closed on demand. Each orifice had an associated actuator that allowed the operator to open/close leaks from the orifices individually. A suggestion is to use the same mechanism for modeling the leak because it is more convenient especially when simulating the offshore environment leak detection where is the pipeline will be sinking in water spool.

The final decision is to use a high precision regulating needle valve. This should allow the engineer running the apparatus to adjust the leak size as desired. It is easy to fix and attach with a motor so it can open with a specific rate remotely by a motor.

### 5.3.8 Pressure Regulator and Oil Filter

After using a compressor for a long time some oil particulates will appear with compressed air. The compressed air available in the laboratories at Texas A&M University at Qatar has been used before so some oil droplets will present with air. Therefore, an oil filter is required to eliminate the presence of these oil particulates.

Commonly, the filters come combined with pressure regulators therefore the selection will be for both filters and pressure regulators.

Need to know the maximum pressure that comes from the air compressor and the connection hoes fitting to decide the type of pressure regulator and kind of filter. However, the **IMI NORGREN** can provide different kinds of pressure regulators and oil filters with some other general-purpose for fitting.

In case Texas A&M University at Qatar orders another new compressor the presence of the filter is still necessary.

The following units will be purchased from the company:

- Model Number: B64G-3GT-AD3-RSN

This is a general-purpose filter (40 microns) with a pressure regulator with an aluminum bowl and maximum pressure 17 bars.

- Model Number: F84C-6AD-AP0

Excelon Plus oil removal filter, automatic drain, 0,01 $\mu$ m filter element

- Model Number: 840014-50KIT general mounting bracket  
840014-51KIT Excelon quick clamp  
840014-52KIT Excelon quick clamp

Those accessories are required to connect the general-purpose filter with the regulator and the oil removal filter units and attached to the wall.

### 5.3.9 Flow and Temperature Sensor

As it is necessary to determine the water and air flow rates before they gathering together to provide a quantitative analysis, flow sensors are required. Instead of having multiple

units that measure the temperature and flow throughout the setup, it is possible to have one sensor that measures both.

The flow sensor measures the fluid velocity, which can be used to determine the volume flowing through, as the dimensions of the pipe are known. The flow meter is available through **OMEGA**.

The previous design for signal phase leak detection at Texas A&M University – Qatar to measure the velocity of air and temperature they suggested to use model number is **FMA1006B-V1** from **Omega company**. It is possible to use the same suggestion model whereas the velocity and temperature are measured before mixture with liquid in a loop.

Based on the pressure drop calculation and the maximum possible air velocity is 20 m/s so, the flow sensor can measure speeds up to 50 m/s. Only fitting problems might face while the connection with the compressor. The out-port compressor connection size needs to be known or it is possible to use a converter to fit the desired size.

### **5.3.10 Tank Design**

Tank design is required for a multiphase leak detection flow loop to simulate the subsea condition. The tank will be fixed above the support structure frame at leak distance in the middle of the flow loop with a capacity of around 250 Liters.

Tank design should be more appreciative of the volume of water with a small size to allow free space for the other equipment. From the safety side, the size should not be large to make it easy to escape while the emergency case without interrupting.

The proposed tank using two metals sides to support the tank and make it stronger to hold the fluid and the other two sides acrylic material to be able to capture or filmed the leak distribution when the leak has occurred. The following figure shows the proposed tank design with dimensions 0.5 x 0.5 x 1 meter.

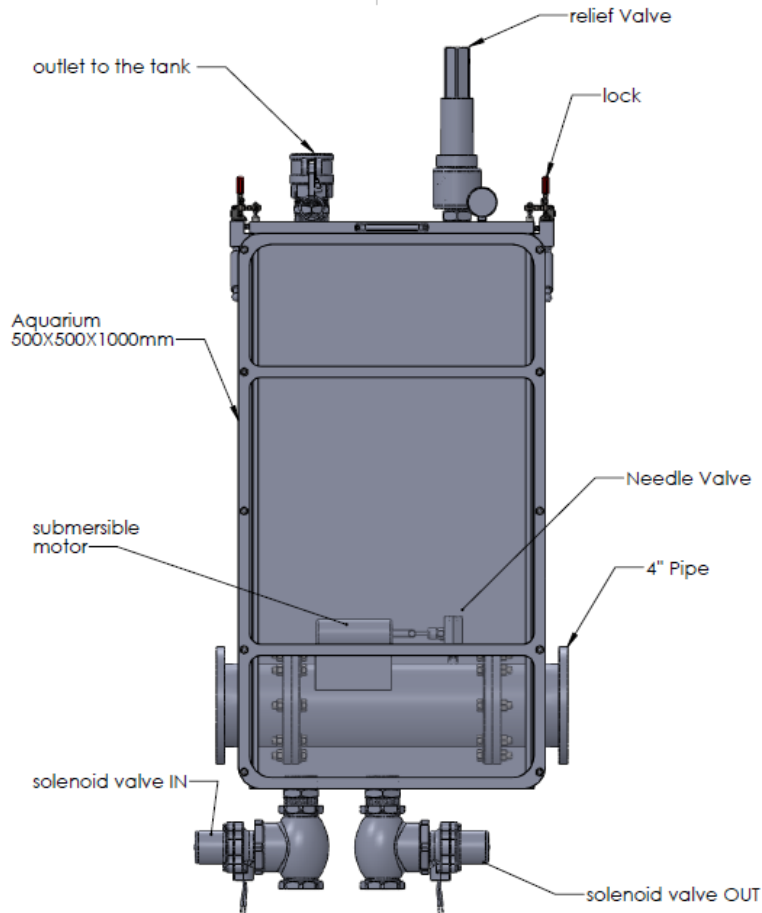


Figure 5. 5 shows the proposed tank design (ant3Dlab)

### 5.3.11 Acoustic Data Acquisition

Bruel & Kjaer hydrophone, BK 8104, with a frequency range between 0.1 Hz to 120kHz will use to measure waterborne sound. This transducer has -205 dB re 1 V/mPa receiving sensitivity. The wide range of the frequency window and exceptional omnidirectional characteristics are reasons why this transducer well-suited to this application.

This kind of hydrophone will give a chance to analyze the acoustic wave once the leak has occurred. It can be used to detect the leak acoustic sound.

### 5.3.12 Air Compressor

The air compressor is needed for the proposed modified flow loop because the working pressure is much higher above 4 bars and the central air supplier at the university for the laboratory is not enough therefore, a separate compressor is required for the experiment.

From the mass and volume flow rate calculation, a proposed to use the **Atlas Copco** air compressor company model **SF 22+**. This model is more appropriate due to the space-limited issue in the lab so it is very small and can handle easily with maximum air up to 10 bars.

**Table 5. 16 Mass Flow rate and volumetric flow rate for Air velocity.**

<b>4.5- inch Pipe 8 Bars</b>				
<b>Air Velocity(m/s)</b>	<b>M<sub>a</sub> (Kg/min)</b>	<b>M<sub>a</sub> (m<sup>3</sup>/min)</b>	<b>M<sub>a</sub> (L/min)</b>	<b>V<sub>a</sub> (L/S)</b>
0	0	0.000	0.00	0.00
0.2	1.15	0.001	1.15	2.05
0.4	2.30	0.002	2.30	4.10
0.6	3.45	0.003	3.45	6.16
0.8	4.60	0.005	4.60	8.21
1	5.75	0.006	5.75	10.26
1.2	6.91	0.007	6.91	12.31
1.4	8.06	0.008	8.06	14.37
1.6	9.21	0.009	9.21	16.42
1.8	10.36	0.010	10.36	18.47
2	11.51	0.012	11.51	20.52
2.2	12.66	0.013	12.66	22.57
2.4	13.81	0.014	13.81	24.63
2.6	14.96	0.015	14.96	26.68
2.8	16.11	0.016	16.11	28.73
3	17.26	0.017	17.26	30.78

Based on the maximum velocity and the volume flow rate for air a decision to use compressor Atlas Capco model SF22<sup>+</sup>.

### **5.3.13 Tilting Frame**

According to the change in the pipeline material from acrylic to stainless steel, the total weight of the flow loop will increase. A proposed to support the frame with a new motor that has the ability to tilting the flow loop up or down. According to the total estimation weight for the new flow loop, a proposed to use motorize model Rev.2.

**Table 5. 17 Shows the total estimation weight for the flow loop**

<b>Components</b>	<b>Weight</b>
4.5” Pipe _stainless steel (114.30mmX6.02thickness) _ 1 meter length = 16.07 X6items	96.42 kg
4.5” stainless steel flanges 14mm thickness X (12 for pipes and 4 for aquarium)	72 kg
Aquarium capacity	300 kg
Aquarium structure	180 kg
Water in the system	100 kg
<b>Total</b>	<b>748.42 kg</b>

## **Chapter 6. Cost Analysis**

Any project or research needs to provide a cost analysis to study the budget possibility to perform the research in reality or not, without cost analysis the project cannot be true.

The objective of this chapter is to describe various types of instruments price and cost analysis according to the proposed modification to change the multiphase flow loop at Texas A&M University – Qatar to Multiphase flow loop leak detection. Develop and explain the total cost of research based on that, the decision of whether to pursue a proposed tool or not.

The cost analysis regarding the proposed modification for the multiphase leak detection composed of three tables

1. experimental components of flow loop set-up table

composed of all the required instruments for modification including the supplier name, model number, and specification of the devices.

2. Image and data acquisition systems table

Including all the data acquisition methods that proposed to use

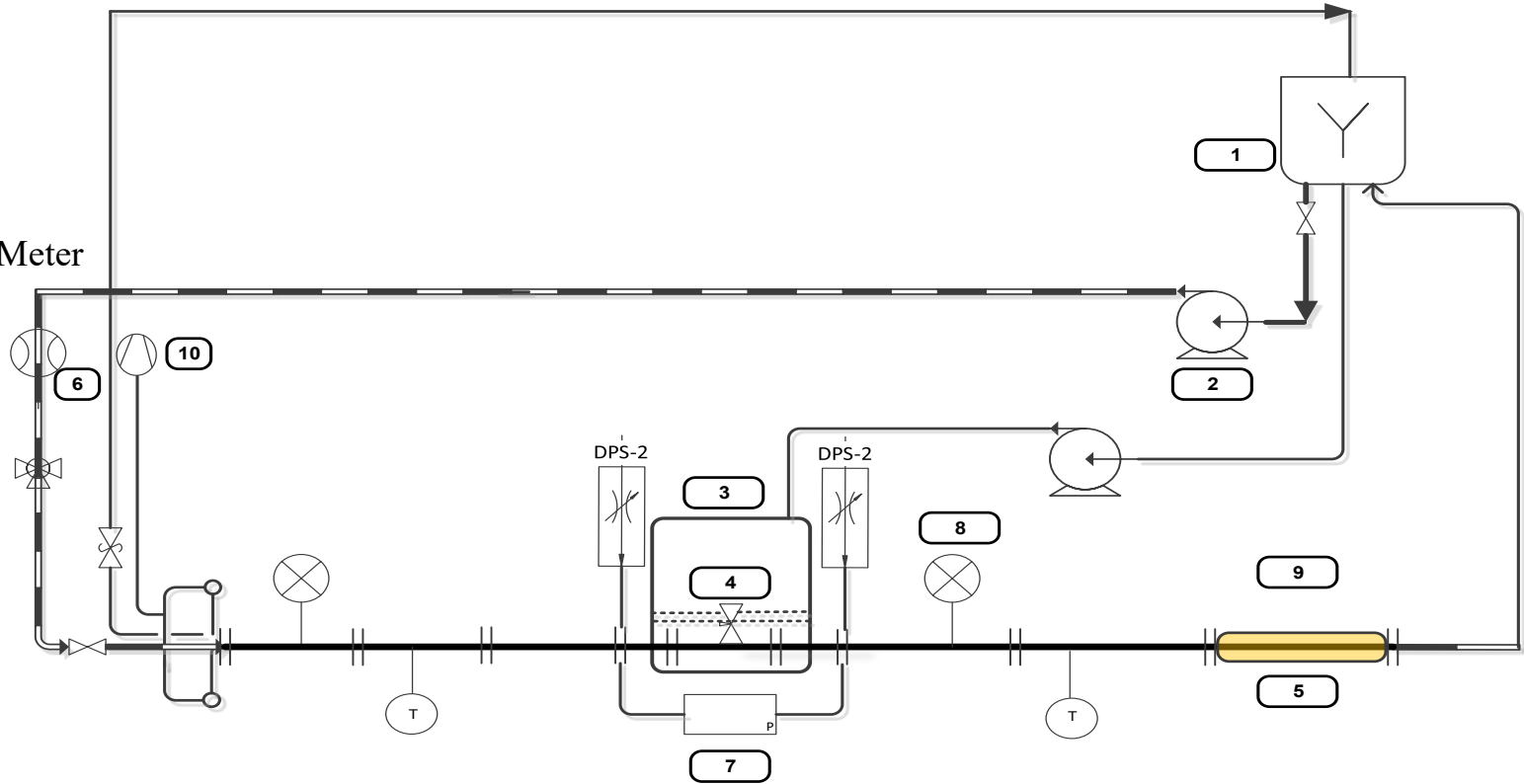
3. Workstation for image and data acquisition table

Composed of extra required tools for imaging and may need during running the experiment.

Finally, the total cost will be mentioned with more information regarding the fitting company and the price for the fitting to assembly the tools and running the test experimentally.

# Facility Report

- 1- Tank
- 2- Pump
- 3- Tank Bath
- 4- Leak Valve
- 5- Visualization Pipe
- 6- Coriolis Liquid Flow Meter
- 7- Differential Pressure
- 8- Pressure Gauge
- 9- Camera
- 10- Compressor



	Pressure gauge		Absolute Digital Pressure (APD)		Flanged		Ball valve (V)		2" Flexible Pipe
	Compressor		Digital pressure sensor (DPS)		Hydrophone		Temperature		2" steel pipe
	Air relief valve (RV)				Air- Non return Valves		Flow Meter (F)		4.5" Steel Pipe

**Table 6. 1 Experimental components of flow loop for two and three-phase leak detection set-up**

<b>Suppliers</b>	<b>Components</b>	<b>Model number</b>	<b>Specifications</b>	<b>Qt.</b>	<b>Unit price</b>	<b>Price (Dollars)</b>
<b>Antonis</b>	Frame	<b>Rev.2</b>	Motorized	1	15340	15340
<b>Vita Needle</b>	Pipeline	<b>N/A</b>	Stainless Steel Tubes 1-9/16” through 5” OD	23 ft		-
<b>Par Group (Perspex®)</b>	Acrylic pipeline	<b>ACT-114X120X2000</b>	Temperature: up to +70°C (+90°C short term). Excellent optical properties. Lightweight and easily fabricated.	3.5 ft	Waiting for Response	-
<b>Antonis</b>	Flanges	1 or 2 meters	4” or 5”	6 meters	8260	8260
<b>Elastic pipes &amp; cam-locks</b>	Connect all the peripheral devices	2” (50X67mm) Or 2 ½”(63X83mm)	Working up to 20 bars	8-12m	1770	1770
<b>Omega</b>	Differential pressure transducer Sensor	<b>PXM409-001BGUSBH</b>	working pressure range of ( 0 to 100000 Pa) High ±0.08% BSL Accuracy <b>Existing gauge (VALIDYNE P61 ) • 0.25% FS Accuracy, 0.7% Max Temperature Error</b> FS Range is 0 – 5 kPa	2	0	0
	Temperature use thermocouple x2	-	-	-	Existing	-
<b>Sensors One</b>	Dynamic pressure transducer	<b>UPS-HSR-B0016-N</b>	0 to 16 bar USB connection to PC	1	750	750
<b>IMI Norgren</b>	Pressure Regulator and filter	-	-	1	Coming with compressor	-

<b>Coriolis</b>	Mass flow meter for water		Micromotion), F200S, 2", 316L stainless steel, 18 to 100 VDC and 85 to 265 VAC, self-switching Analog flow reading measure with 4-20 mA, Density in Frequency using HART. For small range already have	1	Existing	-
<b>Aquarium</b>	500X500X1000 mm	Special design	Open loop max capacity 250 liter	1	11800	11800
<b>Aquarium accessories</b>	Relief valve, pressure gauge, pressure sensor, water level sensor, pumps for fill and drain	-	-	-	3500	3500
<b>Antoni</b>	Mass flow sensor (low-high range) (air)	Control functions also available from PC via RS-232	Accuracy of +/- 1% of full scale Repeatability of +/- 0.25% of full scale	2	4700	4700
<b>Accessories</b>	Tubes for air line, adaptors for dP connections, , power extension cable, USB cables , snubbers, adapters	-	-	-	500	500
<b>Antoni</b>	Air flange 45 degrees	-	2'' connected with cam-locks Non return valve	1	1180	1180
<b>Atlas</b>	Compressor	SF22+	Maximum pressure 10 bars	1	41435.28	41435.28
					<b>Total</b>	<b>89,235 \$</b>

**Table 6. 2 Image and data acquisition systems**

Suppliers	Components	Model number	Specifications	Qt.	Unit price	Price (Dollars)
<b>Bruel &amp; Kjaer</b>	Hydrophone	<b>BK 8104</b>	frequency range between 0.1 Hz to 120kHz	1	10000	10000
Approix	DAQ	-	To control the instrument, compressor and labview	1	5000	5000
					<b>Total</b>	<b>15000\$</b>

**Table 6. 3 Workstation for image and data acquisition**

Suppliers	Components	Model number	Specifications	Qt.	Unit price	Price (Dollars)
<b>Dell</b>	case	Dell Precision T5600	Intel® Xeon® Processor E5-2620; 8GB3 DDR3 SDRAM at 1333 MHz; 1TB, 7200 RPM 3.5" SATA 6Gb/s Hard Drive;2GB NVIDIA® Quadro® 4000, DUAL MON, 2DP & 1DVI	1		
	Monitor	Dell UltraSharp U2413	24inch; One for camera display, one for Labview, one for image acquisition monitor or other works	2		

## **Chapter 7. Risk Analysis**

The objectives of this chapter is to review and study the performance multiphase flow leak detection at Texas A&M University - Qatar and perform risk analysis. Different quantitative and qualitative risk methodologies can be used to indicate all the possible accidents and their damage to people, production, and the environment.

### **7.1 Hazard Identification**

Is part of the process used to evaluate if any situation, item, thing, etc. may have the potential to cause harm. The term often used to describe the full process is risk assessment:

- Identify hazards and risk factors that have the potential to cause harm (hazard identification).
- Analyze and evaluate the risk associated with that hazard (risk analysis, and risk evaluation).
- Determine appropriate ways to eliminate the hazard or control the risk when the hazard cannot be eliminated (risk control).

The primary objective of the HAZOP review was to review the design, develop an understanding of the potential risks in terms of safety and operability, and to propose recommendations designed to mitigate the potential risks and prevent accidents associated with hazard scenarios identified in the HAZOP.

### **7.2 HAZOP Objective**

The objective of this HAZOP was to identify potential hazards and operability issues associated with the equipment design and installation of a leak test lab, document safeguards existing within the current design being proposed, and evaluate (rank) the risks associated with those hazards in terms of risk to people, asset and the environment. Additional protective measures were then proposed if additional safeguards were deemed to be needed to manage these hazards.

### 7.3 Purpose of Risk Analysis

The new leak test lab constructed for use at Texas A&M - Qatar will be used for the study of leak detection behavior of single and multiphase fluids in harsh environments. Although an eventual goal is to study multiphase behavior, this HAZOP covers the experimental setup designed to operate with air as the working fluid and other multiphase working fluid air, water, and solid.

The flow pipeline will be installed to study:

- The effectiveness in using dynamic and differential pressure measurements to detect leaks in pipelines, with a focus on micro-leaks; and
- The possibility of using only dynamic and differential pressure measurements to identify if different leak sizes can be detected and classified accordingly.
- check the ability of the hydrophone sensor to detect the leak acoustic signal.

The proposed setup includes:

- Compressed air supply from the laboratory at Texas A&M University of Qatar, connected to the developed pipeline using flexible piping.
- Compressor machine to supply air that separate from the lap building air supplier
- Pressure regulator with general-purpose filter and oil filter, with downstream pressure relief valve
- T-union with needle valve connected to the setup to model the leak and control the amount leaking from the pipeline
- Pump to supply the water and slurry fluid in flow loop leak detection
- Structure support frame to the flow loop motorized movement
- Water tank bath to simulate the subsea condition
- Tank drained pump.
- Instrumentation (e.g. temperature sensor, differential and dynamic pressure gauge, hydrophone acoustic sensor, Electric Resistance Tomography ERT)

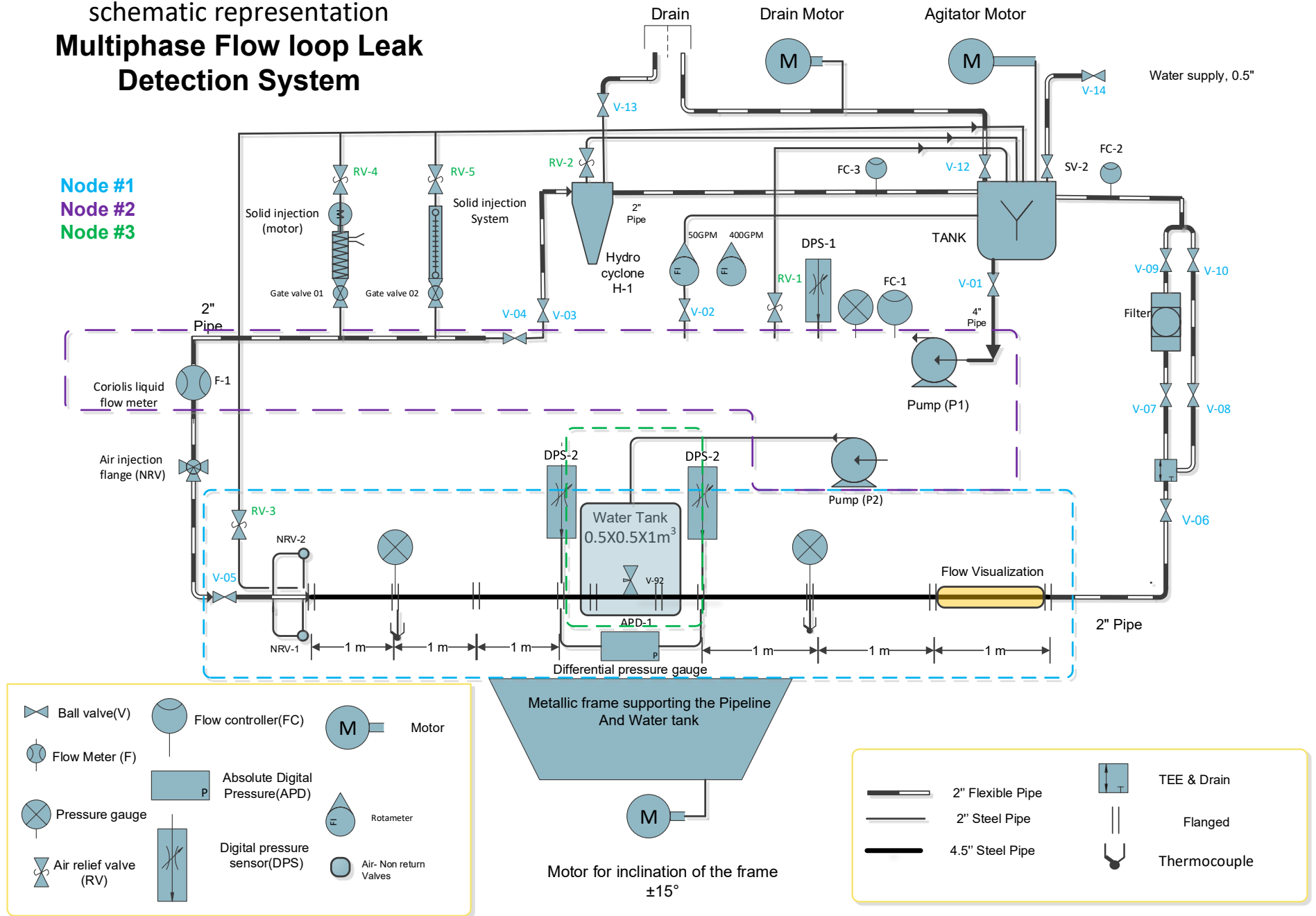
## 7.4 HAZOP Analysis

A hazard and operability study (HAZOP) is a structured and systematic examination of a complex planned or existing process or operation to identify and evaluate problems that may represent risks to personnel or equipment. The intention of performing a HAZOP is to review the design to pick up design and engineering issues that may otherwise not have been found. The technique is based on breaking the overall complex design of the process into a number of simpler sections called 'nodes' which are then individually reviewed.

The process was broken down into the following three (3) HAZOP Nodes for the purposes of this HAZOP review:

- Node 1: Flow loop leak detection
- Node 2: Slurry pump and compressor system
- Node 3: Tank bath and leakage valve

# schematic representation Multiphase Flow loop Leak Detection System



The HAZOP lead to identifying clearly and creatively the risk to:

- Identify any hazards or operability problems associated with each Node, using a set of HAZOP guidewords known as parameters and deviations, considered one at a time, as a prompt.
- Identify the initiating cause of each identified hazard or operability problem.
- Identify the consequences of each identified hazard or operability problem.
- Identify the safeguards currently in place within the existing equipment design and administrative controls, to reduce the likelihood of the hazard arising in the first instance or to minimize the severity of its consequences were it to arise.

The HAZOP is intended to be a rapid identification and description process highlighting potential high-risk areas of the proposed design it is not a forum for trying to solve potential problems. The HAZOP was conducted following the TAMUQ PSA Risk Matrix.

### 7.5 Risk Matrix

The following tables show the criteria established by Texas A&M University at Qatar to calculate risk.

Table 1. Likelihood			
Likelihood (L)	Category	Description	Likelihood as function of number of barriers
Frequent	A	Likely to occur frequently or continuously experienced.	No barriers; or only one Administrative or PPE
Probable	B	Will occur several times during life cycle	Only one Engineering; or combination of no more than two Administrative or PPE
Occasional	C	May occur sometime, but rather rarely	Only one Engineering and at least one Administrative or PPE; or at least three Administrative or PPE Barriers
Remote	D	Unlikely, but possible to occur	At least two Engineering Barriers; or one Engineering, good inherently safer design, and at least one Administrative or PPE
Improbable	E	So unlikely that it can be assumed it will not occur	At least two Engineering Barriers, good inherently safer design and some administrative or PPE

Table 2. Severity of consequences			
Severity (S)	Category	Description	Examples
Catastrophic	1	Death, life-threatening health effects, permanent serious disability. (Irreversible significant environmental impact)	Death or paralysis. Leg or hand amputation.
Critical	2	Permanent partial disability, severe injury or illness that may result in long hospitalization or serious health effects that could impair the ability to take protective action.	A deep burn or a major broken bone.
		(Reversible significant environmental impact. Extensive damage to asset.)	Asphyxiation.
Moderate	3	Mild, transient health effects, injury or illness resulting in more than one lost work day and which may require some hospitalizing, but rather short.	Small burn.
		(Reversible moderate environmental impact. Minor damage to asset.)	A broken finger or toe.
Marginal	4	Minor injury; injury or illness resulting in no more than one lost work day. (Minimal environmental impact or asset damage.)	A small cut or twisted ankle.

Table 3. Risk Matrix						
		Risk (R)				
Severity (S)	1	1E	1D	1C	1B	1A
	2	2E	2D	2C	2B	2A
	3	3E	3D	3C	3B	3A
	4	4E	4D	4C	4B	4A
		E	D	C	B	A
		Likelihood (L)				

Table 4. Risk acceptance criteria		
<b>Acceptable Risk (blue)</b> Medium to low risk, which is fully acceptable with periodic review and control.	<b>Tolerable Risk (yellow)</b> Serious risk, which is tolerable, if demonstrated that is controlled and reduced to ALARP. Make changes if possible.	<b>Unacceptable Risk (red)</b> High risk, which is not acceptable at any time. Do not Operate. Apply risk reduction measures.
Inspect annually	Inspect monthly	Inspect daily until corrected

Figure 7. 1 TAMUQ Risk Matrix

## 7.6 HAZOP Study Details

**Deviation:** a combination of guideword and process parameter. For example, “More” combined with “Temperature” yields the Deviation “Higher Temperature.”

**Causes:** the events or failures that result in a deviation from design intent for a process parameter. For example, “No Flow” may be caused by “pump not pumping.” While it is often adequate to list a “Cause,” it is sometimes preferable to list “root causes” (for example, “pump not turned on,” or “coupling failed”), where Consequences or Safeguards are unique to a particular root cause. By convention, Causes were considered only within the Node under study.

**Consequences:** a description of the worst credible hazard, or series of hazards, or operability problems that would or could result from the Cause, if subsequent events were to proceed without consideration of safeguards which may exist. Consequences may arise beyond the Node under study. If so, these were documented accordingly.

**Safeguards:** existing or proposed (for new projects) measures that detect or warn of a Deviation or Consequence, prevent a Deviation or Consequence or mitigate the effects of a Consequence.

**Recommendations:** recommendations include design, operating, or maintenance changes that reduce or eliminate Deviations, Causes, and/or Consequences. Any recommendations made are for additional safeguards that are not currently in use at the facility.

The focus of the HAZOP recommendations was to first look to see if the hazard could be eliminated, and then if not possible to reduce the risk based on the hierarchy of risk reduction as shown on the bulleted list below:

- Eliminate or minimize HSE hazards by using options with a lower impact on HSE.
- Substitution by using products and/or processes with a lower impact on HSE.
- Isolation/separation of hazards and targets.
- Engineering controls – prevention.
- Engineering controls – mitigation.
- Organizational controls, i.e. competence and communication.
- Procedural controls
- Personal Protective Equipment (PPE)

The list of guidewords used for the Leak Test Lab HAZOP included the following:

<b>Deviation</b>	<b>Guideword</b>	<b>Parameter</b>
1.1. High Pressure	More	Pressure
1.2. Low Pressure	Less	Pressure
1.3. More Flow	More	Flow
1.4. No / Less Flow	Less	Flow
1.5. Reverse / Misdirected Flow	Reverse/Misdirected	Flow

<b>Deviation</b>	<b>Guideword</b>	<b>Parameter</b>
1.6. As well as flow (Contamination)	As well as	Flow
1.7. High Temperature	More	Temperature
1.8. Low Temperature	Less	Temperature
1.9. High Level	More	Level
1.10. Low Level	Less	Level
1.11. Composition Change	As well as	Flow

### **7.6.1 Assumptions and Clarifications**

This study addresses various hazards and operability issues related to the design of the lab based on the following assumptions:

- Work within the lab will comply with the TAMUQ Lab Safety Manual and the Project Safety Analysis (PSA).
- A set of operating procedures has been developed and covers all modes of startup, operation, and shutdown of the lab apparatus.
- The personnel operating the Leak Test Lab apparatus will go through a training and competency assurance protocol before being allowed to run the lab. This training and competency assurance will be done by the TAMUQ Leak Test lab, Principal Investigator.
- The start-up of the laboratory equipment will be such that leak checks will be conducted before starting up.

**Table 7. 1 HAZOP Worksheet for Inlet Line flow loop**

Node 1 Inlet Line Flow Loop									
Guide word	Parameter	Deviation	Cause	Consequence	Safeguards	L	S	R	Recommendation
High	pressure	High pressure	high working pressure	Pipe rupture	Administration control	B	1	1B	Install regulator valve
			Mechanical problem			C	3	3C	
			Signal error			D	4	4D	
Low		Low pressure	Low working pressure	Lower than operation pressure	Administration control	E	4	4E	Install pressure sensor
			Signal error			E	4	4E	
High		Temperature	High temperature	Warm weather	Pipe corrosion	Engineering control	B	2	2B
	Signal error			C			3	3C	
Low	Lower temperature		Cold weather	Lower than operation temperature	Engineering control	D	4	4D	Install temperature sensor
			signal error			D	4	4D	

**Table 7. 2 HAZOP Worksheet for slurry pumping system.**

Node 2 Slurry Pumping System										
Guide word	Parameter	Deviation	Cause	Consequence	Safeguards	L	S	R	Recommendation	
No	Flow rate	no flow	Electric	No fluid delivery	Administration control	C	2	2C	Routine maintenance	
			The main valve locked	Pump failure		D	2	2D		
More		More flow	Fluid delivered at high pressure	High pressure in connection line	Filter damage	Administration control	B	1	1B	Install FC valve
				Filter damage			C	3	3C	
Less		less flow	Partial plug in the supply line	Less fluid delivery (insufficient)		D	3	3D	Install pressure sensor	
High		Pressure	high pressure	Leakage	High pressure in line	Engineering control	B	1		1B
Low	low pressure		Partial plug	Insufficient fluid supply	Engineering control	D	3	3D		
High	Temperature	high temperature	High inlet temperature	Increase pressure in the pipeline		D	2	2D	Install the temperature gauge	
Low		low temperature	Low inlet temperature	Freezing fluid in the pipeline	Engineering control	E	4	E4		
			Low surrounding temperature			E	4	E4		

**Table 7. 3 HAZOP Worksheet for Tank Bath and Leakage Valve.**

Node 3 Tank Bath and Leakage Valve									
Guide word	Parameter	Deviation	Cause	Consequence	Safeguards	L	S	R	Recommendation
High	Pressure	High pressure	Leakage of acrylic sides	The floor gets wet. The operation has to be shut off- tank liquid should be drained out of the tank	Administration control	B	2	2B	Install quick drained pump
Low		Low pressure	No leak	Not likely to cause any significant damage	Administration control	E	4	E4	Regularly check the tank sealing
High	Electricity	High electrical	Short in the electrical actuator valve	Valve will not work	Administration control	B	2	2B	Install electrical regulator
			Signal error						
Low		Lower electrical	The leakage valve will not work	No leakage modeling working	Administration control	D	4	4D	Install electrical regulator
			Signal error						

## Chapter 8. Conclusions and Recommendation

### 8.1 Conclusions

The main aim of this research thesis was to establish a new flow loop leak detection experimental setup including all the required information to change the multiphase flow loop at Texas A&M University – Qatar to leak detection flow loop.

During the entrance of length sensitivity analysis for this study, a sort of points for single-phase and multiphase flow have been noted.

- In the case, single-phase flow, the most contributed parameter is the velocity. When velocity increases the entrance of length increase for all different pipeline diameter. Density has a minor effect on the entrance of length in comparison with viscosity.
- In the case, two-phase flow, the increase of liquid hold up will increase the entrance of length at lower and higher velocity. The increase in viscosity will decrease the entrance of length depending on the liquid hold up. The opposite of density when the density decreases the entrance of length decrease as well for all different velocities.
- In the case, three-phase flow, the increase of solid fraction the entrance of length will decrease for all velocities. The main observed here is that when the viscosity increase as a result of an increase in solid fraction, the entrance of length will decrease for all different velocities.
- The pressure drop calculation for three-phase flow (air, water, and solid) is higher than two-phase flow (air and water).
- Pressure drop calculation with different angles reported that when the angle increases the pressure drop increase as well.
- According to the risk analysis study the high hazard area in case of the high pressure which might affect on pipeline and aquarium tank as well. A fixed relief valve in case of high pressure is highly recommended to avoid failure of the pipeline and other instruments.
- To have the long life of the instruments and electronic devices an Installation electrical regulator is required.

## **8.2 Recommendation**

Knowing the importance of the Leak detection system in the prevention of economic and environmental impacts led pipeline operators to seek for a more detailed understanding of the leak's behavior to determine the best possible technology available.

During this study and searching for experimental setup for leak detection purposes a sort of recommendation can be pointed out as following.

- Using a bigger pipeline diameter for future applications where it is more reliable to the oil industry.
- Better to find another method to collect the leak data rather than use hydrophones or differential pressure for example use fiber optic is more accurate and more interested in the oil industry.
- A suggestion to increase the pipeline length and tilting angles.
- These studies are based on establishing and design work. It would be interesting to compare the result of the flow loop leak detection in the future such as velocity profile and leak rate with the CFD or modeling.

## 9. Reference

1. Sivathanu, Y. "Natural gas leak detection in pipelines". *Technol. Status Report, En'Urga Inc., West Lafayette*(2003). [Online]. Available: [https://netl.doe.gov/sites/default/files/2018-05/scanner\\_technology\\_0104.pdf](https://netl.doe.gov/sites/default/files/2018-05/scanner_technology_0104.pdf)
2. European Gas Pipeline Incident Data Group (EGIG). "10<sup>th</sup> Report of the European Gas Pipeline Incident Data Group (period 1970 – 2016)". 50. Groningen (2018). [Online]. Available: [https://www.egig.eu/startpagina/\\$61/\\$108](https://www.egig.eu/startpagina/$61/$108)
3. Murvay, P. S. & Silea, I. "A survey on gas leak detection and localization techniques". *J. Loss Prev. Process Ind.* **25**, 966–973 (2012). [Online]. Available: [http://www.aut.upt.ro/~pal-stefan.murvay/papers/survey\\_gas\\_leak\\_detection\\_localization\\_techniques.pdf](http://www.aut.upt.ro/~pal-stefan.murvay/papers/survey_gas_leak_detection_localization_techniques.pdf)
4. Yousef, A. Y. "Offshore Pipeline Leak Modeling Using a Computational Fluid Dynamics Approach". Newfoundland, Canada (2018). [Online]. Available: [https://research.library.mun.ca/13506/1/Yousef\\_YousefAbdulhafed\\_master.pdf](https://research.library.mun.ca/13506/1/Yousef_YousefAbdulhafed_master.pdf)
5. M., Golmohamadi. "Pipeline leak detection". Master Thesis. Missouri University. USA.(2015).[Online].Available: <http://merlin.lib.umssystem.edu/record=b10848575~S5>
6. El-Shiekh, T. M. "Leak detection methods in transmission pipelines". *Energy Sources, Part A Recover. Util. Environ. Eff.* **32**, 715–726 (2010). [Online]. Available: <https://doi.org/10.1080/15567030903058618>
7. Zhang, J., Hoffman, A., Murphy, K., Lewis, J. & Twomey, M. "Review of pipeline leak detection technologies". *PSIG Annu. Meet.* 1303. (2013). [Online]. Available: <https://www.atmosi.com/media/1412/review-of-pipeline-leak-detection-technologies.pdf>
8. Geiger, G. "State-of-the-art in leak detection and localization". *Erdoel Erdgas Kohle* **122**, 193–198 (2006). [Online]. Available: <https://www.pipeline-conference.com/sites/default/files/papers/321%20Geiger.pdf>

9. Mishra, A., Al Gabani, S. H. & Al Hosany, A. J. "Pipeline leakage detection using fiber optics distributed temperature sensing DTS". *Soc. Pet. Eng. - SPE Abu Dhabi Int. Pet. Exhib. Conf.* 1–12 (2017). [Online]. Available: <https://www.onepetro.org/conference-paper/SPE-188407-MS>
10. Mohd Ismail, M. I. *et al.* "A review of vibration detection methods using accelerometer sensors for water pipeline leakage". University Teknologi Malaysia, Kuala Lumpur. *IEEE Access* 7, 51965–51981. (2019).[Online].Available: <https://doi.org/10.1109/ACCESS.2019.2896302>
11. Lu, H., Iseley, T., Behbahani, S. & Fu, L. "Leakage detection techniques for oil and gas pipelines: State-of-the-art". *Tunnelling and Underground Space Technology* vol. 98 (2020). [Online].Available: <https://doi.org/10.1016/j.tust.2019.103249>
12. Zhang, J. "Designing a cost-effective and reliable pipeline leak-detection system". *Pipes Pipelines Int.* 42, 20–26 (1997). [Online]. Available: <https://www.semanticscholar.org/paper/Designing-a-cost-effective-and-reliable-pipeline-Zhang/db0dc43828978bb64195c471fe9be2e71ce0db3c?p2df>
13. Murvay, P. S. & Silea, I. "A survey on gas leak detection and localization techniques". *Journal of Loss Prevention in the Process Industries* vol. 25 966–973. Timisoara, Romania.(2012).
14. Adegboye, M. A., Fung, W. K. & Karnik, A. "Recent advances in pipeline monitoring and oil leakage detection technologies: Principles and approaches". (UK),(2019).[Online].Available: <https://doi.org/10.3390/s19112548>
15. K. B. Adedeji, Y. Hamam, B. T. Abe and A. M. Abu-Mahfouz, "Towards achieving a reliable leakage detection and localization algorithm for application in water piping networks: an overview," *IEEE Access*, vol. 5, pp. 20272-20285, (2017) [Online]. Available: <https://ieeexplore.ieee.org/abstract/document/8052087>
16. Rizaldy & Sadiq J. Z. "Pressure Drop in Large Diameter Geothermal Two-Phase Pipelines".University of Acukland. NewZealand.(2016). [Online].Available: <http://hdl.handle.net/2292/32474>

17. Lahey, R. T. "Two-phase flow". *Eng. Handbook, Second Ed.* 42-1-42–12 (2004) .
18. Ortega Malca, Arturo J, and Nieckele, Angela O. "Simulation of horizontal pipe two-phase slug flows using the two-fluid model."( 2005),. Brazil.
19. Streeter, V. L., and E. B. Wylie."Fluid Mechanics (Seventh Ed.)". McGraw-Hill Book Co. (1979).
20. Cengel, Y. A. . & Cimbala, J. M. " Fluid Mechanics: Fundamentals and Applications".McGraw-Hill.(2010).[Online].Available:  
[http://www.academia.edu/download/39343926/Chap02\\_solution.pdf](http://www.academia.edu/download/39343926/Chap02_solution.pdf)
21. Çarpınlioğlu, M. Ö. & Özahi, E. "Laminar flow control via utilization of pipe entrance inserts (a comment on entrance length concept)". *Flow Measurement and instrumentation*, volume, **22**, 165–174(2011).[Online].Available:  
<https://doi.org/10.1016/j.flowmeasinst.2011.01.005>
22. Ofei, T. N. & Ismail, A. Y. "Eulerian-Eulerian Simulation of Particle-Liquid Slurry Flow in Horizontal Pipe". *J. Pet. Eng.* **2016**, 1–10 (2016). [Online]. Available:  
<https://www.hindawi.com/journals/jpe/2016/5743471/>
23. Alina Lozhechnikova, "Determination of slurry viscosity using case based reasoning approach" Master Thesis. Lappeenranta University of Technology (2011). [Online]. Available:  
<https://lutpub.lut.fi/bitstream/handle/10024/73807/nbnfi-fe201112166083.pdf?sequence=1&isAllowed=y>
24. Ryan .Spelay. Saskatchewan Research Council (SRC). "Formula Multiphase." Private Contact with Reseach Council. Canada (2020). [Online]. Available:  
<https://www.src.sk.ca/>
25. Thamarai Chelvi, S. K., Yong, E. L. & Gong, Y. "Preparation and evaluation of calix[4]arene-capped  $\beta$ -cyclodextrin-bonded silica particles as chiral stationary phase for high-performance liquid chromatography". *J. Chromatogr. A* **1203**, 54–58 (2008). [Online]. Available: <https://doi.org/10.1016/j.chroma.2008.07.021>
26. Thomas, D. G. "Transport characteristics of suspension: VIII. A note on the viscosity of Newtonian suspensions of uniform spherical particles". *J. Colloid Sci.* **20**, 267–

277. Texas A&M Electronic Library (1965).
27. Chidamoio, J. F., Akanji, L. & Rafati, R. "Effect of length-to-diameter ratio on axial velocity and hydrodynamic entrance length in air-water two-phase flow in vertical pipes". *J. Oil, Gas Petrochemical Sci.* 18–24. (2017). [Online]. Available: [http://aura.abdn.ac.uk/bitstream/handle/2164/9845/jogps\\_01\\_01\\_00003.pdf?sequence=1](http://aura.abdn.ac.uk/bitstream/handle/2164/9845/jogps_01_01_00003.pdf?sequence=1)
28. N. Mangesana. *et al.* " The effect of particle sizes and solids concentration on the rheology of silica sand based suspensions". *J. South. African Inst. Min. Metall.* **108**, 237–243.(2008).[Online]Available: <http://www.scielo.org.za/pdf/jsaimm/v108n4/05.pdf>
29. Stajanca, P. *et al.* "Detection of leak-induced pipeline vibrations using fiber—Optic distributed acoustic sensing". *Sensors (Switzerland)* (2018) . [Online]Available: <https://doi.org/10.3390/s18092841>
30. Meng, L., Yuxing, L., Wuchang, W. & Juntao, F. "Experimental study on leak detection and location for gas pipeline based on the acoustic method". *J. Loss Prev. Process Ind.* **25**,90–102.(2012).[Online]Available: <https://doi.org/10.1016/j.jlp.2011.07.001>
31. Y.Gao M.J.Brennan P.F.Joseph J.M.Muggleton O.Hunaidi . "A model of the correlation function of leak noise in buried plastic pipes". *journal of sound & vibration*.Unitedkingdom.(2004).[Online]Available: <https://doi.org/10.1016/j.jsv.2003.08.045>
32. Khulief, Y. A., Khalifa, A., Mansour, R. Ben & Habib, M. A. "Acoustic Detection of Leaks in Water Pipelines Using Measurements inside Pipe". *J. Pipeline Syst. Eng. Pract.* **3**, 47–54 (2012). [Online]Available: [https://doi.org/10.1061/\(ASCE\)PS.1949-1204.0000089](https://doi.org/10.1061/(ASCE)PS.1949-1204.0000089)
33. Reddy, H. P., Narasimhan, S., Bhallamudi, S. M. & Bairagi, S. "Leak detection in gas pipeline networks using an efficient state estimator. Part II. Experimental and field evaluation". *Computers and Chemical Engineering* vol. 35 662–670 (2011).

[Online]Available: <https://doi.org/10.1016/j.compchemeng.2010.10.011>

34. Liang, W., Zhang, L., Xu, Q. & Yan, C. "Gas pipeline leakage detection based on acoustic technology". *Engineering Failure Analysis* vol. 31 1–7 (2013). [Online]Available: <https://doi.org/10.1016/j.engfailanal.2012.10.020>
35. Scott, S & Barrufet, M. "Worldwide Assessment of Industry Leak Detection Capabilities for Single & Multiphase Pipelines". Texas A&M University.18133. 125 (2003).[Online]Available:<http://www.celou.com/res/icelou/medicalres/201011/20101116203055479.pdf>
36. Siebenaler, S., Krishnan, V., Nielson, J. & Edlebeck, J. "Fiber-optic acoustic leak detection for multiphase pipelines". *Proc. Int. Offshore Polar Eng. Conf. USA*. 247–255 (2017). [Online]Available: <https://www.onepetro.org/conference-paper/ISOPE-I-17-679>
37. Ji, J., Li, Y., Liu, C., Wang, D. & Jing, H. "Application of EMD technology in leakage acoustic characteristic extraction of gas-liquid, two-phase flow pipelines". *Shock Vib.* (2018). [Online]Available: <https://doi.org/10.1155/2018/1529849>
38. Sassi, P., Pallarès, J. & Stiriba, Y. "Visualization and measurement of two-phase flows in horizontal pipelines". *Exp. Comput. Multiph. Flow* **2**, 41–51 (2020). [Online]Available: <https://doi.org/10.1007/s42757-019-0022-1>
39. Sassi, P., Stiriba, Y., Lobera, J. et al. "Experimental Analysis of Gas–Liquid–Solid Three-Phase Flows in Horizontal Pipelines". *Flow Turbulence Combust* (2020). [Online]Available: <https://link.springer.com/article/10.1007/s42757-019-0022-1>